AWARD NUMBER: W81XWH-12-1-0622

TITLE: Assessment of Biomarkers Associated with Joint Injury and Subsequent Post-Traumatic Arthritis

PRINCIPAL INVESTIGATOR: Virginia B. Kraus

CONTRACTING ORGANIZATION: Duke University Medical Center
Durham, NC 27705

REPORT DATE: December 2016

TYPE OF REPORT: Final

PREPARED FOR: U.S. Army Medical Research and Materiel Command
                        Fort Detrick, Maryland 21702-5012

REPORT DOCUMENTATION PAGE

1. REPORT DATE	2. REPORT TYPE	3. DATES COVERED
December 2016	Final	30 Sep 2012 - 29 Sep 2016

4. TITLE AND SUBTITLE

Assessment of Biomarkers Associated with Joint Injury and Subsequent Post-Traumatic Arthritis

5a. CONTRACT NUMBER
OR110100P1

5b. GRANT NUMBER
W81XWH-12-1-0622

5c. PROGRAM ELEMENT NUMBER

6. AUTHOR(S)

Steven A. Olson, Farshid Guilak, Virginia B. Kraus, Bridgette D. Furman, Kelly A. Kimmerling, Janet L. Huebner, Louis E. DeFrate

E-Mail: vbk@duke.edu

5d. PROJECT NUMBER

5e. TASK NUMBER

5f. WORK UNIT NUMBER

7. PERFORMING ORGANIZATION NAME(S) AND ADDRESS(ES)

Duke University
School of Medicine
2200 West Main St.
Suite 820 Erwin Square Plaza
Durham, NC 27705

8. PERFORMING ORGANIZATION REPORT NUMBER

9. SPONSORING / MONITORING AGENCY NAME(S) AND ADDRESS(ES)

U.S. Army Medical Research and Materiel Command
Fort Detrick, Maryland 21702-5012

10. SPONSOR/MONITOR'S ACRONYM(S)

11. SPONSOR/MONITOR'S REPORT NUMBER(S)

12. DISTRIBUTION / AVAILABILITY STATEMENT
Approved for Public Release; Distribution Unlimited

13. SUPPLEMENTARY NOTES

14. ABSTRACT
The overall objective of this research effort is to identify biomarkers following articular fracture that may be predictive of the development of post-traumatic arthritis (PTA). PTA is a clinically important complication of joint injury with life-long effects for the patient. While PTA can occur rapidly after moderate to severe articular injuries, not every patient will go on to develop this condition. There are no effective screening methods to determine who is at risk. This proposal includes both a clinical observational study and a series of murine experiments, both with the goal of identifying biomarkers that are associated with development of PTA. Patients with knee joint fractures will be enrolled, and we will collect serum, urine, and synovial fluid early after injury. Radiographic imaging will be performed early after injury, again at 18 months, and analyzed to determine which patients developed PTA from those who did not. We will assess the ability of identified biomarkers in serum, urine, and synovial fluid to predict PTA following joint injury. Additionally, biomarkers will be assessed in a murine model of articular fracture using two strains in which one strain develops PTA and the other does not. Comparison of the human and mouse response to knee joint fracture will allow assessment of the potential use of the mouse model to evaluate future therapies to prevent PTA.

15. SUBJECT TERMS

Nothing listed

16. SECURITY CLASSIFICATION OF:			17. LIMITATION OF ABSTRACT	18. NUMBER OF PAGES	19a. NAME OF RESPONSIBLE PERSON USAMRMC
a. REPORT	**b. ABSTRACT**	**c. THIS PAGE**	UU	70	**19b. TELEPHONE NUMBER** (include area code)
U	U	U			

Table of Contents

"Assessment of Biomarkers Associated with Joint Injury and Subsequent Post-Traumatic Arthritis"
Start date: 9/30/2012
PIs – Steven A. Olson **(SAO)**; Farshid Guilak **(FG)**; and Virginia B Kraus **(VBK)**

1. INTRODUCTION:

Post-traumatic arthritis (PTA) is a clinically important complication of joint injury with life-long effects for the patient.[1,2] PTA is a severe burden in active duty and discharged soldiers.[3] While PTA can occur rapidly after moderate to severe articular injuries, not every patient will go on to develop this condition. There are no effective screening methods to determine who is at risk for developing PTA. The overall objective of this proposal is to identify biomarkers following articular fracture that may be predictive of the development of PTA. To accomplish this, we will conduct a two-part study. We will perform a prospective observational study of patients with lower extremity articular fractures requiring operative treatment. Patients with knee joint fractures will be enrolled, and we will collect serum, urine, and synovial fluid from each patient acutely after injury. Radiographic imaging will be performed early after injury and again at 18 months. Both scans will be analyzed to separate the patients that developed PTA from those who did not. We will assess the ability of identified biomarkers in serum, urine, and synovial fluid to predict PTA following joint injury. Additionally, biomarkers will be assessed in a murine model of articular fracture using two strains in which one strain develops PTA and the other does not. Comparison of the human and mouse response to knee joint fracture will allow for assessment of the potential use of the mouse model to evaluate future therapies to prevent PTA. The low cost of mouse models lends itself to this type of work, and the results will provide a validated model to use for studying PTA. The goal of this work is to establish the basis for future use of biomarkers to predict the potential risk for developing PTA after acute joint injury. In addition, this work will elucidate data on biospecimens that may be useful in future registries of acute joint injuries.

2. KEYWORDS:

Post-traumatic arthritis, post-traumatic osteoarthritis, articular fracture, joint injury, trauma, biomarker, inflammation, MRI, knee, mouse model, translational research.

3. OVERALL PROJECT SUMMARY:

The overall objective of this study is to identify biomarkers following articular fracture that may be predictive of the development of PTA. Specifically, patients with a closed unilateral articular fracture of the knee requiring operative treatment will be enrolled over an 18-month period. Biosamples (synovial fluid from the injured and contralateral uninjured knee, serum, and urine) will be collected prior to or at surgical intervention. MRI imaging of the injured knee will be obtained to assess the articular cartilage. Degenerative changes in the cartilage and joint space narrowing will be correlated to biomarkers that may be indicative and predictive of joint degeneration and the development of PTA. We have successfully enrolled patients, collected and stored biosamples, obtained all post-operative MRI scans and are continuing to obtain 18-month MRI scans for study patients. Enrollment was initially slow. However, we addressed this issue by expanding the enrollment criteria and have received a one year no cost extension in order to complete all analyses. Sample collection and processing has been very successful, and we are pleased with the quantity of biosamples collected and MRI analyses.

The second aim of this study is to create closed tibial plateau fractures in the left knee of C57BL/6 mice that develop PTA and MRL/MpJ mice that are protected from PTA. Serum and synovial fluid will be collected from both strains at various time points. Biospecimens will be analyzed for markers of joint inflammation and degradation identified in the human knee following articular injury. Biomarkers will be correlated to joint pathology that will be assessed

from microCT and histology. The human and mouse biomarker profiles associated with PTA will be compared to assess correlations between them. We have successfully completed the short-term data collection (pre-fracture, 0, 1, 7 and 14 days post-fracture), including receiving animals, fracturing, sacrificing, and collection of biosamples. MicroCT and histologic analyses have also been completed for the short-term cohort. We have successfully completed the long-term data collection (8 weeks post-fracture), including receiving the animals, fracturing, sacrificing, and collection of biosamples. MicroCT and histologic analyses are completed.

The details of our progress to date are described below with each task outlined from the approved Statement of Work (SOW).

A. SPECIFIC AIM 1: TASKS

Task 1. Review and approval of IRB protocol (months 1-4) **[SAO, VBK] COMPLETED**
- Duke IRB application submitted on 05/31/2012
- Duke IRB application approved on 07/11/2012
- Amendment to Duke IRB protocol to expand enrollment criteria submitted on 05/06/2013
- Amendment to Duke IRB protocol to expand enrollment criteria approved on 05/17/2013

Task 2. USAMRMC Office of Research Protections review and approval of human use documents (months 1-6) **[SAO] COMPLETED**
- IRB application submitted to USAMRMC Office of Research Protections for review on 09/06/2012
- IRB application approved by USAMRMC Office of Research Protections on 09/21/2012
- Request to expand enrollment criteria was submitted with prior progress report on 04/09/2013
- Response from USAMRMC ORP HRPO received on 05/02/2013.
  - We were informed that the expanded enrollment criteria was not a substantive modification/amendment to our protocol and does not increase risk to subjects. Therefore, the only action needed was to amend the protocol and submit to our Duke IRB for expedited review/approval.

Task 3. Enroll 30 patients in study (months 4-18) **[SAO, FG, VBK] COMPLETED**
3a. Patients with closed unilateral articular fracture of the knee requiring operative treatment will be enrolled in study
3b. Biosamples (synovial fluid, blood, urine) will be collected at time of placing a temporizing spanning external fixator
- First patient enrolled on 12/19/2012 **[SAO]**
  - Synovial fluid, blood, urine processed and stored in -80° freezer **[FG, VBK]**
- Second patient enrolled on 03/06/2013 **[SAO]**
  - Synovial fluid, blood, urine processed and stored in -80° freezer **[FG, VBK]**
- Third patient enrolled on 06/19/2013 **[SAO]**
  - Synovial fluid, blood, urine processed and stored in -80° freezer **[FG, VBK]**
- Fourth patient enrolled on 07/03/2013 **[SAO]**
  - Synovial fluid, blood, urine processed and stored in -80° freezer **[FG, VBK]**
- Fifth patient enrolled on 07/18/2013 **[SAO]**
  - Synovial fluid, blood, urine processed and stored in -80° freezer **[FG, VBK]**
- Sixth patient enrolled on 07/23/2013 **[SAO]**
  - Synovial fluid, blood, urine processed and stored in -80° freezer **[FG, VBK]**
- Seventh patient enrolled on 07/25/2013 **[SAO]**
  - Synovial fluid, blood, urine processed and stored in -80° freezer **[FG, VBK]**
- Eighth patient enrolled on 08/23/2013 **[SAO]**
  - Synovial fluid, blood, urine processed and stored in -80° freezer **[FG, VBK]**

- Ninth patient enrolled on 09/12/2013 **[SAO]**
  - Synovial fluid, blood, urine processed and stored in -80° freezer **[FG, VBK]**
- Tenth patient enrolled on 10/29/2013 **[SAO]**
  - Synovial fluid, blood, urine processed and stored in -80° freezer **[FG, VBK]**
- Eleventh patient enrolled on 05/21/2014 **[SAO]**
  - Synovial fluid, blood, urine processed and stored in -80° freezer **[FG, VBK]**
- Twelfth patient enrolled on 05/29/2014 **[SAO]**
  - Synovial fluid, blood, urine processed and stored in -80° freezer **[FG, VBK]**
- Thirteenth patient enrolled on 06/05/2014 **[SAO]**
  - Synovial fluid, blood, urine processed and stored in -80° freezer **[FG, VBK]**
- Fourteenth patient enrolled on 06/10/2014 **[SAO]**
  - Synovial fluid, blood, urine processed and stored in -80° freezer **[FG, VBK]**
- Fifteenth patient enrolled on 06/25/2014 **[SAO]**
  - Synovial fluid, blood, urine processed and stored in -80° freezer **[FG, VBK]**
- Sixteenth patient enrolled on 06/19/2014 **[SAO]**
  - Synovial fluid, blood, urine processed and stored in -80° freezer **[FG, VBK]**
- Seventeenth patient enrolled on 09/04/2014 **[SAO]**
  - Synovial fluid, blood, urine processed and stored in -80° freezer **[FG, VBK]**
- Eighteenth patient enrolled on 09/25/2014 **[SAO]**
  - Synovial fluid, blood, urine processed and stored in -80° freezer **[FG, VBK]**
- Nineteenth patient enrolled on 12/03/2014 **[SAO]**
  - Synovial fluid, blood, urine processed and stored in -80° freezer **[FG, VBK]**
- Twentieth patient enrolled on 12/04/2014 **[SAO]**
  - Synovial fluid, blood, urine processed and stored in -80° freezer **[FG, VBK]**
- Enrollment closed **[SAO]**

Task 4. *V*isual analog pain score, the Knee injury and Osteoarthritis Outcome Score (KOOS), and the SF-36 will be completed within 2 weeks of injury. **[SAO] COMPLETED**
- Visual analog pain score, KOOS, and SF-36 for first patient was completed on 12/27/2012 **[SAO]**
- Visual analog pain score, KOOS, and SF-36 for second patient was completed on 03/06/2013 **[SAO]**
- Visual analog pain score, KOOS, and SF-36 for third patient was completed on 06/20/2013 **[SAO]**
- Visual analog pain score, KOOS, and SF-36 for fourth patient was completed on 07/01/2013 **[SAO]**
- Visual analog pain score, KOOS, and SF-36 for fifth patient was completed on 07/17/2013 **[SAO]**
- Visual analog pain score, KOOS, and SF-36 for sixth patient was completed on 07/22/2013 **[SAO]**
- Visual analog pain score, KOOS, and SF-36 for seventh patient was completed on 07/23/2013 **[SAO]**
- Visual analog pain score, KOOS, and SF-36 for eighth patient was completed on 08/23/2013 **[SAO]**
- Visual analog pain score, KOOS, and SF-36 for ninth patient was completed on 09/13/2013 **[SAO]**
- Visual analog pain score, KOOS, and SF-36 for ninth patient was completed on 09/13/2013 **[SAO]**
- Visual analog pain score, KOOS, and SF-36 for tenth patient was completed on 10/31/2013 **[SAO]**
- Visual analog pain score, KOOS, and SF-36 for eleventh patient was completed on 05/20/2014 **[SAO]**

- Visual analog pain score, KOOS, and SF-36 for twelfth patient was completed on 05/21/2014 **[SAO]**
- Visual analog pain score, KOOS, and SF-36 for thirteenth patient was completed on 05/28/2014 **[SAO]**
- Visual analog pain score, KOOS, and SF-36 for fourteenth patient was completed on 06/09/2014 **[SAO]**
- Visual analog pain score, KOOS, and SF-36 for fifteenth patient was completed on 06/13/2014 **[SAO]**
- Visual analog pain score, KOOS, and SF-36 for sixteenth patient was completed on 06/20/2014 **[SAO]**
- Visual analog pain score, KOOS, and SF-36 for seventeenth patient was completed on 09/02/2014 **[SAO]**
- Visual analog pain score, KOOS, and SF-36 for eighteenth patient was completed on 09/22/2014 **[SAO]**
- Visual analog pain score, KOOS, and SF-36 for nineteenth patient was completed on 11/25/2014 **[SAO]**
- Visual analog pain score, KOOS, and SF-36 for twentieth patient was completed on 12/04/2014 **[SAO]**

Task 5. Biosamples (synovial fluid, blood, urine) will be collected at time of definitive fixation of closed unilateral articular fracture of the knee requiring operative treatment. Timing of repair will be based on standard of care for treating the clinical injury. **[SAO, FG, VBK] COMPLETED**
- Biosamples from first patient collected at time of definitive fixation on 12/22/2012 **[SAO]**
    - Synovial fluid, blood, urine processed and stored in -80° freezer **[FG]**
- Biosamples from second patient collected at time of definitive fixation on 03/13/2013 **[SAO]**
    - Synovial fluid, blood, urine processed and stored in -80° freezer **[FG]**
- Patients 3 – 9 had definitive fixation at the baseline visit so a second set of biosamples was not collected. **[SAO]**
- Biosamples from the tenth patient collected at time of definitive fixation on 11/12/2013 **[SAO]**
    - Synovial fluid, blood, urine processed and stored in -80° freezer **[FG]**
- Biosamples from the fourteenth patient collected at time of definitive fixation on 06/17/2014 **[SAO]**
    - Synovial fluid, blood, urine processed and stored in -80° freezer **[FG]**
- Patients 11-13 and 15-20 had definitive fixation at the baseline visit so a second set of biosamples was not collected. **[SAO]**

Task 6. Post-operative follow-up of all patients (months 5-18) **[SAO] COMPLETED**
6a. Post-operative T1-rho MRI will be obtained
6b. Analysis of MRI T1-rho imaging of cartilage
- Post-operative MRI obtained from first patient on 01/30/2013 **[SAO]**
- Post-operative MRI obtained for second patient on 04/30/2013 **[SAO]**
- Post-operative MRI attempted for third patient on 08/06/2013; patient experienced claustrophobia associated with the MRI machine and may not return to study **[SAO]**
- Post-operative MRI not obtained for fourth patient because patient will have a total knee replacement; patient does not satisfy enrollment criteria and has been removed from the study **[SAO]**
- Post-operative MRI obtained for fifth patient on 11/01/2013 **[SAO]**
- Post-operative MRI obtained for sixth patient on 09/23/2013 **[SAO]**
- Post-operative MRI obtained for seventh patient on 09/26/2013 **[SAO]**

- Post-operative MRI not obtained for eighth patient because definitive fixation resulted in just an external fixation; patient does not satisfy enrollment criteria and has been removed from the study **[SAO]**
- Post-operative MRI obtained for ninth patient on 10/28/2013; patient withdrew from study so no further MRI will be obtained **[SAO]**
- Post-operative MRI obtained for tenth patient on 01/14/2014 **[SAO]**
- Post-operative MRI obtained for eleventh patient on 07/16/2014 **[SAO]**
- Post-operative MRI not obtained for twelfth patient; patient has been withdrawn from study due to non-compliance **[SAO]**
- Post-operative MRI not obtained for thirteenth patient; patient has been withdrawn from study due to non-compliance **[SAO]**
- Post-operative MRI obtained for fourteenth patient on 08/11/2014 **[SAO]**
- Post-operative MRI obtained for fifteenth patient on 08/15/2014 **[SAO]**
- Post-operative MRI obtained for sixteenth patient on 09/16/2014 **[SAO]**
- Post-operative MRI obtained for seventeenth patient on 11/21/2014 **[SAO]**
- Post-operative MRI obtained for eighteenth patient on 12/12/2014 **[SAO]**
- Post-operative MRI obtained for nineteenth patient on 03/06/2015 **[SAO]**
- Post-operative MRI obtained for twentieth patient on 07/07/2015 **[SAO]**
- Analysis of MRI scans with matched 18-month follow-up scans has been completed and reviewed by radiologist **[SAO]**

Task 7. 18-month follow-up of all patients (months 19-36) **[SAO] COMPLETED**
- 18-month follow-up MRI obtained for first patient on 07/10/2014 **[SAO]**
- 18-month follow-up MRI obtained for second patient on 09/24/2014 **[SAO]**
- 18-month follow-up MRI for fifth patient obtained on 02/04/2015 **[SAO]**
- 18-month follow-up MRI for sixth patient obtained on 03/25/2015 **[SAO]**
- 18-month follow-up MRI for seventh patient obtained on 03/23/2015 **[SAO]**
- 18-month follow-up MRI for tenth patient will not be obtained; patient has withdrawn from study due to relocation outside the area **[SAO]**
- 18-month follow-up MRI for eleventh patient obtained on 12/01/2015 **[SAO]**
- 18-month follow-up MRI for fifteenth patient obtained on 02/16/2016 **[SAO]**
- 18-month follow-up MRI for patients 3-4, 8-9, and 12-13 will not obtained for reasons listed in Task 6 **[SAO]**
- 18-month follow-up MRI for patients 14, 16-20 not obtained due to non-compliance **[SAO]**
- Analysis of MRI scans with matched post-operative scans has been completed and reviewed by radiologist **[SAO]**

Task 8. Perform assays of biosamples to assess acute levels of inflammatory and injury markers (months 18-30) **[VBK] COMPLETED**
- All samples have been transferred to Kraus lab **[FG, VBK]**
- Selection of markers and assay panels has been completed **[VBK]**
- Serum and synovial fluid assayed using inflammatory and injury multiplex array **[VBK]**
- Initial analysis of serum and synovial fluid has been completed **[VBK]**
- Statistical analyses for serum and synovial fluid has been completed **[VBK, SAO]**

*Task 9.* Submit samples for proteomics analysis (months 24-30) **[SAO, VBK] COMPLETED**
- All samples have been transferred to Kraus lab **[SAO, FG, VBK]**
- Selection of targeted proteomics and discovery metabolomics completed **[VBK, SAO]**
- Serum samples submitted for targeted proteomic panel **[VBK]**
- Synovial fluid samples submitted for discovery metabolomics on 01/13/2016 **[VBK, SAO]**

- Discovery metabolomics data received on 03/24/2016 **[VBK, SAO]**
- Additional analyses requested from Metabolon and received on 06/10/2016 **[VBK, SAO]**
- Statistical analyses for targeted proteomics and discovery metabolomics has been completed **[VBK, SAO]**

B. SPECIFIC AIM 1: SUPPORTING DATA

For assessment of degenerative changes to joint tissues, post-operative (post-op) and 18-month follow-up MR scans were evaluates. Sagittal MR images were obtained using a double-echo steady state sequence (DESS; TR: 17 ms; TE: 6 ms; FOV: 15 x 15 cm; Matrix: 512 x 512; Thickness: 1 mm) on a 3.0 T MR scanner (Siemens Healthcare, Malvern, PA).   The outer margin of the patella bone cortex and the surface of the articular cartilage of the patella were outlined from the DESS MR images using solid-modeling software (Rhinoceros, Robert McNeel and Associates, Seattle, WA)[4,5]. Next, each outline was placed in the appropriate spatial plane so that the curves could be compiled to generate 3D surface models of the patella and patellar cartilage (Geomagic Studio, Research Triangle Park, NC). Changes in cartilage thickness between post-operative and 18-month follow-up images were quantified using an in-house analysis program (Wolfram Mathematica, Champaign, IL).

The effect of metal hardware used to fix the articular fracture was evident in the scans, and it obscures the tibial plateau articular surface (**Figure B1**, black shadow). However, the articular cartilage in the patella was clearly visible at the patella-femoral joint. The articular cartilage surface of the patella is outlined in green on sagittal images from both the post-op and 18-month MRI scans in **Figure B1**. Thickness maps of the patella cartilage demonstrate regions of cartilage thinning at 18 months compared to post-operative scans (**Figure B2**). Changes in cartilage thickness were quantified by creating a grid of eleven 2.5 mm radius sampling points spanning the articular surface of the patella (**Figure B3**).

| Post-Operative MRI | 18-Month MRI |
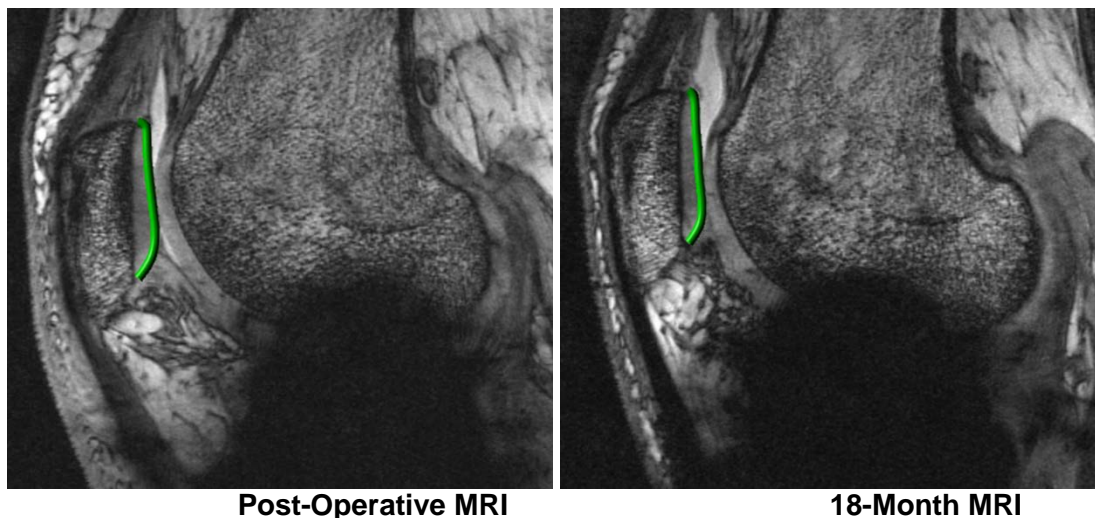
Figure B1. Sagittal view of PTA002 MRI scans. Green outline indicates articular cartilage surface of the patella in both images.
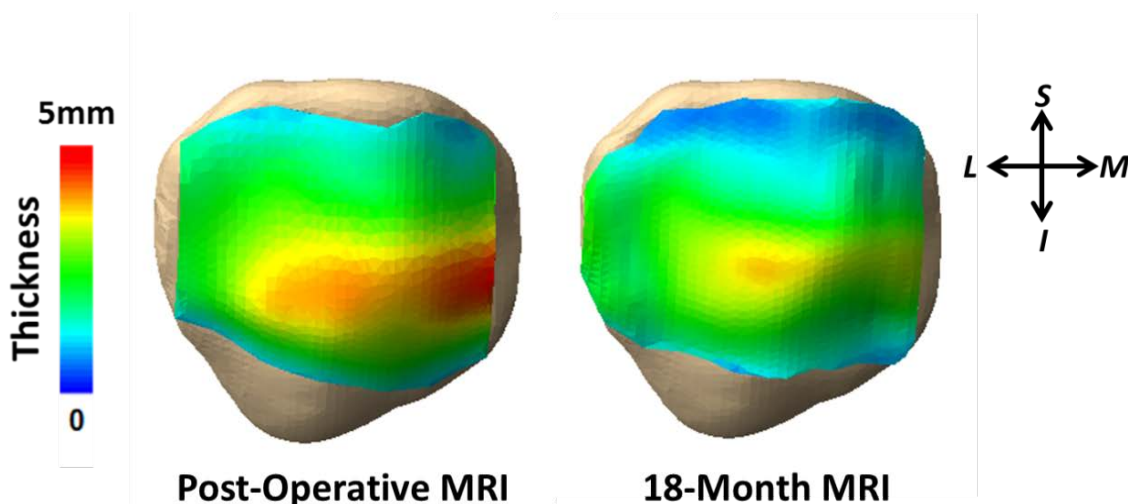
Figure B2. Patella cartilage thickness map of post-operative and 18-month follow-up MRI scans for subject PTA002.
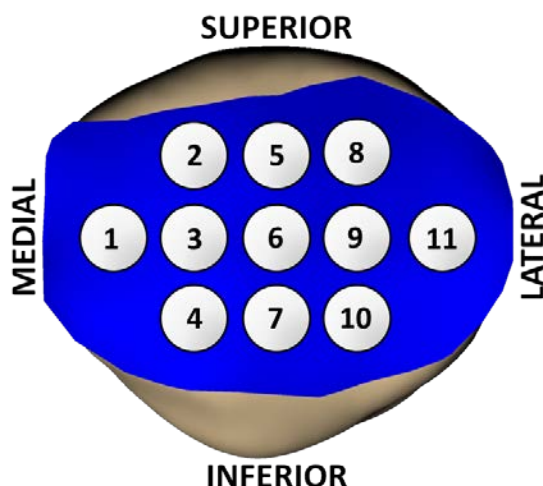
Figure B3. Patella cartilage grid system used to measure localized cartilage thickness changes between the post-operative and 18-month follow-up MRI scans.

Multiplex ELISA assays were used to quantify acute inflammatory and injury markers (40 analytes) in serum and synovial fluid as well as markers of joint degradation including matrix metalloproteinase (MMP)-1, -2, -3, -9, -10, and cartilage oligomeric matrix protein (COMP) in serum and synovial fluid, sulfated glycosaminoglycans (sGAG) in synovial fluid, C-terminal telopeptide of type II collagen (CTXII) in synovial fluid and urine, and markers of bone metabolism (C-terminal telopeptide of type I collagen (CTXI), osteocalcin, osteopontin, and osteonectin) in serum (Table 1). Additionally, a targeted proteomics panel (designed by the Kraus laboratory to identify knee osteoarthritis progressors) was used to assess serum in this cohort. The targeted panel will quantify 20 analytes in sera via mass spectrometry-based multiple reaction monitoring (MRM).

Synovial Fluid Analysis Reveals a Novel Panel of Vascular and Inflammatory Biomarkers that are Altered Following Articular Fracture
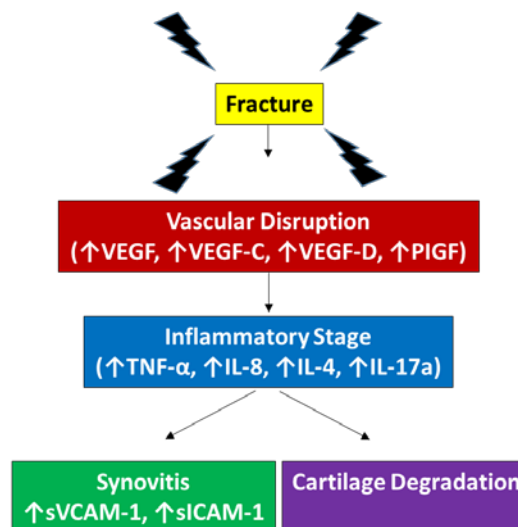
Of the 20 subjects enrolled, eight patients (50% female; 25-83 years of age; average BMI 32.4 kg/m^2) had synovial fluid collected by direct aspiration from both the fractured (Fx) and contralateral non-fractured (Non-Fx) knee. ELISA assays were used to quantify synovial fluid levels of 40 acute inflammatory and injury markers as well as markers of joint metabolism. Joint tissue markers included matrix metalloproteinases (MMP)-1,-2,-3,-9, and -10, sulfated glycosaminoglycans, and C-terminal telopeptide of type II collagen. Paired t-tests were used to test the differences of biomarkers in synovial fluid between the injured limb (Fx) and the contralateral control limb (non-Fx) and corrected for using the Benjamini-Hochberg (BH) method. We identified 16 out of 48 biomarkers meeting BH adjusted p-value <0.05. Ingenuity Pathway Analysis was used to identify pathways of relevance.

Comparisons of biomarker concentrations in SF from Fx and non-Fx knees identified 16 analytes of the 48 measured having significantly higher concentrations in SF from the fractured knee. These biomarkers were associated with inflammatory response (14 of 16) and injury (15 of 16) and are associated with molecular events following fracture. Upon injury, vascular disruption occurs resulting in the release of biomarkers of angiogenesis (VEGF, VEGF-C, VEGF-D, PIGF) which upregulate the expression of MMPs. This is followed by an inflammatory stage in which macrophages and other immune cells are recruited to the fracture sites and secrete pro-inflammatory cytokines (IL-4, IL-8, IL17a, TNF-α), resulting in synovitis and eventual cartilage degradation.

Biomarker	Fold Change (Fx/NonFx)	p-value	Adjusted p (BH FDR)
Tie-2	2.42	0.000144	0.00386
VEGF	8.06	0.000158	0.00386
TNF-α	2.32	0.000734	0.01199
MMP-10	2.72	0.001563	0.01603
ICAM-1	2.28	0.001636	0.01603
IL-8	17.65	0.002963	0.02055
MMP-2	1.39	0.003521	0.02055
MMP-3	1.92	0.003666	0.02055
Flt1	10.48	0.003845	0.02055
VEGF-D	2.09	0.004194	0.02055
PIGF	5.24	0.008368	0.03417
IL-4	26.2	0.013848	0.04860
VCAM-1	1.9	0.014273	0.04860
IL17a	2.59	0.015459	0.04860
VEGF-C	6.11	0.01587	0.04860
Eotaxin	1.96	0.017224	0.04965

Table B1. Synovial fluid biomarkers significantly upregulated by injury.

Upon injury, the articular surface is exposed to inflammatory cytokines and chemokines that may play a role in the development of PTA. Of those identified herein, members of the VEGF family may be indicative of inflammation and are essential to fracture healing and induce soluble Tie-2. TNF-α is a known acute phase inflammatory mediator, IL-8 plays a chemoattractant role in guiding neutrophils through the tissue matrix to the site of injury, and IL-17 promotes joint inflammation and cartilage degradation by enhancing production of pro-inflammatory cytokines and chemokines as well as upregulating the expression of MMPs. Soluble VCAM-1 and ICAM-1 were reported to correlate with synovitis as determined by MRI. Presently, surgical restoration of the articular surface is the only treatment for articular fractures. Adjunctive therapies to surgery may be required to improve outcomes and reduce the prevalence of PTA. Identification of the inflammatory mediators involved in acute injury may provide key insights into potential adjunctive therapies that could improve outcomes following surgery. The patterns of biomarkers following acute injury may aid in identifying those at highest risk for developing PTA.


Figure BX. Model of molecular events following articular fracture.

Finally, discovery metabolomics were run on synovial fluid from this cohort. 710 distinct metabolites were identified from the synovial fluid of patients in both the injured and uninjured limb, when available, and analyses were performed to identify prominent pathways involved in the development of post-traumatic arthritis.

Sphingolipid Metabolites are Upregulated in Human Synovial Fluid Following Articular Fracture

Of the 20 subjects enrolled, eight patients had synovial fluid collected without dilution from both the fractured (Fx) and contralateral non-fractured (Non-Fx) knee. High throughput characterization of the global metabolic profile of synovial fluid samples from both knees of each patient was performed using Ultrahigh Performance Liquid Chromatography-Tandem Mass Spectroscopy (UPLC-MS/MS). Each biochemical analyte was rescaled to set the median equal to 1. Paired t-tests were used to test the differences of biomarkers in synovial fluid between the injured limb and the contralateral control limb. The Benjamini-Hochberg (BH) method was used to control for false discovery rate (FDR) due to multiple testing. We identified 220 out of 710 metabolites meeting BH adjusted p-value < 0.05.

Among the top 19 metabolites most significantly elevated in synovial fluid from the fractured knee (p<0.0002, BH adjusted p = 0.0065), a prominent metabolic pathway involved was complex lipid composition. Evidence of increased sphingomyelin (SPM) synthesis was observed with increases in SPMs (**Figure BX**) and 2-hydroxy- fatty acids that are specialized fatty acids found in SPMs. In addition to accumulation of sphingomyelins, elevated levels of various phospholipid derivatives were also observed in the injured knee relative to the contralateral control limb. Although phospholipids are implicated in joint lubrication, sphingomyelin has been shown to progressively increase in the synovial fluid of, early-stage and late-stage patients with osteoarthritis.[6]
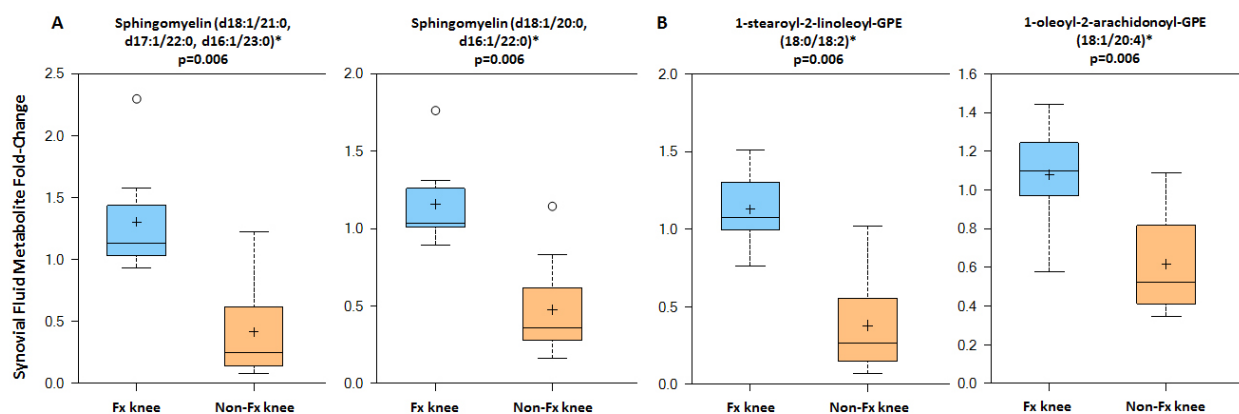
Figure BX. Fractured (Fx) knees showed significant fold increases in (**A**) sphingomyelin and (**B**) phospholipid metabolites following articular fracture.

To date, there are no clinical methods to identify patients at high risk for developing PTA following intra-articular fracture or other joint injuries. Early identification of disease progression in PTA would be valuable for selecting high-risk patients as candidates for interventional therapies and for better understanding of the mechanism of disease progression. This study demonstrates that that altered lipid metabolism could be a risk factor and/or consequence of knee injury. Sphingolipids have been previously identified in synovial fluid [7] and are a class of lipids that include sphingomyelins, ceramide species, and more complex glycosphingolipids. Recent reports on lipidomic analyses of synovial fluid have shown an association of increased sphingomyelin with progression of OA [6] and also altered lipid profiles in synovial fluid following articular fracture in the ankle. [8] Understanding of lipid compositional changes in synovial fluid following joint injury may provide insight into pathologic changes in articular cartilage associated with PTA, as well as potential markers of disease onset and progression. Taken together with the literature, these findings suggest that elevated sphingomyelins, phospholipids, and subsequent lipid metabolites in synovial fluid are biomarkers of knee injury and potential prognostic indicators of risk of post-traumatic arthritis. Further follow-up on the clinical outcomes are necessary to determine the relationships between these biomarker levels and PTA.

C. SPECIFIC AIM 2: TASKS
Task 1. Review and approval of animal protocol (months 1-4) **[FG] COMPLETED**
- Duke IACUC application submitted on 07/02/2012
- Duke IACUC application approved on 07/25/2012
- Duke certification of IACUC Review and Approval/Grant concordance received on 08/21/2012
- Amendment to Duke IACUC to allow use of live microCT scanning submitted 06/10/2013.
- Amendment to Duke IACUC to allow use of live microCT scanning approved 07/17/2013.

Task 2. USAMRMC Office of Research Protections review and approval of animal use documents (months 1-4) **[FG] COMPLETED**
- ACURO animal use appendix submitted to USAMRMC Office of Research Protections for review on 08/29/2012
- Received ACURO approval letter on 11/29/2012
- Amendment to allow use of live microCT scanning submitted to ACURO 08/12/2013.
- Amendment to allow use of live microCT scanning approved to ACURO 08/20/2013.

Task 3. Obtain mice and create closed intra-articular fracture of the left knee of mice (months 5-9) **[FG] COMPLETED**

      3a. Obtain C57BL/6 and MRL/MpJ mice at 8 weeks of age
- 60 mice were ordered on 01/07/2013 **[FG]**
  - 30 C57BL/6 mice were received at 9 weeks of age on 01/16/2013 **[FG]**
  - 30 MRL/MpJ mice were received at 10 weeks of age on 01/24/2013 **[FG]**
- Replacement C57BL/6 mice were ordered after receiving credit for 12 mice on 05/13/2013 **[FG]**
  - 12 C57BL/6 mice were received at 10 weeks of age on 05/22/2013 **[FG]**
  - 2 C57BL/6 mice died due to unidentified health reasons on 05/26/2013 **[FG]**
  - 2 replacement C57BL/6 mice were received after credit on 08/07/2013 **[FG]**

      3b. Allow mice to mature to 16 weeks of age
- Mice (30 MRL/MpJ and 18 C57BL/6) were housed until 03/04/2013 **[FG]**
- 10 C57BL/6 mice were housed until 07/17/2013 **[FG]**

      3c. Create closed intra-articular fractures in the left knee of mice
- Fractures were created 03/05/2013 – 03/13/2013 **[FG]**
- Fractures (n=6) were created on 07/17/2013 **[FG]**

Task 4. Sacrifice mice and harvest samples for analyses (months 10-11) **[FG] COMPLETED**

      4a. Sacrifice mice at pre-fracture, 0, 1, 7 and 14 days
      4b. Collect serum and synovial fluid at time of sacrifice and store at -80°
      4c. Harvest both hind limbs for analyses, store at -20°
- Mice were sacrificed (MRL/MpJ at pre-fracture, 0, 1, 7 and 14 days post-fracture and C57BL/6 at 0,1, and 7 days post-fracture) on 03/04/2013 – 03/27/2013 **[FG]**
  - Serum and synovial fluid were collected at time of sacrifice and stored at -80° **[FG, VBK]**
  - Both hind limbs were harvested at time of sacrifice and stored at -20° **[FG, VBK]**
- Mice were sacrificed (C57BL/6 at pre-fracture & 14 days post-fracture) on 07/31/2013 **[FG]**
  - Serum and synovial fluid were collected at time of sacrifice and stored at -80° **[FG, VBK]**
  - Both hind limbs were harvested at time of sacrifice and stored at -20° **[FG, VBK]**
- Mice were sacrificed (C57BL/6 at pre-fracture) on 08/08/2013. **[FG]**
  - Serum and synovial fluid were collected at time of sacrifice and stored at -80° **[FG, VBK]**
  - Both hind limbs were harvested at time of sacrifice and stored at -20° **[FG, VBK]**

Task 5. Perform microCT analyses on hind limbs (months 12-18) **[FG] COMPLETED**
- Limbs were scanned 09/04/2013-09/09/2013 **[FG]**
- Data processing and analysis complete for both hind legs **[FG]**

Task 6. Perform histologic analyses on hind limbs (months 18-24) **[FG] COMPLETED**
- Limbs were decalcified, dehydrated, and embedded in paraffin for histology **[FG]**
- Histologic grading and statistical analyses complete for both hind legs **[FG]**

Task 7. Obtain 24 additional mice and create closed intra-articular fracture of the left knee of mice (month 12-16) **[FG] COMPLETED**

      7a. Obtain 12 C57BL/6 mice and 12 MRL/MpJ mice at 8 weeks of age
- 24 mice were ordered on 07/29/2013 **[FG]**
  - 12 C57BL/6 mice were received at 9 weeks of age on 08/07/2013
  - 12 MRL/MpJ mice were received at 8 weeks of age on 08/15/2013
  - 2 C57BL/6 mice died due to unidentified health reasons on 08/13/2013 **[FG]**

- 2 replacement C57BL/6 mice were received after credit on 08/28/2013 **[FG]**
  7b. Allow mice to mature to 16 weeks of age **[FG]**
  7c. Create closed intra-articular fractures in the left knee of mice **[FG]**

Task 8. Sacrifice mice and harvest samples for analyses (months 17-18) **[FG, VBK]**
COMPLETED
  8a. C57BL/6 mice and MRL/MpJ mice were sacrificed at 56 days post-fracture **[FG]**
  8b. Collected serum and synovial fluid at time of sacrifice and stored at -80° **[FG, VBK]**
  8c. Both hind limbs were harvested and stored at -20° **[FG]**

Task 9. Perform microCT analyses on hind limbs (months 19-24) **[FG] COMPLETED**
  ▪ Limbs were scanned ex-vivo **[FG]**
  ▪ Data processing and analyses complete for both hind legs **[FG]**

Task 10. Perform histologic analyses on hind limbs (months 25-32) **[FG] COMPLETED**
  ▪ Samples processed, section and stained **[FG]**
  ▪ Histologic grading and statistical analyses complete for both hind legs **[FG]**

Task 11. Determine biomarkers from Aim 1 that should be added to mouse biomarker analysis (months 30-32) **[SAO, FG, VBK] COMPLETED**
  ▪ Biomarkers were selected based on results from Aim 1 and previous studies **[VBK]**

Task 12. Perform assays to assess levels of markers (months 32-36) **[VBK] COMPLETED**
  ▪ Concentrations of bone biomarkers were quantified in longitudinal serum collected from second group of C57BL/6 and MRL/MpJ mice **[VBK]**
  ▪ Selection of markers and assay panels has been completed **[VBK]**
  ▪ Serum biomarkers: MMP-3, VEGF, VCAM-1, TIMP1, MCP-1, IP10, pro-inflammatory panel (IFN-γ, IL-1β, IL-2, IL-4, IL-5, IL-6, KC (IL-8), IL-10, IL-12p70, TNF-α) have been completed **[VBK]**
  ▪ Synovial fluid biomarkers: MMP-3, VEGF, VCAM-1 have been tested for feasibility and the proinflammatory panel (IFN-γ, IL-1β, IL-2, IL-4, IL-5, IL-6, KC (IL-8), IL-10, IL-12p70, TNF-α) and TIMP1 have been completed **[VBK]**
  ▪ Serum and synovial fluid assayed using inflammatory and injury multiplex array **[VBK]**
  ▪ Initial analysis of serum and synovial fluid has been completed **[VBK]**
  ▪ Statistical analyses for serum and synovial fluid has been completed **[VBK, SAO]**

  D. SPECIFIC AIM 2: SUPPORTING DATA

Bone Morphological Changes Correlate with Reduction in PTA after Articular Fracture in the MRL/MpJ Mouse
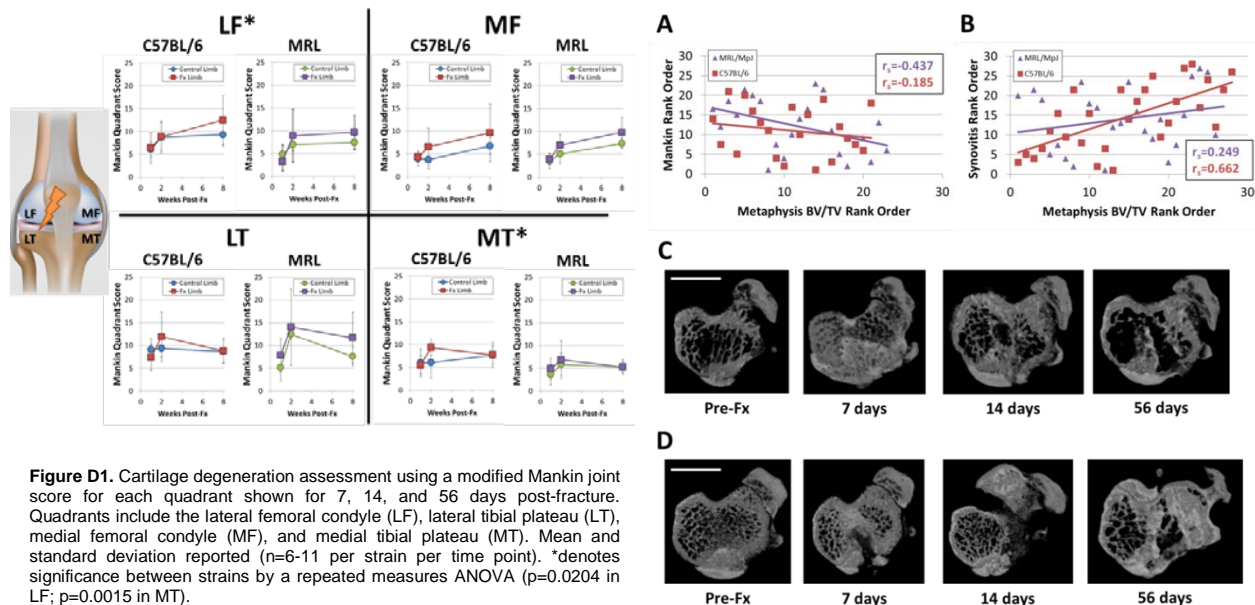The objective was to identify differences in acute joint pathology and degeneration in the articular cartilage as well as other joint tissues, including the synovium and periarticular bone following articular fracture in C57BL/6 and MRL/MpJ mice.

Six mice from each strain (C57BL/6 and MRL/MpJ) did not receive a fracture and served as pre-fracture controls. Mice were sacrificed at 0, 1, 7, 14, and 56 days after fracture (n=6-11 per strain per time point). The left (fractured) and right (non-fractured) limbs were harvested, formalin fixed and scanned with microCT to assess bone morphology in the tibial epiphysis and metaphysis and femoral condyles. Histology sections (FFPE, 8µm thick in coronal plane) of all limbs were assessed for cartilage degeneration in the lateral and medial femoral condyles (LF, MF) and lateral and medial aspects of the tibial plateau (LT, MT) using a modified Mankin score, synovial inflammation using a modified synovitis score with semi-quantitative scales, and

15

osteophyte score. Parametric analyses were performed for bone morphological measures and histological assessment.

Mankin scores of cartilage degeneration (**Figure D1**) were significantly greater in the C57BL/6 strain compared to the MRL/MpJ strain in both the lateral femur (p=0.0204) and the medial tibia (p=0.0015). Subchondral bone thickening was significantly increased in the C57BL/6 mice compared to the MRL/MpJ mice in the medial femur (p=0.03) and the medial tibia (p=0.01), but not on the lateral side. Bone morphological changes in response to fracture were significantly different between the two mouse strains. In the fractured limbs, bone mineral density (BMD), bone volume (BV), and bone fraction (BV/TV) in both the tibial epiphysis and metaphysis were significantly greater (p<0.002) in the MRL/MpJ strain compared to the C57BL/6 strain (p<0.001). However, in the femoral condyles, both BMD and cancellous bone fraction (BV/TV) were significantly increased in the C57BL/6 strain compared to the MRL/MpJ strain (p=0.0001).

Correlations of the histological parameters with the bone morphological parameters (**Figure D2**) showed that in tibial metaphyseal region, the Mankin total joint score negatively correlated with both the BMD (r_s=-0.453, p=0.03) and BV/TV (r_s=-0.437, p=0.04) in the MRL/MpJ strain, but did not correlate with any bone parameters in the C57BL/6 strain. The synovitis total joint score in the fractured limb positively correlated with both the BMD (r_s=0.658, p=0.0001) and BV/TV (r_s=0.662, p=0.0001) in the C57BL/6 strain, but not in the MRL/MpJ strain.

Figure D1. Cartilage degeneration assessment using a modified Mankin joint score for each quadrant shown for 7, 14, and 56 days post-fracture. Quadrants include the lateral femoral condyle (LF), lateral tibial plateau (LT), medial femoral condyle (MF), and medial tibial plateau (MT). Mean and standard deviation reported (n=6-11 per strain per time point). *denotes significance between strains by a repeated measures ANOVA (p=0.0204 in LF; p=0.0015 in MT).

Figure D2. Correlations between Mankin total joint score, synovitis total joint score, and bone fraction (BV/TV) of the tibial metaphysis for both the MRL/MpJ and C57BL/6 strains (rank order within strain for each outcome measure, n=21-28 per strain) with Spearman correlation (R_s). **(A)** Mankin correlated with BV/TV (r_s=-0.437, p=0.0370) in MRL/MpJ strain only. **(B)** Synovitis correlated with BV/TV (r_s=0.662, p=0.0001) in C57BL/6 strain only. **(C-D)** Representative images of tibial metaphysis for **(C)** C57BL/6 strain and **(D)** MRL/MpJ strain at each time point. Scale bar is 0.5mm.

DISCUSSION: The inflammation profiles of these two mice strains differ greatly, which may account for the difference in healing after articular fracture. MRL/MpJ mice are reported to have increased levels of TGF-β_1, which may contribute to the enhanced bone response following fracture found in this study. Interestingly, synovitis in the C57BL/6 mice was associated with greater bone changes. Previous reports have shown that C57BL/6 mice have elevated levels of pro-inflammatory cytokines IL-1 and TNF-α following joint injury. An increased local inflammatory environment may contribute to altered bone morphology and subsequent degenerative changes in the joint tissues. The difference in these arthritic profiles indicates that there may be a benefit to focusing first on fracture healing, then following up with suppression of the pro-inflammatory environment that

leads to subsequent degradation of the joint. Targeted treatment needs to look at all of the joint tissues instead of focusing on a single tissue

SIGNIFICANCE: By characterizing degenerative changes in the C57BL/6 and MRL/MpJ strains, key factors that contribute to the development of PTA can be identified. By understanding what drives disease progression, potential screening methods may be developed to identify patients at high risk of developing PTA.

Novel *In Vivo* Micro-Computed Tomography Metrics of Joint Incongruity in the Mouse Knee Fracture Model

In vivo micro-CT scanning (SkyScan 1176, Bruker) of fractured limbs was performed before and after fracture, and then at 1, 4, and 8 weeks post-fracture. Bone surface deviations (BSD) were measured for all post-fx micro-CT scans. First, surface-rendered 3D digital models of the tibial plateau were generated from *in vivo* scans (CT-Analyser, Bruker). Models were then aligned to their respective pre-fx model's intact medial tibial plateau using an iterative closest point algorithm (Geomagic Studio, Geomagic®). BSDs were measured separately for the medial and lateral sides of the tibial plateau along three anatomic axes: antero-posterior (AP), latero-medial (LM), and axial (Geomagic Control, Geomagic®). Positive and negative deviations of the bone surface were measured, and defined as the distance to a test surface (post-fx bone surface) that was either outside (positive) or inside (negative) of the reference surface (pre-fx bone surface). A deviation of 0% corresponded to perfect alignment of pre-fx and post-fx tibial plateaus. Color maps of BSDs were generated for each anatomical direction. An example of axial deviations in an MRL/MpJ mouse from post-fx to 8 weeks is shown in **Figure D3**. Blood was collected pre-fracture, post-fracture on day 4, and every 2 weeks to 6 weeks post-fracture. Serum concentrations of biomarkers of bone metabolism were measured, including procollagen type I N-propeptide (PINP), a bone formation marker and C-terminal telopeptide of type I collagen (CTXI), a bone resorption marker.

Temporal patterns in BSDs were significantly different between C57BL/6 and MRL/MpJ mice over 8 weeks (**Figure D3**). Significant differences were observed in the lateral tibial plateau as measured by average positive axial deviation ($p = 0.01$), average positive LM deviation ($p = 0.015$), and maximum positive LM deviation ($p = 0.01$). Additionally, a significantly larger average positive axial deviation was observed in C57BL/6 mice at 8 weeks post-fx ($p=0.01$) (**Figure D4**). In the medial plateau, significant differences were seen between strains as measured by average positive axial deviation ($p=0.049$) and average negative LM deviation ($p=0.049$). Concentrations of PINP in the C57BL/6 mice were significantly lower than the MRL/MpJ mice post-fx ($p=0.005$; **Figure D5**), indicating a less robust acute bone anabolic response compared with the superhealer strain. Despite higher levels of CTXI in the C57BL/6 mice compared to the MRL/MpJ at pre-fx, no differences were found in CTXI levels post-fx between strains or at any other time point.

17
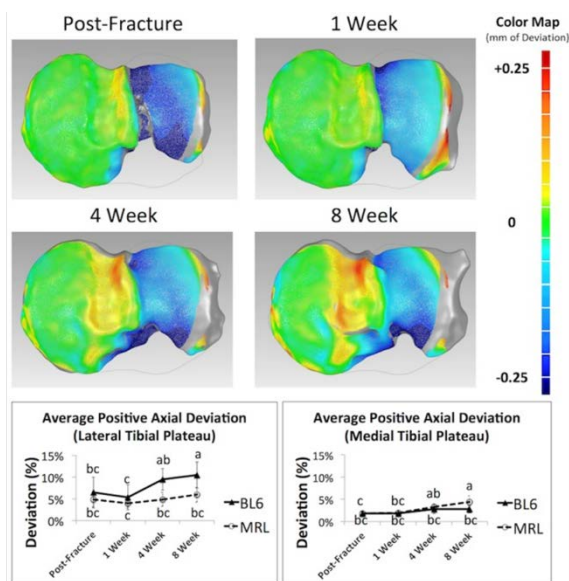
Figure D3. (Top) Representative color map of axial deviation with fracture healing. (Bottom) Significant strain-wise differences in fracture healing to 8 weeks post-fracture *(data with different letters are significantly different).*
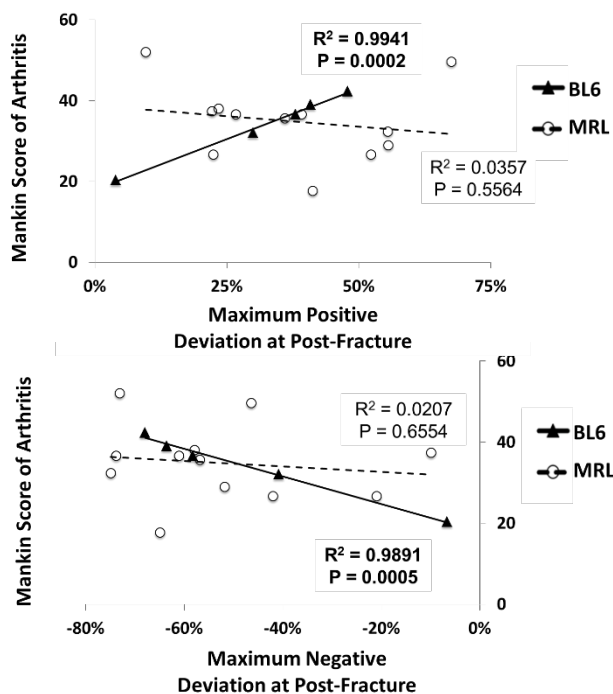
Figure D4. Correlations between total joint Mankin score for arthritis at 8 weeks post-fracture and post-fracture joint incongruity for C57BL/6 (BL6) and MRL/MpJ (MRL) mice.
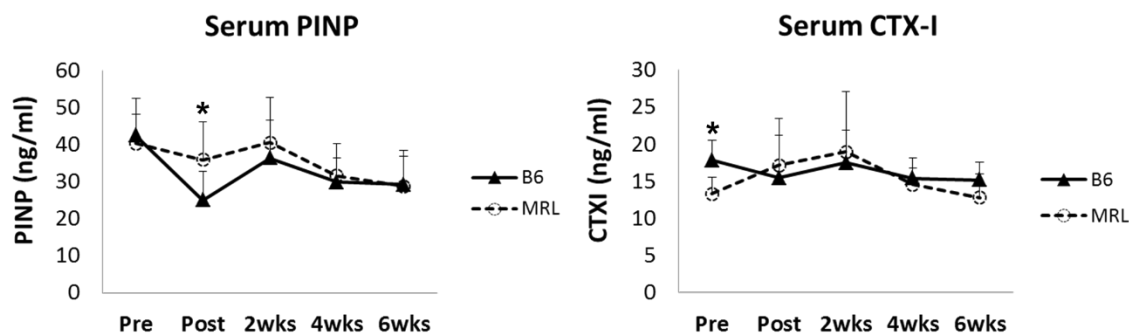
Figure D5. Serum concentrations of bone biomarkers PINP and CTX-I with articular fracture in C57BL/6 (B6) and MRL/MpJ (MRL) mice.

DISCUSSION: Through the development of novel *in vivo* micro-CT metrics of joint incongruity, we analyzed temporal patterns in bone surface deviations that revealed significant differences between C57BL/6 and MRL/MpJ strains over 8 weeks. Acute displacements of the bone surface following articular fracture were predictive of arthritis development in the C57BL/6 but not MRL/MpJ mice. Interestingly, after 8 weeks of fracture healing, we observed significantly larger bone surface deviations in C57BL/6 mice compared to MRL/MpJ mice. Additionally, C57BL/6 mice showed an acute drop in serum PINP following articular fracture compared to MRL/MpJ mice. These results indicate a less robust acute bone anabolic response compared with MRL/MpJ superhealer strain. Previous studies reported that C57BL/6 mice exhibit higher levels of inflammation post-fracture than the MRL/MpJ mice and suggested that this may contribute to the development and progression of PTA in this model. This inflammatory environment may influence fracture healing immediately post-fx, potentially predisposing C57BL/6 mice to PTA. These findings suggest that joint incongruities secondary to articular fracture alone do not predispose mice to the development of PTA, but rather differences in bone metabolism may

18

play a role in early healing, which may have a greater effect on outcome. Our results may provide insights into the physiologic processes determining PTA outcomes that may protect the MRL/MpJ strain from the effects of articular incongruity.

SIGNIFICANCE: Our results provide evidence that the MRL/MpJ superhealer strain is able to overcome the effects of articular incongruity. More work is needed to translate the MRL/MpJ healing response into clinical therapies. *In vivo* micro-CT metrics of joint incongruity provide a method for quantifying bone surface incongruities that have traditionally been difficult to measure and provide new possibilities to guide PTA research and improve fracture management. The translational potential of our joint incongruity metrics is high, as this methodology could be applied to full scale clinical CT scans.

Identification of Biomarkers Indicative of Synovitis in the Mouse Articular Fracture Model of PTA

Male C57BL/6 and MRL/MpJ mice (n=83) were subjected to an articular fracture at 16 weeks of age using an established model. Six mice from each strain did not receive a fracture and served as pre-fracture controls. Mice were sacrificed at 0, 1, 7, 14, and 56 days after fracture (n=6-11 per strain per time point) at which time blood was collected. The left (fractured; Fx) and right (non-fractured; Non-Fx) limbs were harvested. Histology sections (FFPE, 8μm thick in coronal plane) of all limbs were evaluated by three blinded graders for synovial inflammation at the synovial insertion of the lateral tibia, lateral femur, medial tibia, and medial femur and summed, using a modified form of an established standardized, semi-quantitative synovitis score. ELISA assays were used to quantify serum biomarkers including pro-inflammatory cytokines (IFN-γ, IL-1β, IL-2, IL-4, IL-5, IL-6, KC, IL-10, IL-12p70, TNFα), MMP-3, TIMP-1, and VCAM-1. Non-parametric analyses were performed to assess differences in synovitis between Non-Fx and Fx limbs as well as differences in synovitis and biomarkers between strains. Spearman correlations were performed to assess the association of biomarkers with synovitis scores.

Articular fracture was associated with an increase in synovial inflammation in both mouse strains. Compared to the non-fractured contralateral limb at baseline, there were significant increases in synovitis in the fractured limb in the C57BL/6 mice at 7, 14, and 56 days post-fracture, but only at 14 days post-fracture (p<0.05) for the MRL/MpJ strain (Figure 1). Serum concentrations of multiple biomarkers were significantly higher in the C57BL/6 strain: KC (14 and 56 days), MMP-3 (4 hours and 7 days), and VCAM-1 (14 and 56 days). In contrast, serum IL-6 and TIMP-1 (1, 14, and 56 days) were higher post-Fx in the MRL/MpJ strain. Compared to the MRL/MpJ strain, the ratio of MMP-3 to TIMP-1 was significantly higher in the C57BL/6 strain at 1 (p=0.03), 7 (p=0.004), 14 (p=0.002), and 56 days post-Fx (p=0.0008), indicating higher levels of degradation in this strain (Figure 2). Synovitis in the fractured limb was significantly positively correlated with IL-1β (r_s=0.35; p=0.01), IL-6 (r_s=0.29; p=0.04), MMP-3 (r_s=0.54; p<0.0001), and TIMP-1 (r_s=0.35; p=0.01), and significantly negatively correlated with CXCL1/KC (r_s=-0.31; p=0.03), an IL-8 functional homologue. Interestingly, the MMP-3/TIMP-1 ratio was significantly correlated with synovitis of the fractured limb of the C57BL/6 strain (p=0.004).

DISCUSSION: It has become clear that the tissues of the entire joint organ contribute to OA development and contribute to PTA development. Synovitis occurs acutely after injury in both the PTA-susceptible (C57BL/6) and PTA-resistant (MRL/MpJ) strains. Whereas the histological synovitis scoring was unable to distinguish differences between strains, serum analyses revealed higher levels of multiple inflammatory biomarkers and mediators of joint degradation in the PTA-susceptible, C57BL/6 strain. Moreover, the MMP-3/TIMP-1 ratio was strongly
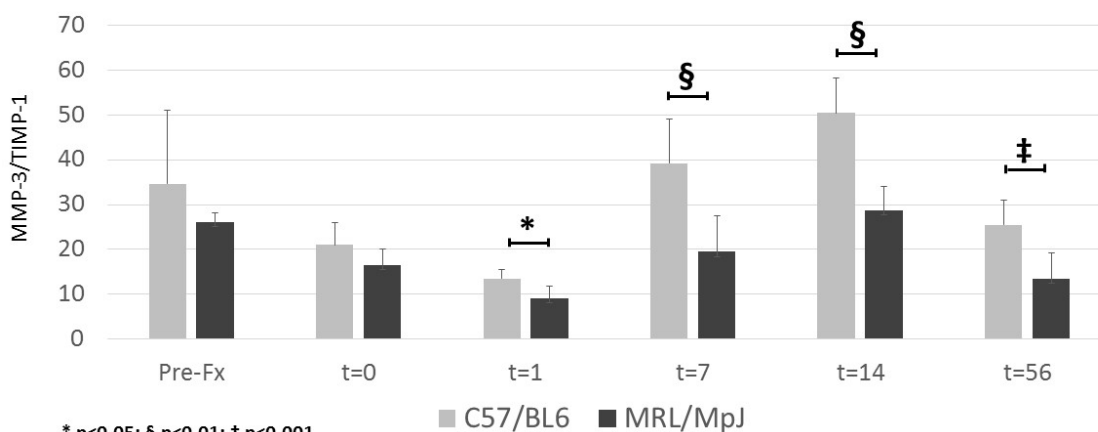
correlated with synovitis in the C57BL/6 strain, indicating its ability to identify a degradative synovial phenotype. These biomarkers should be useful for monitoring the destructive and inflammatory responses that result in the development of OA.

Figure 1. Synovitis Score by Limb
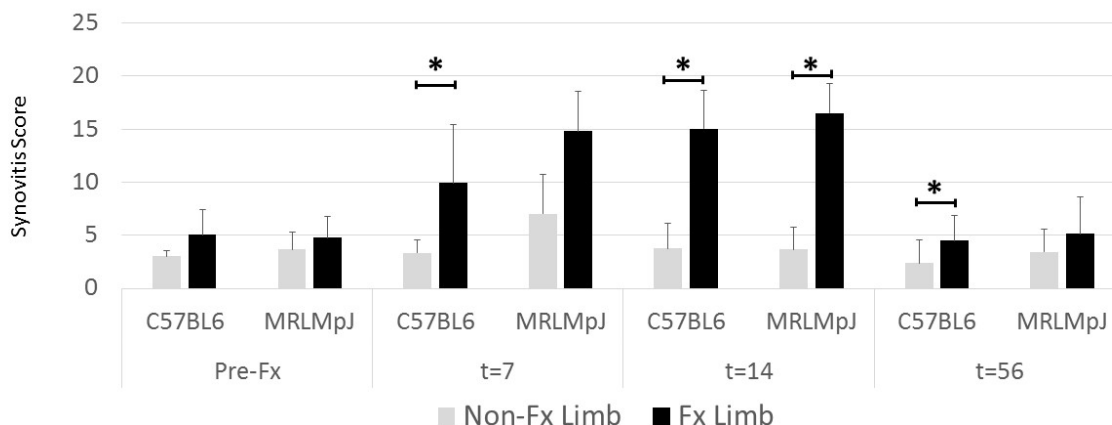
* p<0.05

Figure 2. Ratio of MMP-3/TIMP-1 by Strain

* p<0.05; § p<0.01; ‡ p<0.001

E. PROBLEM AREAS

Specific Aim 1:

The overall objective of this study is to identify biomarkers following articular fracture that may be predictive of the development of PTA. Specifically, patients with a closed unilateral articular fracture of the knee requiring operative treatment will be enrolled over an 18-month period. Biosamples (synovial fluid from the injured and contralateral uninjured knee, serum, and urine) will be collected prior to or at surgical intervention. MR imaging of the injured knee will be obtained to assess the articular cartilage. Degenerative changes in the cartilage and joint space narrowing will be correlated to biomarkers that may be indicative and predictive of joint degeneration and the development of PTA.   After expanding the enrollment criteria and

extending the enrollment period, enrollment has closed with 20 patients successfully enrolled in the study.

Issues:

As previously reported, enrollment was initially slow. However, in response, we expanded the enrollment criteria and extended the enrollment period. The enrollment has closed with 20 patients successfully enrolled in the study. Biosamples from all enrolled patients have been collected, processed and stored at -80°C. Questionnaires have also been collected from all patients. However, there have been issues with patient compliance in obtaining MRI scans, due to various factors including claustrophobia, definitive treatment outside the study criteria, such as conversion to total knee arthroplasty or only open reduction internal fixation, and non-compliance. We have obtained post-op MRI scans for all patients still enrolled in the study. For 18-month follow-up MRI scans, we have obtained 6 scans. Analyses of the paired MRI scans for these six patients have been completed.

Specific Aim 2: No problems/issues to report.

F. ANIMAL USAGE STATISTICS
- DOD Annual Report on Animal Use:
    - Species used: mice
    - Number of each species used: 84
- USDA Pain Category for all animals used:
    - Category C (Non-Painful Procedures): 12
    - Category D (Procedures using anesthesia/analgesia): 72

4. KEY ACCOMPLISHMENTS:
- Human synovial fluid analysis revealed a novel panel of vascular and inflammatory biomarkers that are altered following articular fracture and may provide a means of identifying patients at risk for PTA following articular fracture and serves as a first step in the development of potential therapies and early intervention strategies that could prevent the development of PTA.
- Sphingolipid and phospholipid metabolites were upregulated in human synovial fluid following articular fracture, indicating that they are biomarkers of knee injury and are potential prognostic indicators of risk of PTA development.
- A novel CT-based method was developed for assessing joint incongruity, or bone surface displacements, following articular fracture in the mouse knee that has potential to be used clinically.
- CT-based method for assessing joint incongruity following articular fracture predicted the development of PTA in mouse strain known to develop PTA, C57BL/6 mice.
- The "superhealer" MRL/MpJ mouse strain demonstrated a unique mechanism of fracture healing and bone morphology following articular fracture in which joint incongruities do not predispose this strain to the development of PTA.
- C57BL/6 mice showed a less robust acute bone anabolic response as measure by an acute drop in the bone formation biomarker PINP that was not demonstrated by the MRL/MpJ mice.
- Biomarkers indicative of a degradative synovial phenotype in C57BL/6 mice was identified. These biomarkers should be useful for monitoring the destructive and inflammatory responses that result in the development of PTA.

5. CONCLUSIONS:
Post-traumatic arthritis (PTA) is a severe burden in active duty and discharged soldiers. Recent figures from Operation Iraqi Freedom and Operation Enduring Freedom indicated joint degeneration following injury is the most common cause of a soldier being unfit for duty.[3]

Compared to other forms of arthritis, (PTA) has a more rapid clinical onset.[9] This rapid onset of degenerative arthritis is occurring following joint injuries in a younger population of soldiers. The goal of this work is to identify biomarkers following articular fracture that may be predictive of the development of PTA. This knowledge is needed for future investigations to assess acute interventions to prevent PTA that can be given on the battlefield or at the time of stabilizing medical care in down range medical facilities. To reach this goal, the proposed investigation studies patients who have sustained a closed, displaced articular fracture about the knee requiring operative treatment. While these patients are not suffering battlefield injuries, they do represent significant articular injuries that are at risk for developing PTA. A companion murine bench top series of experiments will allow for the comparison of human and mouse response following joint fracture. An animal model is needed to allow for a low-cost model for the assessment of future therapies to prevent PTA.

6. PUBLICATIONS, ABSTRACTS, AND PRESENTATIONS:

To date, findings from this study have been presented in the following abstracts and detailed in Appendix I.

1. Vovos, T. J., Furman, B. D., Kimmerling, K. A., Uttukar, G., DeFrate, L. E., Guilak, F., Olson, S. A. (2015). Novel in vivo micro-computed tomography metrics of joint incongruity predict arthritis in a knee fracture model. Extemity War Injuries X: Return to Health and Function, Washington, DC. (*podium and poster presentation*)

2. Kimmerling, K. A., Furman, B.D., Vovos, T.J., Huebner, J.L., Guilak, F., Olson, S.A. (2015). Bone Morphological Changes Correlate with Reduction in PTA after Articular Fracture in the MRL/MpJ Mouse. Annual Meeting of the Orthopaedic Research Society, Las Vegas, NV. (*poster presentation*)

3. Vovos, T. J., Furman, B. D., Kimmerling, K. A., Uttukar, G., DeFrate, L. E., Guilak, F., Olson, S. A. (2015). Novel in vivo microCT metrics of joint incongruity predict arthritis in a knee fracture model. Annual Meeting of the Orthopaedic Research Society, Las Vegas, NV. (*podium presentation*)

4. Vovos, T. J., Furman, B. D., Huebner, J. L., Kimmerling, K. A., Utturkar, G. M., DeFrate, L. E., Kraus, V. B., Guilak, F., Olson, S. A. (2015). "Joint incongruity and biomarkers of bone metabolism as predictors of post-traumatic arthritis in mice." Osteoarthritis and Cartilage 23: A242-A243. doi: 10.1016/j.joca.2015.02.449. (*poster presentation*)

5. Huebner, J. L., Furman, B. D., Manson, M. J., Kimmerling, K. A., Olson, S. A., Guilak, F., DeFrate, L. E., Zura, R. D., Reilly, R. M., Kraus, V. B. (2016). "Acute inflammatory response after severe joint injury potentially involved in the development of post-traumatic arthritis." Osteoarthritis and Cartilage 24, Supplement 1: S79-S80. doi: http://dx.doi.org/10.1016/j.joca.2016.01.169. (*poster presentation*)

6. Furman, B. D., Kimmerling, K. A., Ramamoorthy, S., Li, Y. J., Wu, Y. H., Huebner, J. L., Guilak, F., Kraus, V. B., Olson, S. A. (2017). Sphingolipid Metabolites are Upregulated in Human Synovial Fluid Following Articular Fracture. Annual Meeting of the Orthopaedic Research Society, San Diego, CA. (*poster presentation*)

7. Huebner, J. L., Furman, B. D., Kimmerling, K. A., Li, Y. J., Wu, Y. H., Guilak, F., Olson, S. A., Kraus, V. B. (2017). Synovial Fluid Analysis Reveals a Novel Panel of Vascular and Inflammatory Biomarkers that are Altered Following Articular Fracture. Annual Meeting of the Orthopaedic Research Society, San Diego, CA. (*poster presentation*)

8. Olson, S. A., Huebner, J. L., Furman, B. D., Kimmerling, K. A., Li, Y. J., Wu, Y. H., Guilak, F., Kraus, V. B. (2017). <u>Characterization of the Synovial Fluid Milieu after Articular Fracture</u>. Extemity War Injuries XII: Homeland Defense as a Translation of War Lessons Learned, Washington, DC. (*poster presentation*)

Four manuscripts on the findings from the work are in preparation and detailed in Appendix II.

7. INVENTIONS, PATENTS AND LICENSES: Nothing to report.

8. REPORTABLE OUTCOMES:

Potential biomarkers of PTA development following articular fracture have been identified through this work. We are seeking further funding, including through the DoD PRORP Expansion Award W81XWH-16-PRORP-EA (OR160265), to develop and validate a blood screening test that may be able to identify military personnel, veterans or civilians with articular fracture that are at high risk for developing PTA. Additionally, a novel CT-based method for assessing bone surface displacements following articular fracture was developed. Clinically, these deviations in the joint surface have been difficult to measure. This technique has translational potential, as it could readily be applied to full scale clinical CT scans.

9. OTHER ACHIEVEMENTS: None to report.

10. REFERENCES:

1.   Promotion. Arthritis Meeting the Challenge At A Glance 2011. 2011. http://www.cdc.gov/chronicdisease/resources/publications/aag/arthritis.htm#chart1.
2.   Brown TD, Johnston RC, Saltzman CL, Marsh JL, Buckwalter JA. Nov-Dec 2006. Posttraumatic osteoarthritis: a first estimate of incidence, prevalence, and burden of disease. J Orthop Trauma. 20(10):739-744.
3.   Cross JD, Ficke JR, Hsu JR, Masini BD, Wenke JC. 2011. Battlefield orthopaedic injuries cause the majority of long-term disabilities. The Journal of the American Academy of Orthopaedic Surgeons. 19 Suppl 1:S1-7.
4.   Widmyer MR, Utturkar GM, Leddy HA, et al. Oct 2013. High body mass index is associated with increased diurnal strains in the articular cartilage of the knee. Arthritis Rheum. 65(10):2615-2622.
5.   Coleman JL, Widmyer MR, Leddy HA, et al. Feb 1 2013. Diurnal variations in articular cartilage thickness and strain in the human knee. J Biomech. 46(3):541-547.
6.   Kosinska MK, Liebisch G, Lochnit G, et al. Sep 2013. A lipidomic study of phospholipid classes and species in human synovial fluid. Arthritis Rheum. 65(9):2323-2333.
7.   Kosinska MK, Liebisch G, Lochnit G, et al. 2014. Sphingolipids in human synovial fluid--a lipidomic study. PloS one. 9(3):e91769.
8.   Leimer EM, Pappan KL, Nettles DL, et al. Feb 29 2016. Lipid profile of human synovial fluid following intra-articular ankle fracture. J Orthop Res.
9.   Furman BD, Olson SA, Guilak F. Nov-Dec 2006. The development of posttraumatic arthritis after articular fracture. J Orthop Trauma. 20(10):719-725.

10. TABLES:

Table 1. Categories of Biomarkers Measured by ELISA.

Proinflammatory Cytokines*	Cytokines*	Chemokines*	Angiogenesis*	Vascular Injury*	Joint Metabolism	Bone Metabolism (serum only)
IFN-γ	GM-CSF	Eotaxin	bFGF	CRP	COMP‡	CTXI†
IL-1β	IL-1α	Eotaxin-3	Flt-1	SAA	CTXII†	Osteocalcin*
IL-2	IL-5	IP-10	PIGF	VCAM-1	sGAGΨ	Osteopontin*
IL-4	IL-7	MIP-1α	Tie-2	ICAM-1	HA¶	Osteonectin*
IL-6	IL-12/IL-23p40	MIP-1β	VEGF		MMP-1*	
IL-8	IL-15	MCP-1	VEGF-C		MMP-2*	
IL-10	IL-16	MCP-4	VEGF-D		MMP-3*	
IL-12p70	IL-17A	MDC			MMP-9*	
IL-13	TNF-β	TARC			MMP-10*	
TNF-α	VEGF					

11. APPENDICES:

Appendix I: Abstracts
Abstracts (8 in total) are included from the following with scientific meetings in which findings supported by this award were presented: 2015 Extremity War Injuries X symposium, 2015 Annual Meeting of the Orthopaedic Research Society (2), 2015 World Congress on Osteoarthritis, 2016 World Congress on Osteoarthritis, and 2017 Annual Meeting of the Orthopaedic Research Society (2), 2017 Extremity War Injuries XII symposium.

Appendix II: Manuscripts for Publication
Summaries for the four manuscripts in progress are listed. Paper 1 has been drafted for submission to JBJS-Am. Papers 2-4 are currently being drafted.

Appendix III: Personnel
A list of personnel receiving pay from the research effort is provided.

Appendix IV: Quad Chart

Appendix I. Abstracts

DoD-TRP Award – Assessment of Biomarkers Associated with Joint Injury and Subsequent Posttraumatic Arthritis

Abstracts are attached and listed below in which findings supported by this award were presented at scientific meetings in both poster and podium format.

Vovos, T. J., Furman, B. D., Kimmerling, K. A., Uttukar, G., DeFrate, L. E., Guilak, F., Olson, S. A. (2015). Novel in vivo micro-computed tomography metrics of joint incongruity predict arthritis in a knee fracture model. Extemity War Injuries X: Return to Health and Function, Washington, DC. (*podium and poster presentation*)

Kimmerling, K. A., Furman, B.D., Vovos, T.J., Huebner, J.L., Guilak, F., Olson, S.A. (2015). Bone Morphological Changes Correlate with Reduction in PTA after Articular Fracture in the MRL/MpJ Mouse. Annual Meeting of the Orthopaedic Research Society, Las Vegas, NV. (*poster presentation*)

Vovos, T. J., Furman, B. D., Kimmerling, K. A., Uttukar, G., DeFrate, L. E., Guilak, F., Olson, S. A. (2015). Novel in vivo microCT metrics of joint incongruity predict arthritis in a knee fracture model. Annual Meeting of the Orthopaedic Research Society, Las Vegas, NV. (*podium presentation*)

Vovos, T. J., Furman, B. D., Huebner, J. L., Kimmerling, K. A., Utturkar, G. M., DeFrate, L. E., Kraus, V. B., Guilak, F., Olson, S. A. (2015). "Joint incongruity and biomarkers of bone metabolism as predictors of post-traumatic arthritis in mice." Osteoarthritis and Cartilage 23: A242-A243. doi: 10.1016/j.joca.2015.02.449. (*poster presentation*)

Huebner, J. L., Furman, B. D., Manson, M. J., Kimmerling, K. A., Olson, S. A., Guilak, F., DeFrate, L. E., Zura, R. D., Reilly, R. M., Kraus, V. B. (2016). "Acute inflammatory response after severe joint injury potentially involved in the development of post-traumatic arthritis." Osteoarthritis and Cartilage 24, Supplement 1: S79-S80. doi: http://dx.doi.org/10.1016/j.joca.2016.01.169. (*poster presentation*)

Furman, B. D., Kimmerling, K. A., Ramamoorthy, S., Li, Y. J., Wu, Y. H., Huebner, J. L., Guilak, F., Kraus, V. B., Olson, S. A. (2017). Sphingolipid Metabolites are Upregulated in Human Synovial Fluid Following Articular Fracture. Annual Meeting of the Orthopaedic Research Society, San Diego, CA. (*poster presentation*)

Huebner, J. L., Furman, B. D., Kimmerling, K. A., Li, Y. J., Wu, Y. H., Guilak, F., Olson, S. A., Kraus, V. B. (2017). Synovial Fluid Analysis Reveals a Novel Panel of Vascular and Inflammatory Biomarkers that are Altered Following Articular Fracture. Annual Meeting of the Orthopaedic Research Society, San Diego, CA. (*poster presentation*)

Olson, S. A., Huebner, J. L., Furman, B. D., Kimmerling, K. A., Li, Y. J., Wu, Y. H., Guilak, F., Kraus, V. B. (2017). Characterization of the Synovial Fluid Milieu after Articular Fracture. Extemity War Injuries XII: Homeland Defense as a Translation of War Lessons Learned, Washington, DC. (*poster presentation*)

Extremity War Injuries X: Return to Health and Function

January 26-28, 2015 / Mandarin Oriental Hotel / Washington, DC
Symposium Co-Chairs: Marc Swiontkowski, MD and Col Jeffrey Davila, MD
EWI Project Team Chair: COL (Ret.) James Ficke, MD

POSTER SESSION CALL FOR ABSTRACTS
Deadline: December 1, 2014

The American Academy of Orthopaedic Surgeons (AAOS) is accepting abstracts for combat casualty and/or trauma related research. Up to 16 abstracts will be selected for display at the 2015 Extremity War Injuries Symposium (EWI), January 26-28, at the Mandarin Oriental Hotel in Washington, DC.

If your abstract is accepted for exhibition, your poster will be displayed January 27 and 28, with a poster session from 6:00 – 8:00 PM on Tuesday, January 27. You must be present to participate in the poster session. Selected posters will be invited to give a brief podium presentation on Wednesday, January 28. The $600 EWI registration fee will be waived for poster presenters. Presenters will be responsible for hotel and travel costs associated with attending the EWI symposium. CME (up to 14.75 hours) will be available for EWI X attendees/participants.

Please complete this form and submit with a copy of your CV to Erin Ransford, AAOS Manager, Research Advocacy, at ransford@aaos.org by Monday, December 1, 2014.

Full Name: Steven A. Olson
Military Rank (if applicable):
Institution/Organization: Duke University School of Medicine
Mailing Address: DUMC 3389
City /State/Zip: Durham, NC 27710
Email: olson016@dm.duke.edu
Phone: 919-668-3000

Abstract Title: Novel In Vivo micro-Computed Tomography Metrics of Joint Incongruity Predict Arthritis in a Knee Fracture Model

Abstract Text (limited to 3,000 characters, including spaces [~500 words])
The form will expand as you type/paste text.
Introduction: Post-traumatic arthritis (PTA) is an accelerated form of arthritis that develops following joint injury and occurs most predictably after intraarticular fracture. The MRL/MpJ strain of mice is protected from PTA following intraarticular fracture, thus providing valuable insight into the mechanisms of progression of PTA. We hypothesized that quantitative measures of joint incongruity could be used to predict PTA development following intraarticular fracture by assessing in vivo micro-CT metrics of joint incongruity after joint fracture. Furthermore, we hypothesized that the MRL/MpJ mouse would have an altered fracture healing response compared to the C57BL/6 mouse.

Methods: This is an IACUC-approved protocol. Skeletally mature male C57BL/6 (n=12, Charles River) and MRL/MpJ mice (n=12, Jackson Labs) were subjected to a closed intraarticular fracture (fx) of the lateral tibial plateau using an established model. In vivo micro-CT (SkyScan 1176, Bruker) of fractured limbs was performed pre and post fracture, and then at 1, 4, & 8 weeks post-fx. The articular surface alignment was assessed as bone surface deviations (BSD) for all post-fx micro-CT scans. Surface-rendered 3D digital models of the tibial plateau were generated from in vivo scans. Models were aligned to their respective pre-fx model's intact medial tibial plateau using an iterative closest point algorithm. BSDs were measured separately for the medial and lateral tibial plateau along three anatomic axes: anteroposterior (AP), latero-medial (LM), and axial. Positive and negative deviations of the bone surface were measured as the distance a displaced surface that was either outside (positive) or inside (negative) of the intact surface. A deviation of 0% corresponded to perfect alignment of pre-fx and post-fx tibial plateaus.

Results: Intraarticular fractures were successfully created in all mice. Temporal patterns in BSDs were significantly different between C57BL/6 and MRL/MpJ mice over 8 weeks. The initial displacement of BSD was similar in each strain and was observed to increase over time in the C57BL/6 to be significantly different from the MRL/MpJ at 8 weeks post fracture (p=.01).

In assessing the relationship between BSDs of the joint after fracture and the development of PTA, total joint Mankin scores of PTA changes were correlated to all BSDs measured in both mouse strains. Measures of BSDs from scans obtained immediately after fracture showed the strongest correlations with PTA development. In C57BL/6 mice, BSDs on post-fx day 0 were highly predictive of PTA severity at 8 weeks post-fx (R^2=0.94, p=0.006). In contrast, MRL/MpJ mice post-fx day 0 BSDs did not predict the development of PTA (R^2=0.25, p=0.10).

Significance: The MRL/MpJ mice are protected against development of PTA, and their post injury response overcomes the effect of articular misalignment. Whereas the C57BL/6 post injury response enhances the effect of articular misalignment.

Bone Morphological Changes Correlate with Reduction in PTA after Articular Fracture in the MRL/MpJ Mouse

Kelly A. Kimmerling, MEng[1], Bridgette D. Furman, B.S.[2], Tyler J. Vovos, BS[1], Janet L. Huebner, MS[3], Virginia B. Kraus, MD, PhD[2], Farshid Guilak, PhD[2], Steven A. Olson, MD[2].
[1]Duke University, Durham, NC, USA, [2]Duke University Medical Center, Durham, NC, USA, [3]Duke Molecular Physiology Institute, Durham, NC, USA.

Introduction: Post-traumatic arthritis (PTA) occurs after joint trauma, such as articular fractures, but the mechanism is not well-understood [1, 2, 3]. While PTA can occur rapidly after moderate to severe articular injuries, not every patient will go on to develop this condition. Currently, there are no effective screening methods to determine who is at risk. Characterizing degenerative changes in joint tissues following articular fracture in an animal model provides an opportunity to study the pathology of joint injury and the development of PTA. In previous studies, we have shown that C57BL/6 mice exhibit arthritic changes following articular fracture, whereas the MRL/MpJ strain is protected from PTA [1, 4]. The objective of this study was to identify differences in acute joint pathology and degeneration in C57BL/6 and MRL/MpJ mice as measured in the articular cartilage, synovium, and periarticular bone following articular fracture.

Methods: All animal procedures were performed in accordance with an IACUC-approved protocol. Male C57BL/6 and MRL/MpJ mice (n=83) were subjected to an articular fracture at 16 weeks of age using an established model [5]. Six mice from each strain did not receive a fracture and served as pre-fracture controls. Mice were sacrificed at 0, 1, 7, 14, and 56 days after fracture (n=6-11 per strain per time point). The left (fractured) and right (non-fractured) limbs were harvested, formalin fixed and scanned with microCT to assess bone morphology in the tibial epiphysis and metaphysis and femoral condyles. Histology sections (FFPE, 8µm thick in coronal plane) of all limbs were assessed for cartilage degeneration in the lateral and medial femoral condyles (LF, MF) and lateral and medial aspects of the tibial plateau (LT, MT) using a modified Mankin score, synovial inflammation using a modified synovitis score with semi-quantitative scales, and osteophyte score [1,5,6,7,8]. Parametric analyses were performed for bone morphological measures and histological assessment.

Results: Mankin scores of cartilage degeneration were significantly greater in the C57BL/6 strain compared to the MRL/MpJ strain in both the lateral femur (p=0.0204) and the medial tibia (p=0.0015). No strain differences were seen in the lateral tibia, where the fracture occurred, or in the medial femur. Synovial inflammation did not differ by strain; however, there was a significant increase in the fractured limb compared to the control limb at 1 and 2 weeks post-fracture (p<0.05). Osteophyte scores did not show any trends, but were present in both strains at 7 and 14 days and were not present at 56 days. Subchondral bone thickening was significantly increased in the C57BL/6 mice compared to the MRL/MpJ mice in the medial femur (p=0.0278) and the medial tibia (p=0.0077), but not on the lateral side.

Bone morphological changes in response to fracture were significantly different between the two mouse strains. In the fractured limbs, bone mineral density (BMD), bone volume (BV), and bone fraction (BV/TV) in both the tibial epiphysis and metaphysis were significantly greater (p<0.0015) in the MRL/MpJ strain compared to the C57BL/6 strain (p<0.001). However, in the femoral condyles, both BMD and cancellous bone fraction (BV/TV) were significantly increased in the C57BL/6 strain compared to the MRL/MpJ strain (p=0.0001).

Correlations of the histological parameters with the bone morphological parameters showed that in tibial metaphyseal region, the Mankin total joint score negatively correlated with both the BMD (rs=-0.453, p=0.0298) and BV/TV (rs=-0.437, p=0.0370) in the MRL/MpJ strain, but did not correlate with any bone parameters in the C57BL/6 strain. The synovitis total joint score in the fractured limb positively correlated with both the BMD (rs=0.658, p=0.0001) and BV/TV (rs=0.662, p=0.0001) in the C57BL/6 strain, but not in the MRL/MpJ strain.

Discussion: Analysis of both histologic and bone morphologic measures in this study suggest that the differences between the C57BL/6 and MRL/MpJ strains may be associated with bone morphological changes. Despite the lack of difference in synovial inflammation between strains, cartilage degradation and bone parameters were significantly different, which may account for the altered healing response after articular fracture [4]. MRL/MpJ mice are reported to have increased levels of TGF-β1, which may contribute to the enhanced bone response following fracture found in this study [9]. Interestingly, synovitis in the C57BL/6 mice was associated with greater bone changes. Previous reports have shown that C57BL/6 mice have elevated levels of pro-inflammatory cytokines IL-1 and TNF-α following joint injury [1]. An increased local inflammatory environment may contribute to altered bone morphology and subsequent degenerative changes in the joint tissues. The difference in these arthritic profiles indicates that there may be a benefit to focusing first on fracture healing, then following up with suppression of the pro-inflammatory environment that leads to subsequent degradation of the joint. Clinically, surgical restoration of the articular surface is the only treatment for articular fractures. To date, there is no method of identifying patients that are at risk for developing PTA. In addition to measures of joint pathology, serum and synovial fluid from both strains of mice will be analyzed for biomarkers. The comparison of early imaging or biochemical biomarkers between mice strains and humans, which are predictive of PTA, may be useful in assessing clinical risk in articular fracture patients.

Significance: By characterizing degenerative changes in the C57BL/6 and MRL/MpJ strains, key factors that contribute to the development of PTA can be identified. By understanding what drives disease progression, potential screening methods may be developed to identify patients at high risk of developing PTA.
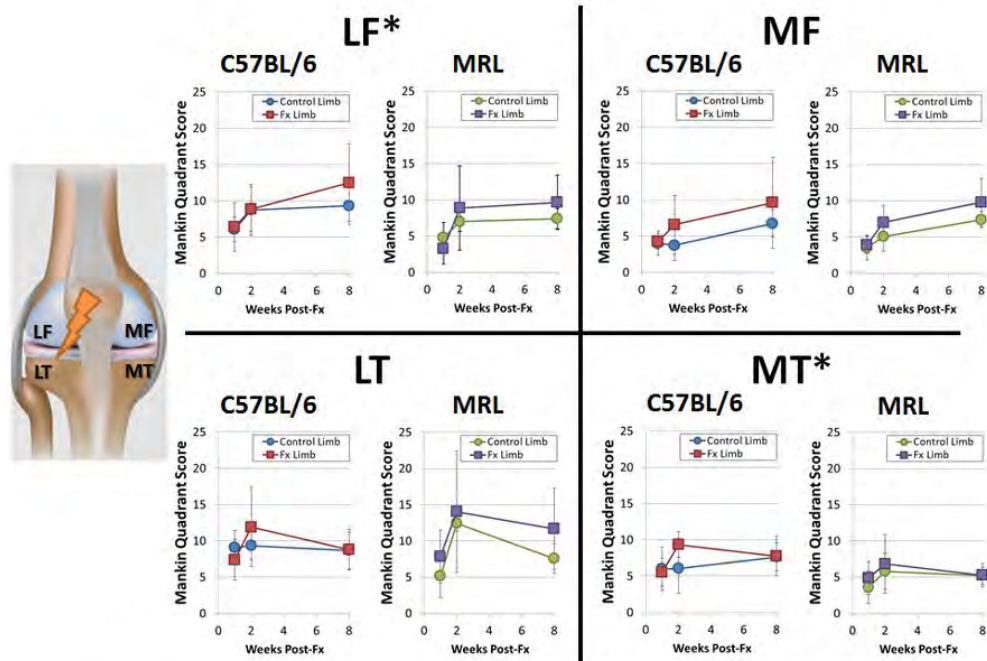
Figure 1
Cartilage degeneration assessment using a modified Mankin joint score for each quadrant shown for 7, 14, and 56 days post-fracture. Quadrants include the lateral femoral condyle (LF), lateral tibial plateau (LT), medial femoral condyle (MF), and medial tibial plateau (MT). Mean and standard deviation reported (n=6-11 per strain per time point). * denotes significance between strains by a repeated measures ANOVA (p=0.0204 in LF; p=0.0015 in MT).
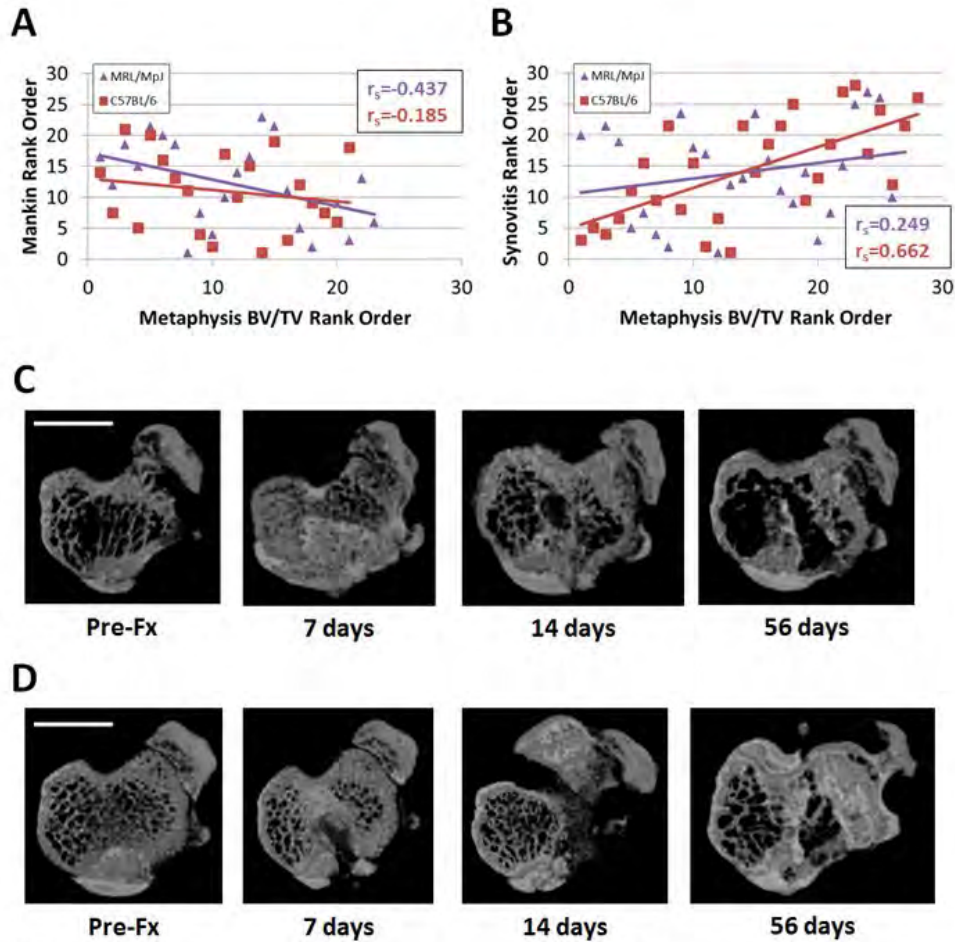
Figure 2
Correlations between Mankin total joint score, synovitis total joint score, and bone fraction (BV/TV) of the tibial metaphysis for both the MRL/MpJ and C57BL/6 strains. Values are displayed as a rank order within strain for each outcome measure (n=21-28 per strain). R_s values indicate Spearman correlation coefficient for each strain. **(A)** Mankin correlated with BV/TV (r_s=-0.437, p=0.0370) in the MRL/MpJ strain only. **(B)** Synovitis correlated with BV/TV (r_s=0.662, p=0.0001) in the C57BL/6 strain only. **(C)** Representative images of the tibial metaphysis for the C57BL/6 strain at each time point. Scale bar is 0.5mm. **(D)** Representative images of the tibial metaphysis for the MRL/MpJ strain at each time point. Scale bar is 0.5mm.

Novel In Vivo Micro-Computed Tomography Metrics of Joint Incongruity Predict Arthritis in a Knee Fracture Model

Tyler J. Vovos[1], Bridgette D. Furman, B.S.[1], Kelly A. Kimmerling, MEng[2], Gangadhar Utturkar[1], Louis E. DeFrate[1,2], Farshid Guilak[1,2], Steven A. Olson, MD[1].
[1]Duke University Medical Center, Durham, NC, USA, [2]Duke University, Durham, NC, USA.

Introduction: Post-traumatic arthritis (PTA) is an accelerated form of arthritis that develops following joint injury and occurs most predictably after intraarticular fracture [1, 2]. Joint degeneration may result from damage to the articular surface upon injury, or from residual joint instability or incongruity after injury [3]. Radiographic classification systems (e.g. Schatzker and AO/OTA) traditionally used to classify tibial plateau fracture severity do not account for 3D geometry of the joint surface [4]. A few research studies have used CT-based measures of joint fracture severity to predict PTA development [5]. To further characterize PTA development following joint trauma we developed a murine model of closed intraarticular fracture of the tibial plateau [6]. Interestingly, the MRL/MpJ "superhealer" strain of mice is protected from PTA following intraarticular fracture, thus providing valuable insight into the mechanical and inflammatory progression of PTA [7, 8]. Currently, the relationship between initial injury severity, articular surface displacement, and the development of PTA following intraarticular fracture in the MRL/MpJ and other mouse strains remains unknown. The objective of the current study was to develop in vivo micro-CT metrics of joint incongruity after intraarticular fracture to further characterize the pathomechanism of PTA. We hypothesized that quantitative measures of joint incongruity could be used to predict PTA development following intraarticular fracture. Furthermore, we hypothesized that the MRL/MpJ mouse would have an altered fracture healing response compared to the C57BL/6 mouse.

Methods: All animal procedures were performed in accordance with an IACUC-approved protocol. Skeletally mature male C57BL/6 (n=12, Charles River) and MRL/MpJ mice (n=12, Jackson Labs) were subjected to a closed intraarticular fracture (fx) (Fig 1) of the lateral tibial plateau using an established model [6, 9]. To generate similar fractures, indenter displacement was scaled relative to the size of the tibial plateau for each strain [7]. Fracture energy was calculated from the area under the load-displacement curve. At 8 weeks post-fx, all mice were sacrificed and arthritic changes in both fractured and non-fractured contralateral control knees were quantified using a modified Mankin score [6,10] of histologic sections (8 µm thick, FFPE, Safranin O/fast green). In vivo micro-CT (SkyScan 1176, Bruker) of fractured limbs was performed before and after fracture, and then at 1, 4, and 8 weeks post-fx. Bone surface deviations (BSD) were measured for all post-fx micro-CT scans. First, surface-rendered 3D digital models of the tibial plateau were generated from in vivo scans (CT-Analyser, Bruker). Models were then aligned to their respective pre-fx model's intact medial tibial plateau using an iterative closest point algorithm (Geomagic Studio, Geomagic®). BSDs were measured separately for the medial and lateral tibial plateau along three anatomic axes: antero-posterior (AP), latero-medial (LM), and axial (Geomagic

Control, Geomagic®). Positive and negative deviations of the bone surface were measured (Fig 1), and defined as the distance to a test surface (post-fx bone surface) that was either outside (positive) or inside (negative) of the reference surface (pre-fx bone surface). A deviation of 0% corresponded to perfect alignment of pre-fx and post-fx tibial plateaus. Color maps of BSDs were generated for each anatomical direction. An example of axial deviations in an MRL/MpJ mouse from post-fx to 8 weeks is shown in Fig 2.
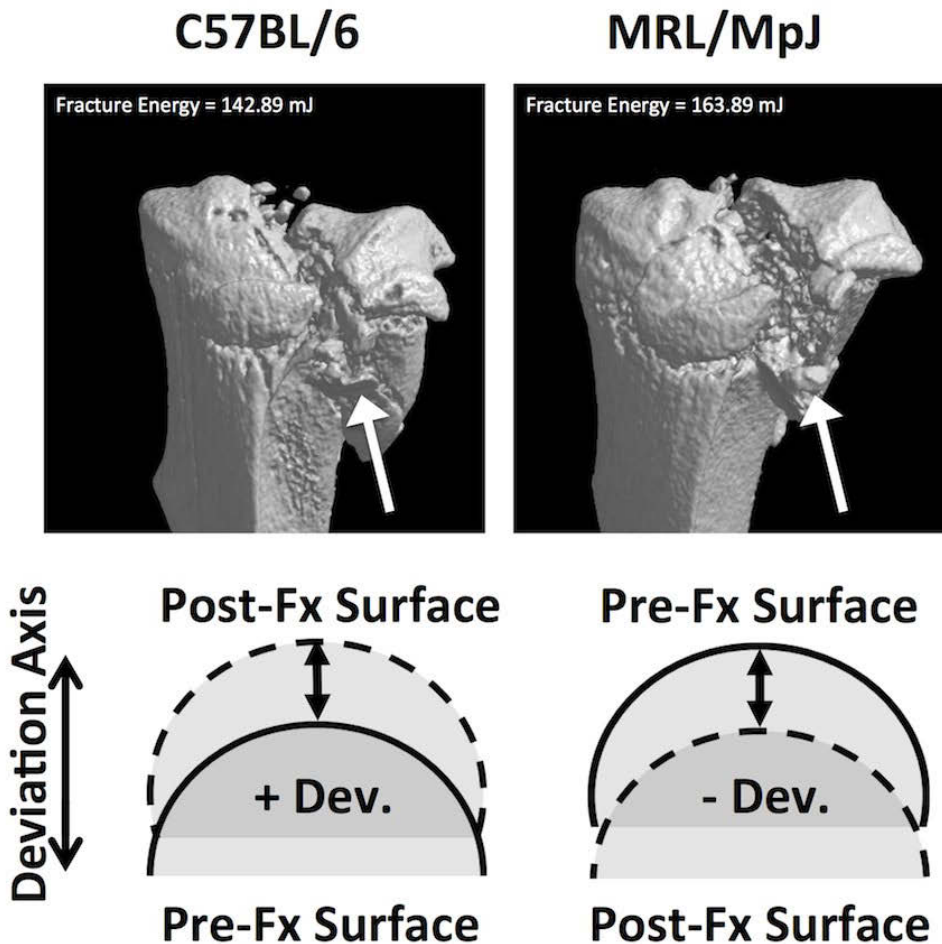
Results: Intraarticular fractures were successfully created in all mice. Consistent with previous data [7], fracture energy was significantly greater for MRL/MpJ mice (148.1 ± 22.1 mJ) compared to C57BL/6 mice (106.6 ± 20.3 mJ) (p<0.001). Temporal patterns in BSDs were significantly different between C57BL/6 and MRL/MpJ mice over 8 weeks (Fig 2). Significant differences were observed in the lateral tibial plateau as measured by average positive axial deviation (p = 0.01), average positive LM deviation (p = 0.015), and maximum positive LM deviation (p = 0.01). Additionally, a significantly larger average positive axial deviation was observed in C57BL/6 mice at 8 weeks post-fx (p=0.01) (Fig 2). In the medial plateau, significant differences were seen between strains as measured by average positive axial deviation (p=0.0487) and average negative LM deviation (p=0.0491).

In assessing the relationship between BSDs of the joint after fracture and the development of PTA, total joint Mankin scores of degenerative changes were correlated to all BSDs measured in both mouse strains. Measures of BSDs from scans obtained immediately after fracture showed the strongest correlations with PTA development. In C57BL/6 mice, axial BSDs on post-fx day 0 were highly predictive of PTA severity at 8 weeks post-fx (Fig 3). In contrast, MRL/MpJ mice post-fx day 0 BSDs did not predict the development of PTA (Fig 3). Average positive AP deviation at the post-fx scan was also highly correlated to Mankin score in C57BL/6 mice (R^2 =0.94, p=0.006) but not in MRL/MpJ mice (R^2 =0.25, p=0.10).

Discussion: Through the development of novel in vivo micro-CT metrics of joint incongruity, we analyzed temporal patterns in bone surface deviations that revealed significant differences between C57BL/6 and MRL/MpJ strains over 8 weeks. Interestingly, after 8 weeks of fracture healing, we observed significantly larger bone surface deviations in C57BL/6 mice compared to MRL/MpJ mice. Furthermore, when applied to in vivo scans of the knee joint obtained immediately after fracture, our metrics of joint incongruity were capable of predicting the development of PTA in wild-type C57BL/6 mice, but not MRL/MpJ mice. These findings suggest that the MRL/MpJ strain undergoes a unique mechanism of fracture healing following intraarticular fracture, and that joint incongruities secondary to intraarticular fracture do not predispose MRL/MpJ mice to the development of PTA. Combined with an evolving knowledge of the biology of PTA development, our metrics hold potential as a tool for guiding PTA research in identifying physiologic processes that protect the MRL/MpJ strain from the effects of articular incongruity. Clinically, our metrics of joint incongruity could be used to predict which injuries are at risk for progression to PTA. Our observation that early measures of joint incongruity predict PTA in wild-type C57BL/6 mice corroborates previous findings that small articular incongruities after surgical fixation of intraarticular tibial plateau fractures predispose patients to the development of PTA [11]. Further, the translational potential of our joint incongruity metrics is high, as they could be readily applied to full scale clinical CT scans [12].

Significance: In vivo micro-CT metrics of joint incongruity provide a method for quantifying bone surface incongruities that have traditionally been difficult to measure and provide new possibilities to guide PTA

research and improve fracture management. The translational potential of our joint incongruity metrics is high, as they could readily be applied to full scale clinical CT scans.

Figure 1. (Top) Micro-CT images of representative fractures. (Bottom) Metrics of joint incongruity after intra-articular fracture. Reference surface = pre-fracture; test surface = post-fracture.
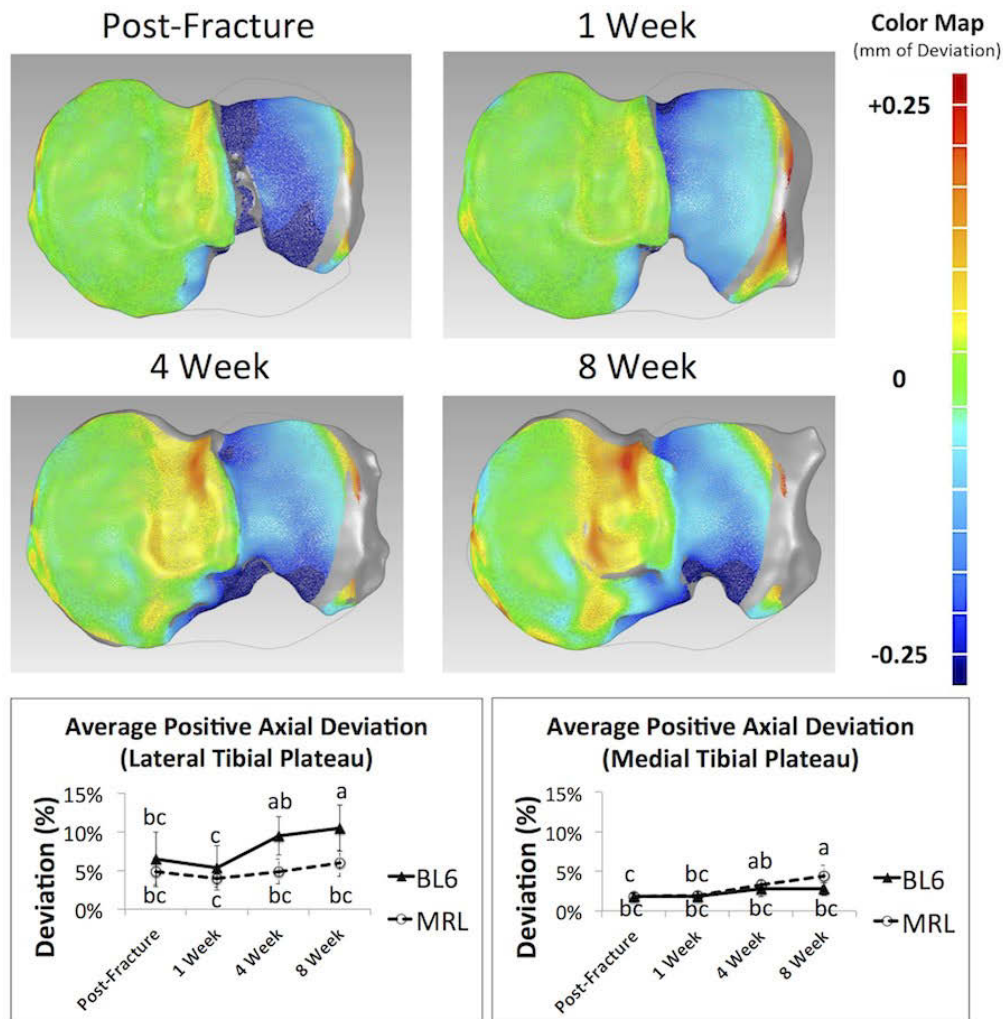
Figure 2. (Top) Representative color map of axial deviation with fracture healing. (Bottom) Significant strain-wise differences in fracture healing from post-fracture to 8 weeks.
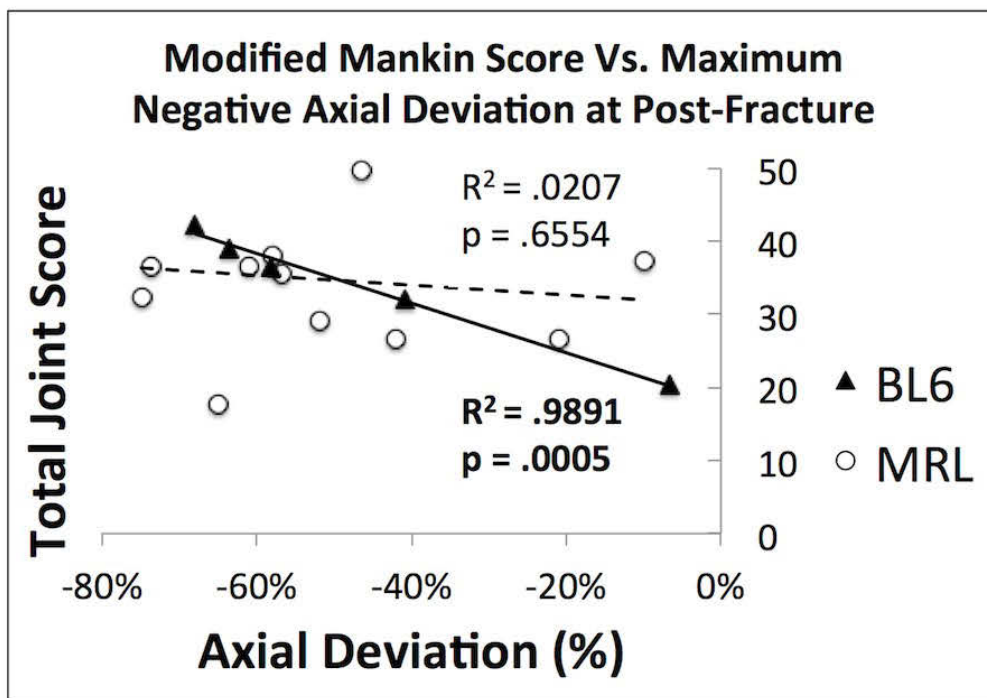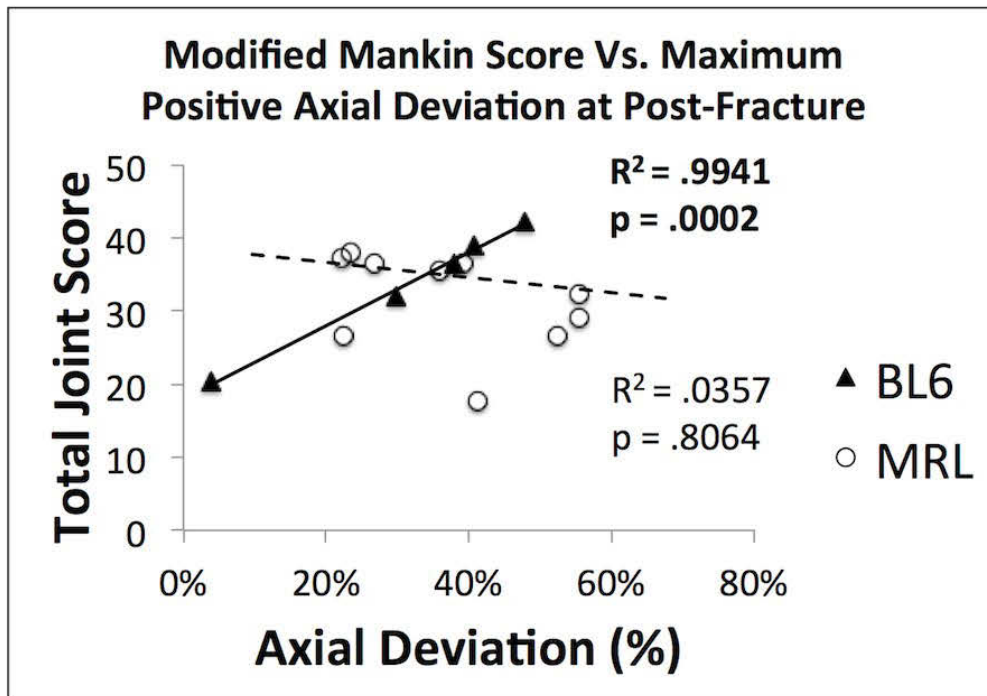
Figure 3. Correlations between total joint Mankin score for arthritis at 8 weeks post-fracture and post-fracture joint incongruity.

studied the correlation of sonographic measurements of the articular cartilage of the knee joint obtained from the posterolateral and posteromedial aspects to that obtained from the anterior aspect by the traditional method in patients with osteoarthritis of the knee.

Methods: We selected and studied the right knee of thirty one patients diagnosed with knee osteoarthritis, age ranging from 54 to 85 years who presented to our outpatient clinic. We used questionnaires to calculate Western Ontario and McMaster Ostoearthitis (WOMAC) scores and categorize patients into mild, moderate and severe osteoarthritis. and determined the correlation of the measurements to the severity of osteoarthritis. We excluded patients who could not extend the knee past 5 degrees or could not flex the knee beyond 135 degrees, patients with a knee effusion, and patients who had received an intra articular injection within the past month.

We measured the articular cartilage by the standard sonographic method using a GE Logiq e machine equipped with an 8-13 MHz linear transducer. We first measured cartilage thickness with the knee held in full flexion and at 140 degrees, at the medial and lateral aspects. We then measured the articular cartilage from the posterior aspect with the knee extended, over the medial and lateral condyles. We then compared the measurements obtained from the anterior aspect in full flexion to that obtained at 140 degrees and from the posterior aspect. We assumed a linear correlation between standard and posterior aspect measurements, hypothesized that a Pearson correlation coefficient greater than 0.77, corresponding to the lower bound of the 95% confidence interval of 0.6, would show satisfactory correlation between measurements.

Results: We demonstrated very good interobserver and intraobserver correlation between the two observers, with a correlation coefficient of 0.975 or higher at all sites. We compared the anterior and posterior measurements with Pearson correlation in both observers 1 and 2. Among the two observers, the greatest correlation for observer 1 was between the fully flexed anterolateral measurement to the posteromedial measurement with a Pearson correlation coefficient of 0.613, p-value = 0.000. Among measurements for observer 2, we found a Pearson correlation coefficient of 0.611, p-value = 0.000 between the fully flexed lateral and posteromedial measurements. We did not find correlation coefficients among the other measurements. We also noted that measurements from the posterior aspect appeared to be generally greater than those from the anterior aspect.

Conclusions: We did not find significant correlation between anterior and posterior measurements in patients with knee osteoarthritis. The highest correlation was found between anterolateral fully flexed and posteromedial measurements in both observers, with a Pearson correlation coefficient of 0.6. Posterior measurements, especially the posterolateral measurement appeared to be larger than anterior measurements indicating that posterior measurements of the articular cartilage by ultrasound may overestimate the cartilage measurements. We were unable to correlate the articular correlation with severity of osteoarthritis as majority of the patients had severe osteoarthritis (27/34 patients). Hence, although significant correlation between anterior and posterior measurements of the articular cartilage of the knee joint was observed in healthy volunteers, this was not the case in patients with osteoarthritis of the knee joint.

377

JOINT INCONGRUITY AND BIOMARKERS OF BONE METABOLISM AS PREDICTORS OF POST-TRAUMATIC ARTHRITIS IN MICE

T.J. Vovos †, B.D. Furman †, J.L. Huebner †‡, K.A. Kimmerling †§, G.M. Utturkar †, L.E. DeFrate †§, V.B. Kraus †‡, F. Guilak †§, S.A. Olson †. † Duke Univ. Med. Ctr., Durham, NC, USA; ‡ Duke Molecular Physiology Institute, Durham, NC, USA; § Duke Univ., Durham, NC, USA

Purpose: Post-traumatic arthritis (PTA) develops predictably after articular fracture and may result from joint inflammation, hemarthrosis, or damage to the articular surface and residual joint instability or incongruity after injury. The MRL/MpJ "superhealer" mouse strain is protected from PTA and has reduced serum and synovial fluid levels of IL-1 and TNF-α acutely following fracture. The role of initial injury severity on PTA development following articular fracture is unclear. The objectives of this study were: 1) to measure acute and longitudinal displacement of the articular surface of the bone using in vivo microCT, and 2) to quantify serum bone markers following articular fracture. We hypothesized that quantitative measures of joint incongruity could predict PTA development and that MRL/MpJ mice would have an altered fracture healing response compared to C57BL/6 mice.

Methods: With an IACUC-approved protocol, male C57BL/6 and MRL/MpJ mice (n=12 each) were subjected to a closed articular fracture (fx) (Fig 1) of the lateral tibial plateau. Mice were sacrificed at 8wks post-fx, and arthritic changes were assessed in fractured and contralateral control knees (modified Mankin score). In vivo microCT was performed pre- and post-fx, and at 1, 4, and 8wks post-fx. Displacements of the articular surface of the bone, or Bone Surface Deviations (BSD), were quantified for the lateral and medial tibial plateau (Fig 1), defined as the displacement of the post-fx bone surface either outside (positive) or inside (negative) of the pre-fx bone surface (Fig 2). Blood was collected pre-fx, post-fx on day 4, and every 2wks to 6wks post-fx. Serum
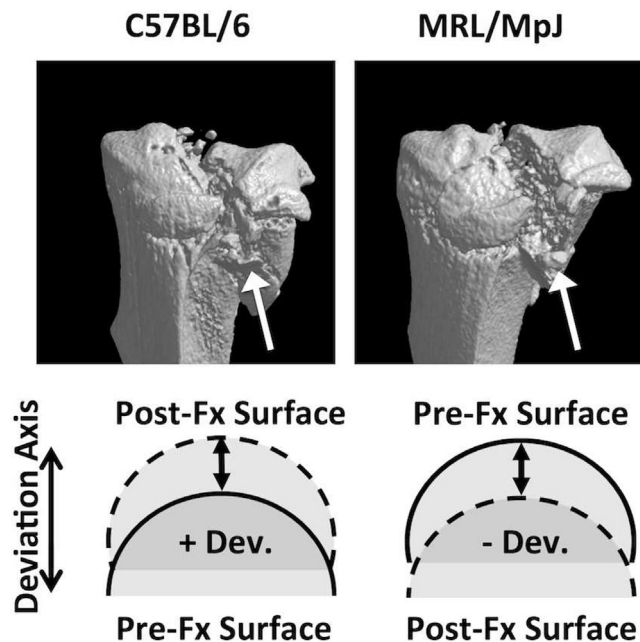

Figure 1(Top) Micro-CT images of representative fractures. (Bottom) Metrics of joint incongruity after intra-articular fracture. Reference surface = prefracture; test surface = post-fracture.
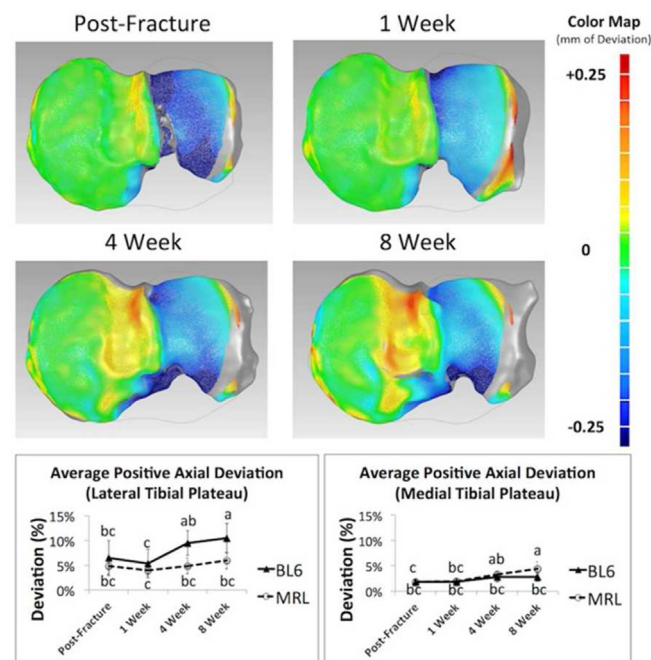

Figure 2(Top) Representative color map of axial deviation with fracture healing. (Bottom) Significant strain- wise differences in fracture healing to 8 weeks post- fracture *(data with different letters are significantly different).*
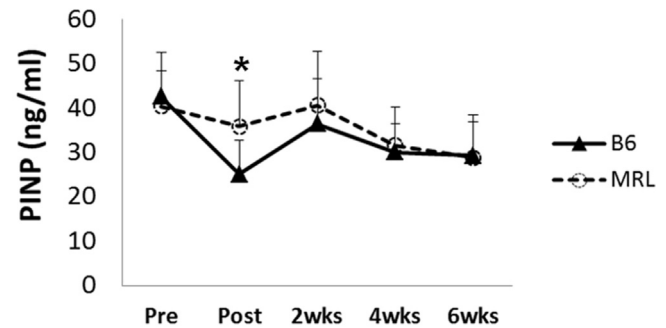
concentrations of biomarkers of bone metabolism were measured: procollagen type I N-propeptide (PINP), a bone formation marker; and C-terminal telopeptide of type I collagen (CTXI), a bone resorption marker. BSDs were analyzed using ANOVA. Bone marker concentrations were analyzed by Friedman test for repeated measures, and mouse strains were compared at each time point using the Holm-Sidak multiple t-test. Regression analysis was used to analyze the relationship between measured outcomes.

Results: Temporal patterns in BSDs were significantly different between C57BL/6 and MRL/MpJ mice with larger average positive axial deviations found in C57BL/6 mice at 8wks post-fx (p=0.01;Fig 2). Mankin scores were correlated to all BSDs in both mouse strains. Acute BSDs showed the strongest correlations with PTA development. In C57BL/6 mice, axial BSDs on post-fx day 0 were highly predictive of PTA severity at 8wks post-fx (Fig 3). In contrast, MRL/MpJ mice post-fx day 0 BSDs did not predict the development of PTA. Concentrations of PINP in the C57BL/6 mice were significantly lower than the MRL/MpJ mice post-fx (p=0.005;Fig 4), indicating a less robust acute bone anabolic response compared with the superhealer strain. Despite higher levels of CTXI in the C57BL/6 mice compared to the MRL/MpJ at pre-fx, no differences were found in CTXI levels post-fx between strains or at any time point.

Conclusions: Acute BSDs following articular fracture were predictive of arthritis development in C57BL/6 but not MRL/MpJ mice. C57BL/6 mice also showed an acute drop in serum PINP compared to MRL/MpJ mice. Larger BSDs were also observed in C57BL/6 mice compared to MRL/MpJ mice after 8 wks. Previous studies reported that C57BL/6 mice exhibit higher levels of inflammation post-fx than the MRL/MpJ mice and suggested that this may contribute to the development and progression of PTA in this model. This inflammatory environment may influence fracture healing immediately post-fx, potentially predisposing C57BL/6 mice to PTA. These findings suggest that joint incongruities secondary to articular fracture alone do not predispose mice to the development of PTA, but rather differences in bone metabolism may play a role in early healing, which may have a greater effect on outcome. Our results may provide insights into the physiologic processes determining PTA outcomes that may protect the MRL/MpJ strain from the effects of articular incongruity. Further, the translational potential of these incongruity metrics is high, as they could be readily applied to clinical CT scans.
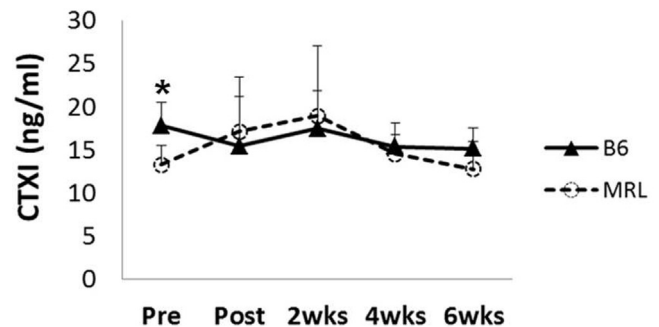

Figure 4. Serum concentrations of bone biomarkers PINP and CTX-I with articular fracture in C57BL/6 (B6) and MRL/MpJ (MRL) mice.

378

CLINICAL SIGNIFICANCE OF A KNEE EFFUSION DETECTED ON MRI BY MOAKS OR KIMRISS IN A PATIENT WITH KNEE OA

J.L. Jaremko, D. McDougall, B. Smith, R.G. Lambert, W.P. Maksymowych. *Univ. of Alberta, Edmonton, AB, Canada*

Purpose: Presence of a joint effusion in knee osteoarthritis (OA) is thought to represent potentially treatable active inflammation. However, reliable assessment of presence and size of an effusion is surprisingly difficult. Effusions can be graded in a holistic fashion as present or absent, or by the MOAKS system which generates a whole-joint score from 0 (absent) to 3 (large). The volume of fluid can be directly measured by segmentation of T2-intense voxels, but this process requires workstation post-processing and some supervision. The KIMRISS semi-quantitative grading system offers an intermediate approach in which the width of joint fluid is measured and graded 0-3 in each of 4 standardized locations at the knee joint on axial and sagittal fluid-sensitive sequences, maximum score 12. The relative merits of each of these methods, and the clinical significance of detecting an effusion in a patient with knee OA, have been little studied. Accordingly, we used data from the Osteoarthritis Initiative to determine whether an effusion of different sizes detected by MOAKS or KIMRISS was associated with increased knee pain and disability at presentation or with an increased rate of use of intra-articular steroid injection over the next year.

Methods: Patients: This cohort study included knees from 40 subjects from the Osteoarthritis Initiative (OAI) that went on to have a knee steroid injection within 1 year of baseline evaluation, and 40 that did not, matched by age, sex, and Kellgren-Lawrence (K-L) grade of radiographic OA. Subjects averaged 62.3 years of age (range: 45-78), K-L grade 2.8±1.0 (mean±standard deviation), 78% were women, and body mass index (BMI) averaged 30.3±4.6. For each patient we extracted the

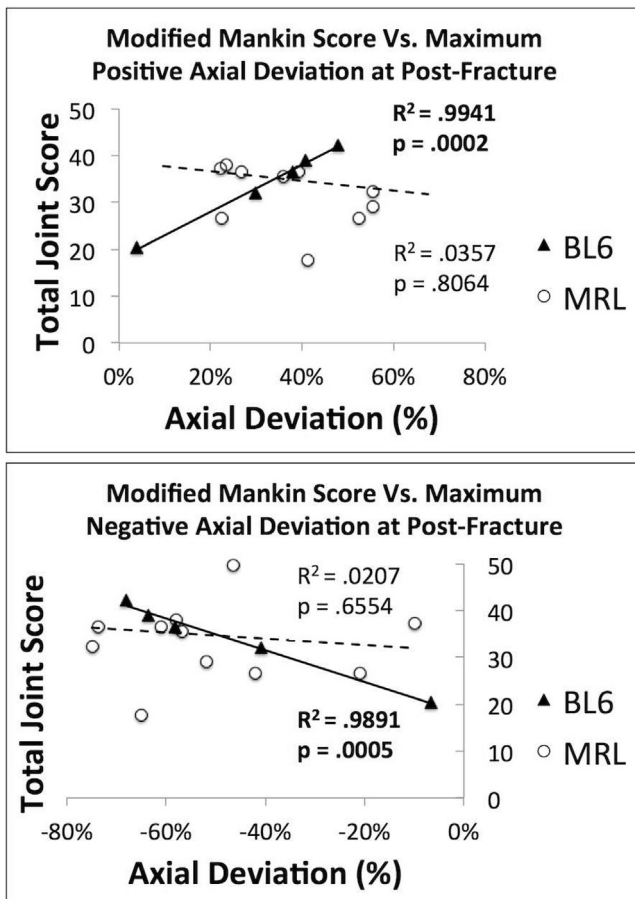Figure 3. Correlations between total joint Mankin score for arthritis at 8 weeks post-fracture and post-fracture joint incongruity.

surgery, and investigated its associations with inflammatory factors and matrix degrading MMP enzymes in an attempt to understand the role of YKL-40 in OA.

Methods: The patients in the present study fulfilled the American College of Rheumatology classifications for OA. Blood and cartilage tissue were collected from 100 OA patients undergoing total knee replacement surgery, and simultaneously collected synovial fluid samples were available from 49 of them. Body mass index was 29.7 (8.3) kg/m^2, age 72 (14) years, median (IQR); and 62% of the patients were female. For cartilage cultures full-thickness pieces of articular cartilage from femoral condyles and tibial plateaus showing macroscopic features of early OA were removed aseptically from sub-chondral bone, cut into small pieces, and cultured for 42h at 37°C in humidified 5% CO_2 atmosphere. The cartilage explants were weighted after the incubation and the results were expressed per milligram of cartilage. For primary chondrocyte cultures the OA cartilage was processed as for tissue culture and chondrocytes were isolated by enzymatic digestion for 16h at 37°C in a shaker by using collagenase enzyme blend. Isolated chondrocytes were washed, plated and treated with the compounds of interest for 24h at 37°C in humidified 5% CO_2 atmosphere. Levels of YKL-40, IL-6, IL-17, MMP-1, and MMP-3 were measured by ELISA.

Results: YKL-40 levels in SF were considerably higher than those in plasma (1027.9 ± 78.3 vs 67.2 ± 4.5 ng/ml, p<0.001, Figure 1A). No correlation between plasma and SF YKL-40 levels or with plasma / SF YKL-40 levels and BMI were found. Interestingly, YKL-40 in SF showed a positive correlation with YKL-40 released from the corresponding cartilage into the culture medium (r = 0.37, p = 0.010). These data indicate that OA cartilage is a major source of YKL-40 in OA joints.

In synovial fluid samples, YKL-40 correlated positively with MMP-1 and MMP-3 (r = 0.36, p = 0.014, and r = 0.46, p = 0.001, respectively, Figure 1B). Concentrations of YKL-40 released into the culture media from cartilage samples showed also a positive correlation with the levels of MMP-1 and MMP-3 in culture medium after incubation for 42h (r = 0.34, p = 0.001, and r = 0.38, p<0.001, respectively). Interestingly, YKL-40 in SF was also associated with the inflammatory factors IL-6 and IL-17 (r = 0.57, p<0.001, and r = 0.52, p = 0.010, respectively, Figure 1C and D). In support, both of these cytokines stimulated YKL-40 production in primary OA chondrocytes when cultured *in vitro*.

Conclusions: The present study introduces YKL-40 as a cartilage-derived factor associated with inflammatory mediators and cartilage degrading enzymes in the pathogenesis of OA.
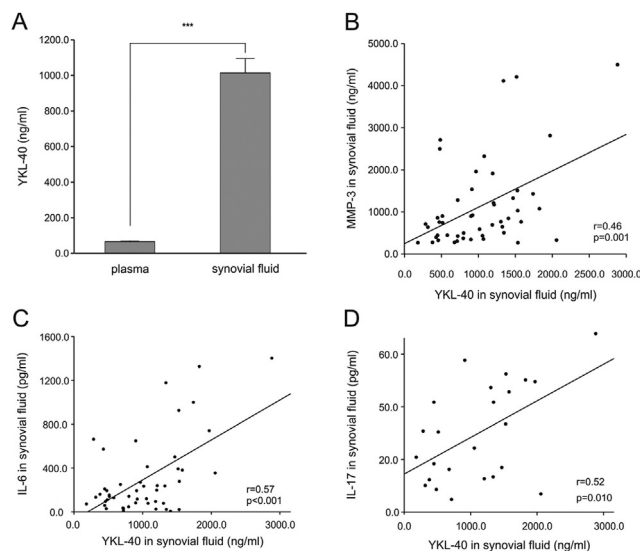

Figure 1. A Concentrations of YKL-40 in OA synovial fluid were significantly higher than those in plasma, mean + SEM. YKL-40 correlated with MMP-3 (B), IL-6 (C), and IL-17 (D) in synovial fluid from OA patients. Reprinted with permission from: Väänänen et al. 2014, Mediators of Inflammation, ID 215140.

120
ACUTE INFLAMMATORY RESPONSE AFTER SEVERE JOINT INJURY POTENTIALLY INVOLVED IN THE DEVELOPMENT OF POST-TRAUMATIC ARTHRITIS

J.L. Huebner, B.D. Furman, M.J. Manson, K.A. Kimmerling, S.A. Olson, F. Guilak, L.E. DeFrate, R.D. Zura, R.M. Reilly, V.B. Kraus. *Duke Univ. Med. Ctr., Durham, NC, USA*

Purpose: Post-traumatic arthritis (PTA) is a frequent and clinically important complication of joint injury. While PTA can occur rapidly after moderate to severe articular fractures, not every patient will develop this condition. There are currently no effective screening methods to determine who is at risk for developing PTA. The overall objective of this study was to identify biomarkers following articular fracture that may be associated with joint injury and predictive of the development of PTA.

Methods: Patients (n = 14) with a closed unilateral articular fracture (Fx) of the knee requiring operative treatment were enrolled in this study under IRB approval. The type of articular fracture was classified using the Orthopaedic Trauma Association/ AO Foundation/ (OTA/AO) classification of fractures. This is the standard used worldwide for classifying long bone fractures into several levels: type B include simple fractures, in which part of the articular surface remain intact with the diaphysis; type C are complex fractures with a greater degree of comminution with the articular surface disconnected from the diaphysis (Table 1). Fractures with more comminution have been shown clinically and in animal models to have significantly higher fracture energies resulting in a greater incidence of PTA. Serum, urine and synovial fluid (SF), were collected prior to or at the time of surgical intervention representing a mean 5.8 (SD 4.5) days from injury. SF was collected by direct aspiration from the injured and contralateral uninjured knees with a total of n = 9 paired samples of serum, SF and urine obtained. ELISA assays were used to quantify 40 acute inflammatory and injury markers as well as markers of joint metabolism (13 analytes) in serum and SF. Joint tissue markers included matrix metalloproteinases (MMP)-1, -2, -3, -9, and -10, cartilage oligomeric matrix protein (COMP) in serum and SF, sulfated glycosaminoglycans (sGAG) in SF, hyaluronic acid (HA) in the serum, C-terminal telopeptide of type II collagen (CTXII) in SF and urine, and markers of bone metabolism (C-terminal telopeptide of type I collagen (CTXI), osteocalcin, osteopontin, and osteonectin) in serum. Biomarkers were compared in synovial fluids from Non-Fx and Fx knees by the non-parametric, Wilcoxon matched-pairs signed rank test. The non-parametric Kruskal-Wallis test was used to assess differences in biomarker concentrations by the degree of fracture and Spearman correlations were performed to assess the association of biomarkers.

Results: Comparisons of biomarker concentrations in SF from Fx and non-Fx knees identified 27 analytes with significant differences; the concentrations of all of these analytes were significantly higher in SF compared to serum suggesting a joint tissue origin. Significant correlations were observed between SF and matched serum for seven of these analytes: MMP-10 (p = 0.004, rs = 0.88); IL-6 (p = 0.0005, rs = 0.92); MDC (p = 0.0002, rs = 0.93); Tie-2 (p = 0.05, rs = 0.67); VEGF (p = 0.03, rs = 0.72); ICAM (p = 0.002, rs = 0.88); and VCAM (p = 0.005, rs = −0.83). There were significant differences in biomarker concentrations by OTA/AO classification for serum IL-6 (p = 0.005), SF IL-10 (p = 0.01), SF VEGF (p = 0.02), SF MMP-9 (p = 0.03), SF COMP (p = 0.04) (Figure 2). Serum IL-6 was significantly correlated with serum IL-10 and sfVEGF. SF IL-6 was significantly correlated with markers of joint tissue metabolism (sCOMP, uCTXII, sfMMP-9, sfMMP-2), cytokines (sIL-6, sIL-15, sfIL-4, sfIL-10, sfIL-15, sfIL-16, sfVEGF), and a marker of bone metabolism, sCTXI.

Conclusions: Upon injury, the articular surface is exposed to a multitude of inflammatory cytokines and chemokines that may play a role in the development of post-traumatic arthritis. The data for sfIL-6 and sfVEGF suggest that these analytes are released from and actively report on the status of the injured knee. Understanding the complex changes that occur acutely in the joint after injury is critical for the development of potential therapies and early intervention strategies that could prevent the development of PTA.

Table 1
Description of OTA/AO fracture classifications used in this study

OTA/AO Partial Articular Fracture Type B Groups (1-3)		OTA/AO Complete Articular Fracture Type C Groups (1-3)	
B1	Simple split	C1	Articular simple + metaphyseal simple
B2	Depression	C2	Articular simple + metaphyseal multifragmentary
B3	Split + Depression multifragmentary	C3	Articular multifragmentary + metaphyseal multifragmentary

Type B and C fractures were included in this study. Type B fractures are partial articular fractures, and type C fractures are complete articular fractures. Within each type, fractures are then grouped according to the number of fracture lines (simple versus multifragmentary).
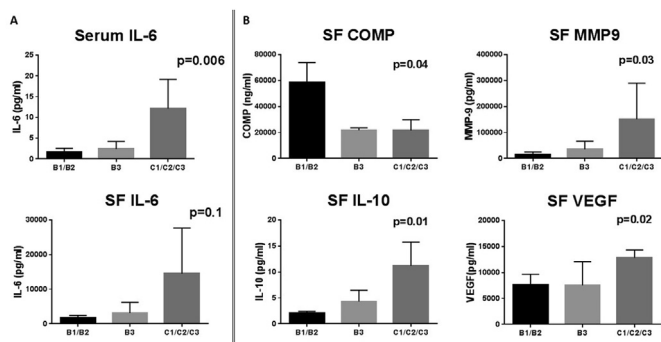
Figure 1. B1/B2, B3 and C1/C2/C3 describe the fractures by OTA/AO classification criteria.

121

CALCITONIN GENE-RELATED PEPTIDE (CGRP) LEVELS ARE ELEVATED IN THE PLASMA AND KNEE SYNOVIAL FLUID OF PATIENTS WITH KNEE OSTEOARTHRITIS (OA)

T. McNearney, X. Chai, J. Xu, C.-Y. Chang, E. Collins, K. Cox, W. Anderson, P. Mitchell, J. Talbot, J. Dage, B. Miller, K. Johnson. *Eli Lilly and Company, Indianapolis, IN, USA*

Purpose: Sensory neurons expressing calcitonin gene-related peptide (CGRP) innervate most joint structures including synovial membrane, ligaments and subchondral bone. CGRP contributes to peripheral sensitization and inflammation, and evidence suggests a role for CGRP in the pain and inflammation associated with osteoarthritis (OA). This study measured and compared CGRP levels in plasma and synovial fluid (SF) from OA patients and matched healthy controls. Analyses were performed to determine if CGRP levels correlated with available clinical and radiographic parameters from the OA patients. Finally, descriptive statistics were performed to summarize the frequency for different ranges of fold change of OA SF over plasma CGRP levels.
Methods: Plasma collected in EDTA-tubes and knee SF collected in red top tubes (N = 145 paired samples), from OA patients being assessed for knee pain and/or joint replacement were obtained from the Indiana University Methodist Research Institute Biorepository Program. Similarly prepared plasma (N = 51) and SF (N = 10), unpaired samples from healthy volunteers, were obtained from additional repositories. CGRP levels were assessed by an in-house, sensitive CGRP quantitation assay validated for plasma and SF in the pg/ml range. The assay detected both α-CGRP and β-CGRP isoforms. Additional data considered when available were age, gender, race/ethnicity, knee radiographs and/or knee radiograph reports sufficient to calculate Kellgren-Lawrence (K-L) scores, comorbidities and medications. Statistical analyses were performed by two-sample t-tests and Pearson Correlation Analysis using GraphPad Prism statistical software. A significant p-value cutoff was set at 0.05.
Results: Of the 145 OA patients, 57 had available medical information and 49 had available knee radiographs and/or reports. The average K-L score was 3.2, average age was 64 years, 63% were female and 88% were white. The average plasma CGRP levels from OA patients were higher than those from matched healthy controls, (3.37 +/-2.34 vs 2.46+/- 1.23 pg/ml, p = 0.007). The average plasma CGRP levels from OA patients were 1.4-fold higher than the plasma from matched healthy controls. Increased plasma CGRP levels in the OA patients trended with more severe K-L scores and with additional evidence of joint pathology, namely fixed or loose joint bodies, chondrocalcinosis, or pronounced bony deformities. SF CGRP levels from OA patients were 16-fold higher than SF levels from healthy controls, (3.35+/-1.65 vs 0.20+/- 0.19, p3 (N = 36), more severe OA joint pathology (N = 14), or increased joint space narrowing (N = 29) had higher SF and plasma CGRP level correlations, (Pearson r = 0.58 vs 0.60 vs 0.64, respectively). The percentage of coefficient variation for OA SF duplicate samples was 20%. Seventy-nine % of the ratios of OA SF and plasma CGRP levels were within 2-fold. In 13%, the SF CGRP levels were ≥ 2 fold higher than plasma levels (fold change range = 2-9).
Conclusions: Significantly elevated CGRP levels were demonstrated in the plasma and knee SF of OA patients being evaluated for knee pain and/or arthroplasty. This study was limited by incomplete clinical data on many of the OA patients. Moreover, pain levels of these patients were not recorded and therefore could not be included in analysis. In 79% of the OA sample pairs, the ratio of OA and plasma CGRP levels highly agreed, with each other, as ratios were within 2 fold. The above results suggest that diffusion from plasma and/or components of the OA joint itself are sources of CGRP in the SF. Plasma CGRP levels represent a potentially novel, minimally-invasive disease biomarker and therapeutic tailoring opportunity to identify OA patients who might benefit from CGRP-modulating therapies.

122

HIGH SERUM LEPTIN LEVELS ARE ASSOCIATED WITH LOW SERUM VITAMIN D, MUSCLE STRENGTH, AND PHYSICAL PERFORMANCE IN KNEE OSTEOARTHRITIS PATIENTS

P. Manoy, P. Yuktanandana, A. Tanavalee, W. Anomasiri, S. Honsawek. *Chulalongkorn Univ., Bangkok, Thailand*

Purpose: Vitamin D and leptin play a critical role in energy metabolism; however, the relationship between vitamin D and leptin in osteoarthritis (OA) is not well established. The purpose of this study was to examine serum levels of leptin and vitamin D in knee OA patients and to explore the possible relationship between serum leptin, vitamin D, physical performance, and disease severity in OA patients of a South-East Asian country.
Methods: In a cross-sectional study, 235 adult patients (112 women and 23 men, aged 65.6 ± 6.5 years) with established diagnosis of OA were consecutively recruited. Serum 25-hydroxycholecalciferol (25(OH)D), serum leptin, calcium, phosphorus, and intact parathyroid hormone (iPTH) were measured. Physical performance including grip strength and muscle strength were also assessed.
Results: Serum vitamin D insufficiency (≤ 75 nmol/L) was found in 48% of patients with OA, whereas serum vitamin D deficiency (≤ 25 nmol/L) was detected in 35% of osteoarthritis patients. Our results demonstrated a positive association between serum 25(OH)D and physical performance in osteoarthritis patients (P<0.001). In addition, serum 25(OH)D concentration was inversely associated with fat mass and iPTH in the knee OA patients (P<0.001). Serum leptin expression was significantly elevated in OA patients when compared with the controls (P = 0.02). There was a negative correlation between serum 25(OH)D concentration and serum leptin in patients with knee OA (P<0.001). In a multivariate regression analysis, serum leptin was inversely related to significant serum 25(OH)D, muscle strength, and physical performance after accounting for age, gender, body mass index, and fat mass.
Conclusions: Vitamin D insufficiency and deficiency is highly prevalent in OA patients and is associated with higher serum leptin. Elevated serum leptin and low serum 25(OH)D levels were associated with poor physical performance in osteoarthritis patients. These findings suggest that high serum leptin could be used for predicting low vitamin D, poor muscle strength, and physical performance in osteoarthritis patients.

Sphingolipid Metabolites are Upregulated in Human Synovial Fluid Following Articular Fracture

Bridgette D. Furman[1], Kelly K. Kimmerling[1], Sivapriya Ramamoorthy[2], Yi-Ju Li[1], Yi-Hung Wu[1], Janet L. Huebner[1], Farshid Guilak[3], Virginia B. Kraus[1], Steven A. Olson[1]

[1]Duke University, Durham, NC, [2]Metabolon, Durham, NC, [3]Washington University and Shriners Hospitals for Children, St. Louis, MO

Disclosures: Bridgette Furman (N), Kelly Kimmerling (N), Sivapriya Ramamoorthy (3A-Metabolon), Yi-Ju Li (N), Yi-Hung Wu (N), Janet Huebner (N), Farshid Guilak (N), Virginia Kraus (N), Steven Olson (5)

INTRODUCTION: Post-traumatic arthritis (PTA) is a clinically important complication of joint injury with life-long effects for the patient,[1,2] and associated with a severe burden in active duty and discharged soldiers.[3] While PTA can occur rapidly after moderate to severe articular injuries, not every patient will go on to develop this condition. There are no effective screening methods to determine who is at risk for developing PTA. The knee is a complex joint with many components, making it vulnerable to a variety of injuries, including articular fracture. Articular synovial fluid (SF) is a complex mixture of components that regulate nutrition, communication, shock absorption and lubrication of the knee joints. A precise profile of the chemical composition of SF during disease-related alteration will increase our knowledge about the pathogenesis and possible options to treat these joints. Importantly, understanding the relationship between specific compositional changes in the synovial fluid and the onset of PTA could provide biomarkers that could be useful for stratifying patients for therapeutic intervention. This global metabolic profiling study was conducted to identify synovial fluid biomarkers to discriminate the healthy from the injured knee and the metabolic pathways affected by knee injury.

METHODS: Patients with unilateral articular fracture of the knee were enrolled in an IRB and USAMRMC Human Research Protection Office (HRPO) approved study. Of the 20 subjects enrolled between October 2012 and December 2014, eight patients had synovial fluid collected without dilution from both the fractured (Fx) and contralateral non-fractured (Non-Fx) knee. Synovial fluid was centrifuged at 3500 rpm and stored in aliquots at -80° until analyses. High throughput characterization of the global metabolic profile of synovial fluid samples from both knees of each patient was performed using Ultrahigh Performance Liquid Chromatography-Tandem Mass Spectroscopy (UPLC-MS/MS). Each biochemical analyte was rescaled to set the median equal to 1. Paired t-tests were used to test the differences of biomarkers in synovial fluid between the injured limb and the contralateral control limb. The Benjamini-Hochberg (BH) method was used to control for false discovery rate (FDR) due to multiple testing. We identified 220 out of 710 metabolites meeting BH adjusted p-value < 0.05.

RESULTS: Among the top 19 metabolites most significantly elevated in synovial fluid from the fractured knee (p<0.0002, BH adjusted p = 0.0065), a prominent metabolic pathway involved was complex lipid composition. Evidence of increased sphingomyelin (SPM) synthesis was observed with increases in SPMs (Figure 1) and 2-hydroxy- fatty acids that are specialized fatty acids found in SPMs. In addition to accumulation of sphingomyelins, elevated levels of various phospholipid derivatives were also observed in the injured knee relative to the contralateral control limb. Although phospholipids are implicated in joint lubrication, sphingomyelin has been shown to progressively increase in the synovial fluid of, early-stage and late-stage patients with osteoarthritis.[4]
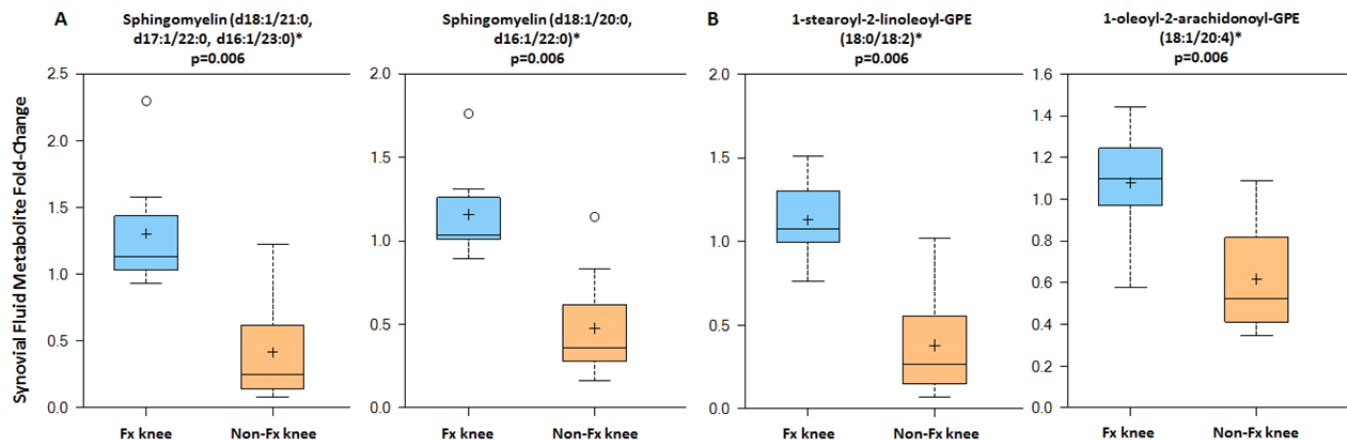

Figure 1. Fractured (Fx) knees showed significant fold increases in (**A**) sphingomyelin and (**B**) phospholipid metabolites following articular fracture.

DISCUSSION: To date, there are no clinical methods to identify patients at high risk for developing PTA following intra-articular fracture or other joint injuries. Early identification of disease progression in PTA would be valuable for selecting high-risk patients as candidates for interventional therapies and for better understanding of the mechanism of disease progression. This study demonstrates that that altered lipid metabolism could be a risk factor and/or consequence of knee injury. Sphingolipids have been previously identified in synovial fluid[5] and are a class of lipids that include sphingomyelins, ceramide species, and more complex glycosphingolipids. Recent reports on lipidomic analyses of synovial fluid have shown an association of increased sphingomyelin with progression of OA[4] and also altered lipid profiles in synovial fluid following articular fracture in the ankle.[6] Understanding of lipid compositional changes in synovial fluid following joint injury may provide insight into pathologic changes in articular cartilage associated with PTA, as well as potential markers of disease onset and progression. Further followup on the clinical outcomes are necessary to determine the relationships between these biomarker levels and PTA.

SIGNIFICANCE: Taken together with the literature, these findings suggest that elevated sphingomyelins, phospholipids, and subsequent lipid metabolites in synovial fluid are biomarkers of knee injury and potential prognostic indicators of risk of post-traumatic arthritis.

REFERENCES: 1. CDC 2011; 2. Brown JOR 2006; Cross JAAOS 2011; 4. Kosinska A&R 2013; 5. Kosinska PLOSone 2014; 6. Leimer JOR 2016

Synovial Fluid Analysis Reveals a Novel Panel of Vascular and Inflammatory Biomarkers that are Altered Following Articular Fracture

Janet L Huebner[1], Bridgette D. Furman[1], Kelly K. Kimmerling[1], Yi-Ju Li[1], Yi-Hung Wu[1], Farshid Guilak[2], Steven A. Olson[1], Virginia B. Kraus[1]
[1]Duke University, Durham, NC, [2]Washington University and Shriners Hospitals for Children, St. Louis, MO

INTRODUCTION: Post-traumatic arthritis (PTA) is a frequent and clinically important complication of joint injury. While PTA can occur rapidly after articular fracture, not every patient will develop this condition. There are currently no effective screening methods to determine who is at risk for developing PTA. The overall objective of this study was to identify biomarkers following articular fracture that may be associated with joint injury and predictive of the development of PTA.

METHODS: Patients with unilateral articular fracture of the knee were enrolled in an IRB- and USAMRMC Human Research Protection Office (HRPO)-approved study. Of the 20 subjects enrolled between October 2012 and December 2014, eight patients (50% female; 25-83 years of age; average BMI 32.4 kg/m^2) had synovial fluid collected by direct aspiration (without dilution) from both the fractured (Fx) and contralateral non-fractured (Non-Fx) knee. Synovial fluid was centrifuged at 3500 rpm and stored in aliquots at -80° until analyses. ELISA assays were used to quantify synovial fluid levels of 40 acute inflammatory and injury markers as well as markers of joint metabolism (8 analytes). Joint tissue markers included matrix metalloproteinases (MMP)-1, -2, -3, -9, and -10, cartilage oligomeric matrix protein (COMP), sulfated glycosaminoglycans (sGAG), and C-terminal telopeptide of type II collagen (CTXII). Paired t-tests were used to test the differences of biomarkers in synovial fluid between the injured limb (Fx) and the contralateral control limb (non-Fx). The Benjamini-Hochberg (BH) method was used to control for false discovery rate (FDR) due to multiple testing. Biomarkers meeting BH adjusted p-value < 0.05 were identified. Ingenuity Pathway Analysis (IPA) was used to identify pathways of relevance.

RESULTS: Comparisons of biomarker concentrations in SF from Fx and non-Fx knees identified 16 analytes of the 48 measured having significantly higher concentrations in SF from the fractured knee (Table 1). These biomarkers were associated with inflammatory response (14 of 16) and injury (15 of 16) and are illustrated as they are associated with molecular events following fracture (Figure 1). Upon injury, vascular disruption occurs resulting in the release of biomarkers of angiogenesis (VEGF, VEGF-C, VEGF-D, PIGF) which upregulate the expression of MMPs[1]. This is followed by an inflammatory stage in which macrophages and other immune cells are recruited to the fracture sites and secrete proinflammatory cytokines (IL-4, IL-8, IL17a, TNF-α)[2], resulting in synovitis and eventual cartilage degradation.

DISCUSSION: Upon injury, the articular surface is exposed to a multitude of inflammatory cytokines and chemokines that may play a role in the development of post-traumatic arthritis. Of those identified herein, members of the VEGF family may be indicative of inflammation and are essential to fracture healing and induce soluble Tie-2.[3,4] TNF-α is a known acute phase inflammatory mediator, IL-8 plays a chemoattractant role in guiding neutrophils through the tissue matrix to the site of injury[5], and IL-17 promotes joint inflammation and cartilage degradation by enhancing production of proinflammatory cytokines and chemokines as well as upregulating the expression of MMPs[6]. Soluble VCAM-1 and ICAM-1 were reported to correlate with synovitis as determined by MRI.[7] Presently, surgical restoration of the articular surface is the only treatment for articular fractures. Adjunctive therapies to surgery may be required to improve outcomes and reduce the prevalence of PTA. Identification of the inflammatory mediators involved in acute injury may provide key insights into potential adjunctive therapies that could improve outcomes following surgery. In addition, the patterns of biomarkers following acute injury may aid in risk stratification and identification of those at highest risk for developing PTA.

SIGNIFICANCE: Characterizing the synovial fluid milieu after fracture may provide a means of identifying patients at risk for PTA following articular fracture, and serves as a first step in the development of potential therapies and early intervention strategies that could prevent the development of PTA.

REFERENCES: 1. Wang and Keiser, *Circ. Res*. 1998; 2. Marzona and Pavolini, *Clin Cases Min Bone Metab*, 2009; 3. Beamer, *HSS J*, 2010; 4. Findley, *J Am Col Cardio,* 2008; 5. deOliveira, *J Immunol*, 2013; 6. Kirkham, *Immunol*, 2014; 7. Anderson, *Arthritis Rheum*, 2009.

Table 1. Synovial fluid biomarkers significantly upregulated by injury.

Biomarker	Fold Change (Fx/NonFx)	p-value	Adjusted p (BH FDR)
Tie-2	2.42	0.000144	0.00386
VEGF	8.06	0.000158	0.00386
TNF-α	2.32	0.000734	0.01199
MMP-10	2.72	0.001563	0.01603
ICAM-1	2.28	0.001636	0.01603
IL-8	17.65	0.002963	0.02055
MMP-2	1.39	0.003521	0.02055
MMP-3	1.92	0.003666	0.02055
Flt1	10.48	0.003845	0.02055
VEGF-D	2.09	0.004194	0.02055
PIGF	5.24	0.008368	0.03417
IL-4	26.2	0.013848	0.04860
VCAM-1	1.9	0.014273	0.04860
IL17a	2.59	0.015459	0.04860
VEGF-C	6.11	0.01587	0.04860
Eotaxin	1.96	0.017224	0.04965

Figure 1. Model of molecular events following articular fracture.
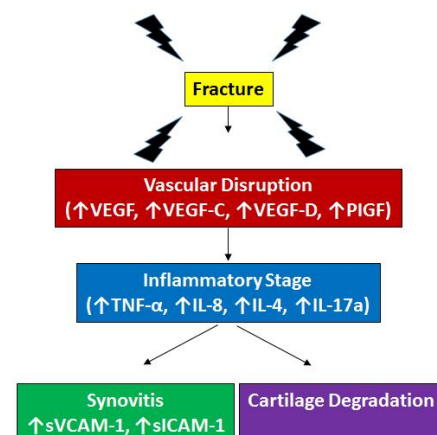
Extremity War Injuries XII:
Homeland Defense as a Translation of War Lessons Learned

January 30 – February 1, 2017 / Mandarin Oriental Hotel / Washington, DC
Symposium Co-Chairs: Andrew Schmidt, MD and MAJ Daniel Stinner, MD
Scientific Director: LTC Justin Orr, MD
EWI Project Team Chair: COL (Ret.) James Ficke, MD

POSTER SESSION CALL FOR ABSTRACTS
Deadline: ~~October 10, 2016~~ EXTENDED TO October 24, 2016

The American Academy of Orthopaedic Surgeons (AAOS) is accepting abstracts for combat casualty, trauma-related, and extremity war injury / rehabilitation research. Up to 20 abstracts will be selected for display at the 2017 Extremity War Injuries Symposium (EWI), January 18-20, at the Mandarin Oriental Hotel in Washington, DC.

If your abstract is accepted for exhibition, your poster will be displayed January 31 and February 1, with a dedicated poster session from 6:00 – 7:00 PM on Tuesday, January 31. You must be present to participate in the poster session. **Selected posters will be invited to give a brief podium presentation during the symposium.** The $600 EWI registration fee is waived for poster presenters. Presenters will be responsible for hotel and travel costs associated with attending the EWI symposium. CME (up to 15.5 hours) will be available for EWI XII attendees/participants.

Please complete this form and submit with a copy of your CV to Erin Ransford, AAOS Manager, Research Advocacy, at ransford@aaos.org by October 24, 2016.

Full Name: Steven A. Olson, MD
Military Rank (if applicable):
Institution/Organization: Duke University Medical Center
Mailing Address: Box 3389 200 Trent Drive, Room 5332, Orange Zone 5th floor
City /State/Zip: Durham NC 27710
Email: steven.olson@duke.edu
Phone: 919-668-3000

Abstract Title: Characterization of the Synovial Fluid Milieu after Articular Fracture

Abstract Text (limited to 3,000 characters, including spaces [~500 words])
The form will expand as you type/paste text.
Post-traumatic arthritis (PTA) is a severe burden in active duty and discharged soldiers. While PTA can occur rapidly after an articular fracture, not every patient will develop PTA. There are currently no screening methods to determine who is at risk for developing PTA. The overall objective of this study was to identify biomarkers following articular fracture that may be associated with joint injury.

Patients with unilateral articular fracture of the knee were enrolled in an IRB- and USAMRMC HRPO-approved study. Of the 20 subjects enrolled, 8 patients (50% female; 25-83 years of age; average BMI 32.4 kg/m2) had synovial fluid (SF) collected from both knees, fractured (Fx) and contralateral non-fractured (Non-Fx). SF levels of inflammatory, injury, and joint metabolism markers were quantified using ELISA assays. Paired t-tests were used to test the differences of biomarkers in SF between Fx and non-Fx limbs and were corrected for multiple comparisons using the Benjamini-Hochberg (BH) method. Ingenuity Pathway Analysis was used to identify pathways of relevance.

Comparisons of biomarker concentrations in SF from Fx and non-Fx knees identified 16 analytes of the 48 measured having significantly higher concentrations in SF from the fractured knee (BH adjusted p-value <0.05). These biomarkers were associated with inflammation (14 of 16) and injury (15 of 16), and are associated with molecular events following fracture. Our data indicate that vascular disruption occurs resulting in the release of biomarkers of angiogenesis (VEGF, VEGF-C, VEGF-D, PIGF) which upregulate the expression of MMPs. This is followed by an inflammatory phase in which macrophages and other immune cells are recruited to the fracture sites and secrete proinflammatory cytokines (IL-4, IL-8, IL17a, TNF-α), resulting in synovitis (VCAM-1, ICAM-1) and eventual cartilage degradation.

Upon injury, articular cartilage is exposed to inflammatory cytokines and chemokines that may play a role in PTA development. Of those identified here, members of the VEGF family may be indicative of inflammation and are essential to fracture healing . TNF-α is a known acute phase inflammatory mediator, IL-8 plays a chemoattractant role in guiding neutrophils through the tissue matrix to the site of injury, and IL-17 promotes joint inflammation and cartilage degradation by enhancing production of proinflammatory cytokines and chemokines, as well as upregulating the expression of MMPs. VCAM-1 and ICAM-1 are reported to correlate with synovitis as determined by MRI. Presently, surgical restoration of the articular surface is the only treatment for articular fractures. Identification of the inflammatory mediators involved in acute injury may provide key insights into potential adjunctive therapies that could improve outcomes following surgery. In addition, these patterns of biomarkers following acute injury may aid in identifying those at highest risk for developing PTA.

Appendix II. Manuscripts for Publication

DoD-TRP Award – Assessment of Biomarkers Associated with Joint Injury and Subsequent Posttraumatic Arthritis

Summaries for the four manuscripts in progress are listed below and the draft of paper 1 is attached.

1. Acute *In Vivo* Metrics of Joint Incongruity Following Articular Fracture Predict Post-Traumatic Arthritis in Mice – in preparation for submission to JBJS-Am (draft attached)

2. Articular Fracture in the Human Knee Increases Local Biomarkers and Metabolites – in preparation based on findings summarized in attached abstracts presented at OARSI 2016 and ORS 2017

3. Regional Loss of Cartilage is the Patella following Human Knee Articular is correlated to Biomarkers and Metabolites – in preparation

4. Comparison of Biomarkers of PTA in Murine Model to Findings from Human Knee Fracture – in preparation

Acute *In Vivo* Metrics of Joint Incongruity Following Articular Fracture Predict Post-Traumatic Arthritis in Mice

Tyler J. Vovos, BS[1]
Bridgette D. Furman, MS[1,2]
Kelly A. Kimmerling, BS[1,2]
Cindy L. Green, PhD[3]
Louis E. Defrate, PhD[1,2]
Farshid Guilak, PhD[1,2]
Steven A. Olson, MD[1]

1. Department of Orthopaedic Surgery
   Duke University Medical Center
   Durham, NC

2. Department of Biomedical Engineering
   Duke University Medical Center
   Durham, NC

3. Department of Biostatistics and Bioinformatics
   Duke University Medical Center
   Durham, NC

Please address all correspondence to:

Tyler J. Vovos, BS
375 Medical Sciences Research Building
DUMC Box 3093
Duke University Medical Center
Durham, NC 27710
Phone: (608)577-3701
Fax: (919)684-2521
Email: Tyler.Vovos@dm.duke.edu

Abstract

Objectives: Post-traumatic arthritis (PTA) occurs commonly after articular fracture. Joint degeneration may arise in part from surface incongruity after injury. Radiographic classification systems do not account for 3D geometry of the joint surface. CT-based measures of joint fracture severity have been used to predict ankle PTA development. Interestingly, the MRL/MpJ "superhealer" mouse strain is protected from PTA following articular fracture, thus providing valuable insight into the progression of PTA. Currently, the relationship between initial injury severity, articular displacement, and PTA development following articular fracture remains unknown. The objective of this study was to develop *in vivo* microCT metrics of joint incongruity after articular fracture to further characterize the pathomechanism of PTA.

Methods: C57BL/6 and MRL/MpJ mice (n=12/strain) received closed articular fractures (fx) of the tibia (Fig 1). At 8wks, mice were sacrificed and assessed for arthritic changes (Mankin score). *In vivo* microCT was performed pre- and post-fx, 1, 4, and 8wks post-fx. Displacements of the bone surface, or Bone Surface Deviations (BSD), were quantified for the lateral and medial tibial plateau (Fig 1). Serum biomarkers of bone metabolism were measured pre- and post-fx to 6wks. BSDs were analyzed using ANOVA and bone markers using nonparametric analyses.

Results: Temporal patterns in BSDs were significantly different between mice with larger average positive axial deviations found in C57BL/6 mice at 8wks post-fx (p=0.01;Fig 2). Mankin scores were correlated to all BSDs in both mouse strains. Acute BSDs showed the strongest correlations with PTA development. In C57BL/6 mice, axial BSDs on post-fx day 0 were highly predictive of PTA severity at 8wks post-fx (Fig 3). In contrast, MRL/MpJ mice post-fx day 0 BSDs did not predict PTA development. Serum PINP, a bone formation marker, in the C57BL/6 mice were significantly lower than the MRL/MpJ mice post-fx (p=0.005), indicating a less robust acute response compared with the superhealer strain.

Conclusions: Acute displacements of the bone surface following articular fracture were predictive of arthritis development in C57BL/6 but not MRL/MpJ mice. C57BL/6 mice also showed an acute drop in serum PINP compared to MRL/MpJ mice. These findings suggest that MRL/MpJ mice undergo a unique mechanism of fracture healing following articular fracture and that joint incongruities secondary to articular fracture do not predispose MRL/MpJ mice to PTA development. Whereas, PTA development in C57BL/6 mice is predicted by acute bone displacements and decreased bone metabolism. *In vivo* CT metrics of joint incongruity provide a method for quantifying bone surface incongruities that have traditionally been difficult to measure. The translational potential of our joint incongruity metrics is high, as they could readily be applied to full scale clinical CT scans.

Introduction

Posttraumatic arthritis (PTA) is the clinical syndrome of progressive joint degeneration that occurs following injury to weight bearing joints. PTA represents a significant challenge for orthopaedic surgeons and the US healthcare system. Estimates suggest that PTA is responsible for 12% of the 27 million cases of osteoarthritis (OA) in the US. The financial burden of PTA is significant, as it is estimated to cost the US economy over $7 billion annually in work productivity and medical expenses [1].

Importantly, PTA occurs predictably after articular fracture [1-3]. The current standard of care for articular fractures is surgical reduction and fixation. Despite optimal surgical management of fractures, the incidence of post-traumatic arthritis remains high [4]. Articular surface incongruity, or "step-off", may contribute to poor outcomes after articular fracture. Even the smallest incongruities are thought to cause long-term alterations in joint loading and degeneration of cartilage [4, 5]. Recently, Parkkinen et al. reported increased PTA severity in patients with residual articular incongruity greater than 2 mm after surgical fixation of intraarticular tibial plateau fractures[6]. While classification systems and prior CT-based metrics have accounted for fracture severity, they have not accounted for incongruities in the articular surface [7-9].

To further characterize arthritis development following articular fracture, we developed a physiologically relevant murine model of closed intraarticular fracture of the tibial plateau [10]. Using this model, we can reproducibly create clinically relevant articular fractures of moderate severity in the murine lateral tibial plateau. Repeated studies have shown that in the absence of surgical fixation fractured limbs progress to arthritis after 8 weeks[10-13].

To differentiate favorable from non-favorable healing in post-traumatic arthritis we have studied the MRL/MpJ "Superhealer" mouse strain with our fracture model. The MRL mouse has a unique ability to regenerate a number of tissues including articular cartilage [14-16]. Further, the mouse strain is protected from post-traumatic arthritis after articular fracture relative to the wild-type C57BL/6, or Black6 mouse strain, and has reduced serum and synovial fluid levels of IL-1 and TNF-α acutely following fracture [11, 17]. Despite this knowledge, the relationship between articular surface incongruities and the development of post-traumatic arthritis following articular fracture in the MRL and other mouse strains remains unknown.

In the current study, we hypothesized that quantitative measures of joint incongruity can predict arthritis after articular fracture. Further, we hypothesized that the MRL/MpJ mouse strain has an altered fracture healing response relative to the Black6 mouse strain. The objective of the current study was to develop in vivo microCT metrics of joint incongruity after articular fracture and correlate these metrics to arthritis development.

Materials and Methods

Animal Selection

All animal procedures were performed in accordance with protocols approved by the Duke University Institutional Animal Care and Use Committee (IACUC) and the United States Army Medical Research and Materiel Command Animal Care and Use Review Office (USAMRMC ACURO). Male C57BL/6 mice (n=12) were obtained from Charles River (Wilmington, MA) and Male MRL/MpJ mice (n=12) were obtained from The Jackson Laboratory (Bar Harbor, ME).

Closed Intra-Articular Fracture

Mice were housed until 16 weeks of age to ensure skeletal maturity [18, 19], at which time all mice received intraarticular fracture as previously described [10]. Animals were anesthetized using isoflurane gas then placed in a custom cradle with the left hind limb in a neutral position of 90° flexion and secured at the ankle, the right hind limb served as a control. The location of the tibial plateau was determined by manual blunt probing. A 10N compressive preload was applied using a wedge-shaped stainless steel indenter mounted to a materials testing system (ELF3200; Bose, Framingham, MA, USA). Moderately severe fractures were created in the lateral tibial plateau of all mice by loading the tibial plateau in compression at a rate of 20N/second to a maximum load of 55N. As previously described [11], indenter displacement limits were scaled relative to the size of the tibial plateau in mouse strains to create fractures of similar severity; a limit of 2.7 mm was used for C56BL/6 mice and a limit of 3.2 mm was used for the larger MRL/MpJ mice. No surgical or fixative interventions were employed. All mice received an analgesic (buprenorphine, 48 h) immediately after fracture and allowed immediate weight bearing and motion. Fracture energy was calculated from the area under the load-displacement curve.

Measuring Biomarkers of Bone Metabolism

Serum was collected via retro-orbital bleed at pre-fracture, post-fracture, on day 4, and every 2 weeks until 6 weeks post-fracture. Serum concentrations of biomarkers of bone metabolism were measured: procollagen type I N-propeptite (PINP), a bone formation marker; and C-terminal telopeptide of type 1 collagen (CTXI), a bone resorption marker.

Histological Assessment of Arthritis Severity

All animals were sacrificed 8 weeks post-fracture and knees were harvested for histologic assessment of arthritis. Limbs were formalin fixed for 48 hours then decalcified (Cal-Ex Decalcification Solution, Fisher Scientific, Pittsburgh, PA) for 120 hours, processed, and paraffin-embedded for histology using a commercially available automated tissue processor (ASP300S, Leica Biosystems, Buffalo Grove, IL). Histological sections were taken at 8µm in the coronal plane of the joint. Sections that captured the tibiofemoral articulation were selected. Each quadrant–lateral tibia, lateral femur, medial tibia, and medial femur–was evaluated separately. The degree of arthritic changes was assessed from Safranin-O and fast green stained sections using a modified Mankin score [10, 20, 21]. The maximum possible score was 30 for each quadrant. The scores from all quadrants were summed for a total joint score with a possible maximum joint score of 120. A total of

three graders, blinded to treatment group, scored all specimens. The mean scores of the 3 graders were used for statistical analysis.

In Vivo Micro-Computed Tomography Scanning

In vivo micro-CT (SkyScan 1176, Bruker Corporation, Billerica, MA; 55 kV, 455 µA, 16.76 µm isotropic spatial resolution, 0.7° rotation step, 180° rotation, 242 ms exposure time) of fractured limbs was performed immediately pre- and post-fracture, then at 1, 4, and 8 weeks post-fracture. To reduce radiation exposure and anesthesia time, control hind limbs were scanned at the pre-fracture and 8 week time points. Mice were anesthetized with isoflurane gas and secured in a custom rigid foam bed to reduce motion artifact. The hind limb was then secured on a rigid foam wedge in a position of 90° flexion. Scanning regions were centered at the tibial plateau. Micro-CT datasets were reconstructed (NRecon, Bruker Corporation) using a ring artifact correction of 1 and beam hardening correction of 40%. Hydroxyapatite calibration phantoms were scanned at the start and end of the study to scale values (mg/cm^3).

Measuring Joint Incongruity

Image processing was performed using CT-Analyser software (Bruker Corporation). First, bony regions of interest were manually selected. Binary data sets were then generated using a global density threshold (454.26 mg/cm^3) to automatically segment for cortical bone. Manual contouring of binarized images was performed to segment the tibia from surrounding bony structures. Finally, surface-rendered 3D models of binary data sets were generated.

To achieve our goal of measuring joint incongruities in these models, we registered, or aligned, the intact medial plateaus of all post-fracture models to their corresponding pre-fracture model using CAD software (Figure 1) (Geomagic Studio Version 11 software, Geomagic®). This was accomplished with an iterative closest point algorithm. After registration was complete the intact portions of both scans were well aligned and joint incongruities could be measured in the disrupted portion of the post-fracture joint surface.

Joint incongruity was quantified using 3D directional deviation analysis (Figure 2) (Geomagic Control 2014 Software, Geomagic®). For the purpose of the current study, directional deviation was defined as the distance from a pre-fracture model surface to a post-fracture model surface along a single axis, or unit vector. Positive deviations represent outward projections of the post-fracture surface and negative deviations represent inward projections. We chose to measure bone surface deviations along the axial, antero-posterior, and latero-medial anatomic axes.

Ultimately, we were able to collect bone surface deviation (BSD) data at all post-fracture time points along each anatomic axis. Positive and negative deviations were reported as average and maximum values for the medial and lateral plateaus of 3D models. To normalize for size differences between mice, deviations were reported as percentages of pre-fracture 3D model size as determined by anatomic landmarks (Figure 3). Finally,

mouse strains were compared with regards to post-fracture deviation changes over time and correlations were drawn between deviation and Mankin scores for arthritis.

Statistical Analysis

Statistical analysis of differences between group means was performed using ANOVA (Tukey HSD post-hoc). Statistical analysis of within strain differences between contralateral control and fractured limbs was performed using a one-sample t-test. Regression analysis was used to analyze the relationship between measured outcomes. A Bonferroni correction was applied to regression analysis when appropriate. Repeated measures analysis was performed to determine differences between strain-wise changes across limb and over time. Bone marker concentrations were analyzed by Friedman test for repeated measures, and mouse strains were compared at each time point using the Holm-Sidak multiple t-test. For all tests, significance was reported at a 95% confidence level.

Results

Sample Population and Data Quality Assurance

Two mice from the C56BL/6 strain died during anesthesia induction and were excluded from our study. At the end of our study we had a sample population of n=22, comprised of n=10 C56BL/6 mice and n=12 MRL/MpJ mice. Images were carefully scrutinized for motion artifact and all images with evidence of such were excluded, these include: three post-fracture, three 1 week, and two 4 week datasets from the C56BL/6 strain; as well as one 1 week and one 8 week control dataset from the MRL/MpJ strain.

Bone surface deviation (BSD) analysis resulted in 24 unique measures of joint incongruity for each scan analyzed. For the purpose of quality control, deviation analysis was performed on contralateral control limbs. Contralateral control limb deviations at 8 weeks post-fracture represent the combined effects of model registration and bone remodeling. As expected, average deviations at 8 weeks post-fracture in contralateral control limbs were small. At 8 weeks post-fracture the most and least precise measures of deviation were average positive anterior-posterior deviation in the medial plateau (Mean ± SD: 0.55 ± 0.20%) and average positive axial deviation in the lateral plateau (Mean ± SD: 3.71 ± 3.15%), respectively.

Intraarticular Fracture Creation and Fracture Energy

Intraarticular fractures were successfully created in all mice (Figure 4). Fracture energy was significantly different between strains (P < 0.001), ranging from 62.83 mJ to 142.89 mJ (mean ± SD, 106.61 ± 20.31 mJ) in C57BL/6 mice and from 113.19 mJ to 182.65 mJ (mean ± SD 148.11 ± 22.09 mJ) in MRL/MpJ mice. The ratio of fracture energies in the C57BL/6 and MRL/MpJ mice was ~0.7, which is consistent with the difference in their relative tibial plateau size [11]. In C57BL/6 mice, a significant correlation between fracture energy and the total joint Mankin score for the fractured limbs was observed (R^2 = 0.8405, P = 0.0014).

No significant correlation between fracture energy and arthritis was seen in the MRL/MpJ mice.

Markers of Bone Metabolism

Concentrations of PINP in the C57BL/6 mice were significantly lower than the MRL/MpJ mice post-fx (p=0.005; Figure 5), indicating a less robust acute bone anabolic response compared with the superhealer strain. Despite higher levels of CTXI in the C57BL/6 mice compared to the MRL/MpJ at pre-fracture, no differences were found in CTXI levels post-fracture between strains or at any time point.

Progression of Post-Fracture Deviations

Application of colored bone surface deviation maps to 3D models across time points allowed for visualization of the fracture healing process (Figure 6). Repeated measures analysis was used to compare temporal patterns in bone surface deviations between C57BL/l6 and MRL/MpJ mice from post-fracture to 8 weeks post-fracture. Strain wise differences were observed for the several key measures: average positive axial deviation in the lateral and medial tibial plateau (Figure 7), average positive LM deviation in the lateral tibial plateau, average negative LM deviation in the medial tibial plateau, and maximum positive LM deviation in the lateral tibial plateau (p<0.05). For all significant differences in the lateral tibial plateau, C57BL/6 mice demonstrated a significant increase in deviation between 1 and 4 weeks post-fracture. At 8 weeks post-fracture, C57BL/6 mice demonstrated significantly larger average positive axial deviations in the lateral plateau compared to MRL/MpJ mice (p=0.006, Figure 7).

Post-Fracture Bone Surface Deviations Correlate with Arthritis Development in C57BL/6 Mice

All measures of BSD were correlated with the development of arthritis. Acute measures of BSD demonstrated a strong correlation with PTA development. Correlations between BSDs measured immediately post-fracture and total joint Mankin score for arthritis at 8 weeks post-fracture are reported (Table 1). In C57BL/6 mice, average axial BSDs in the lateral tibial plateau on post-fracture day 0 were highly predictive of PTA severity at 8 weeks post-fracture (Figure 8A and 8B). In contrast, MRL/MpJ post-fracture day 0 axial BSDs in the lateral plateau were not predictive of PTA.

Discussion

Our work resulted in the development of novel *in vivo* micro-CT metrics of joint incongruity. Applying these metrics after articular fracture allowed us to draw correlations between joint incongruity, or step-off, and the development of post-traumatic arthritis. Furthermore, analysis of bone surface deviations overtime revealed differences in fracture healing between the MRL/MpJ and C57BL/6 mouse strains.

Measurements of bone surface deviation made immediately after articular fracture were highly predictive of arthritis development in C57BL/6 mice, but not MRL/MpJ mice.

Further, C57BL/6 mice demonstrated an acute post-fracture drop in serum PINP compared to MRL/MpJ mice. Ultimately, C57BL/6 mice showed significantly larger bone surface deviations at 8 weeks post-fracture compared to the MRL/MpJ mice. Taken together, these findings suggest that the MRL/MpJ strain may undergo a unique mechanism of fracture healing following articular fracture. Further, they suggest that the MRL/MpJ strain is capable of compensating for joint incongruity following articular fracture.

Previous studies reported that C57BL/6 mice exhibit higher levels of inflammation post-fracture than the MRL/MpJ mice and suggested that this may contribute to the development and progression of PTA in this model. This inflammatory environment may influence fracture healing immediately post-fracture, potentially predisposing C57BL/6 mice to PTA. Results of the current study suggest that joint incongruities secondary to articular fracture alone do not predispose mice to the development of PTA, but rather differences in bone metabolism may play a role in early healing, which may have a greater effect on outcome. Our results may provide insights into the physiologic processes determining PTA outcomes that may protect the MRL/MpJ strain from the effects of articular incongruity. A better understanding bone metabolism in MRL/MpJ mice could provide valuable insight into the strains altered fracture healing and resistance to arthritis.

Our, novel in vivo microCT metrics of joint incongruity provide a new method for quantifying bone surface incongruities that have traditionally been difficult to measure, and provide new possibilities to improve fracture management and guide post-traumatic arthritis research. There is potential to translate microCT metrics to full scale clinical CT scans. Using a mirrored 3D model of the contralateral limb for registration, Islam et al. [22] was able to demonstrate a strong degree of symmetry between left and right human ankle joints using bone surface deviation analysis. Applying this registration method to our surface incongruity metric would allow for bone surface deviation analysis to be performed between fractured joints and intact contralateral limbs. Measures of joint incongruity could then be used as a prognostic tool for the development of PTA either before, or after surgical reduction of the fracture.

This study had some limitations. The 3D model registration process we used to derive our measures of tibial plateau surface incongruities is based off of the assumption that minimal bone remodeling occurs in the medial tibial plateau, making misinterpretation of lateral tibial plateau incongruities possible. To mitigate this effect, we selected large regions of the medial plateau for the registration of scans, and in doing so, minimized the effect small bony deviations may have on registration. Further, our measures of maximum deviation are based off of single point calculations, which are inherently subject to noise. In the future, we will address this issue by lowering the sensitivity of the maximum deviation measurement. Finally, recent studies have shown that misalignment of the knee correlates with the development of PTA [6]. Unfortunately, we were unable to measure joint alignment in the mouse knee, as *in vivo* micro-CT requires positioning the limb in a way that may misrepresent its natural alignment.

Future work includes optimization of our surface deviation metrics and the creation of a refined predictive model for PTA that encompasses all 96 metrics of surface deviation.

Achieving reproducibility by applying this advanced model to future knee fracture studies will further validate our metrics. The present study is a sub-study of a larger project funded by a Department of Defense Translational Research Partnership Award, for which we hope to draw comparisons between our animal model and humans with regards to the mechanical and inflammatory progression of PTA. In the current study, we collected small volumes of serum longitudinally in mice. These serum samples will be analyzed for markers of bone remodeling for comparison with our measures of joint incongruity. We hope to use our understanding of the differences in joint incongruity and bone healing response between the C57BL/6 and MRL/MpJ strains to better understand differences between human subjects who develop PTA and those that are protected from PTA, respectively.

In summary, acute displacements of the bone surface following articular fracture were highly predictive of arthritis development in Black6 but not MRL mice. Black6 mice showed significantly larger bone surface deviations at 8 weeks post-fracture compared to MRL mice. Together, these findings suggest that the MRL mouse strain undergoes a unique mechanism of fracture healing following articular fracture. We hope to better understand these differences through serum analysis of bone remodeling biomarkers. The metric derived from this study provides a powerful tool for PTA research and provides new possibilities for improving the management of fractures.

Bibliography

1. Brown, T.D., et al., *Posttraumatic osteoarthritis: a first estimate of incidence, prevalence, and burden of disease.* J Orthop Trauma, 2006. **20**(10): p. 739-44.
2. Olson, S.A. and J.L. Marsh, *Posttraumatic osteoarthritis.* Clin Orthop Relat Res, 2004(423): p. 2.
3. Buckwalter, J.A. and T.D. Brown, *Joint Injury, Repair, and Remodeling.* Clinical Orthopaedics and Related Research, 2004. **423**: p. 7-16.
4. Matta, J.M., *Fractures of the acetabulum: accuracy of reduction and clinical results in patients managed operatively within three weeks after the injury.* J Bone Joint Surg Am, 1996. **78**(11): p. 1632-45.
5. Llinas, A., et al., *Healing and remodeling of articular incongruities in a rabbit fracture model.* J Bone Joint Surg Am, 1993. **75**(10): p. 1508-23.
6. Parkkinen, M., et al., *Factors predicting the development of early osteoarthritis following lateral tibial plateau fractures Mid-term clinical and radiographic outcomes of 73 operatively treated patients.* Scand J Surg, 2014.
7. Dirschl, D.R. and P.A. Dawson, *Injury Severity Assessment in Tibial Plateau Fractures.* Clinical Orthopaedics and Related Research, 2004. **423**: p. 85-92.
8. Anderson, D.D., et al., *Quantifying tibial plafond fracture severity: absorbed energy and fragment displacement agree with clinical rank ordering.* J Orthop Res, 2008. **26**(8): p. 1046-52.
9. Thomas, T.P., et al., *Objective CT-based metrics of articular fracture severity to assess risk for posttraumatic osteoarthritis.* J Orthop Trauma, 2010. **24**(12): p. 764-9.

10. Furman, B.D., et al., *Joint degeneration following closed intraarticular fracture in the mouse knee: a model of posttraumatic arthritis.* J Orthop Res, 2007. **25**(5): p. 578-92.

11. Ward, B.D., et al., *Absence of posttraumatic arthritis following intraarticular fracture in the MRL/MpJ mouse.* Arthritis Rheum, 2008. **58**(3): p. 744-53.

12. Diekman, B.O., et al., *Intra-articular delivery of purified mesenchymal stem cells from C57BL/6 or MRL/MpJ superhealer mice prevents posttraumatic arthritis.* Cell Transplant, 2013. **22**(8): p. 1395-408.

13. Louer, C.R., et al., *Diet-induced obesity significantly increases the severity of posttraumatic arthritis in mice.* Arthritis Rheum, 2012. **64**(10): p. 3220-30.

14. Clark, L.D., R.K. Clark, and E. Heber-Katz, *A new murine model for mammalian wound repair and regeneration.* Clin Immunol Immunopathol, 1998. **88**(1): p. 35-45.

15. Bedelbaeva, K., et al., *Lack of p21 expression links cell cycle control and appendage regeneration in mice.* Proc Natl Acad Sci U S A, 2010. **107**(13): p. 5845-50.

16. Fitzgerald, J., et al., *Evidence for articular cartilage regeneration in MRL/MpJ mice.* Osteoarthritis Cartilage, 2008. **16**(11): p. 1319-26.

17. Lewis, J.S., Jr., et al., *Genetic and cellular evidence of decreased inflammation associated with reduced incidence of posttraumatic arthritis in MRL/MpJ mice.* Arthritis Rheum, 2013. **65**(3): p. 660-70.

18. Beamer, W.G., et al., *Genetic variability in adult bone density among inbred strains of mice.* Bone, 1996. **18**(5): p. 397-403.

19. Sheng, M.H.C., et al., *Histomorphometric studies show that bone formation and bone mineral apposition rates are greater in C3H/HeJ (high-density) than C57BL/6J (low-density) mice during growth.* Bone, 1999. **25**(4): p. 421-429.

20. Mankin, H.J., M.E. Johnson, and L. Lippiello, *Biochemical and metabolic abnormalities in articular cartilage from osteoarthritic human hips. III. Distribution and metabolism of amino sugar-containing macromolecules.* J Bone Joint Surg Am, 1981. **63**(1): p. 131-9.

21. Carlson, C.S., et al., *Synovial fluid biomarker levels predict articular cartilage damage following complete medial meniscectomy in the canine knee.* J Orthop Res, 2002. **20**(1): p. 92-100.

22. Islam, K., et al., *Symmetry analysis of talus bone: A Geometric morphometric approach.* Bone Joint Res, 2014. **3**(5): p. 139-45.

Acknowledgments

			C57BL/6	MRL/MpJ
Axial	Lateral Plateau	Average Positive	R2 = .507902; P = .1767	R2 = .043317; P = .5163
		Average Negative	R2 = .670472; P = .0900	R2 = .235678; P = .1096
		Maximum Positive	**R2 = .994132; P = .0002**	R2 = .035706; P = .5564
		Maximum Negative	**R2 = .989104; P = .0005**	R2 = .020712; P = .6554
	Medial Plateau	Average Positive	R2 = .000020; P = .9943	R2 = .138081; P = .2343
		Average Negative	R2 = .26187; P = .3781	R2 = .403871; P = .0264
		Maximum Positive	R2 = .027227; P = .7909	R2 = .006291; P = .8064
		Maximum Negative	R2 = .034164; P = .7660	R2 = .300458; P = .0650
AP	Lateral Plateau	Average Positive	**R2 = .943727; P = .0058**	R2 = .251188; P = .0969
		Average Negative	R2 = .715259; P = .0710	R2 = .403218; P = .0265
		Maximum Positive	R2 = .847584; P = .0265	R2 = .00005539; P = .9817
		Maximum Negative	R2 = .734391; P = .0635	R2 = .028634; P = .5991
	Medial Plateau	Average Positive	R2 = .016568; P = .8366	R2 = .087822; P = .3496
		Average Negative	R2 = .093639; P = .6166	**R2 = .54222; P = .0063**
		Maximum Positive	R2 = .023703; P = .8048	R2 = .251041; P = .0970
		Maximum Negative	R2 = .078003; P = .6491	R2 = .017647; P = .6807
LM	Lateral Plateau	Average Positive	R2 = .535194; P = .1601	R2 = .018326; P = .6749
		Average Negative	R2 = .509161; P = .1759	R2 = .235861; P = .1095
		Maximum Positive	R2 = .265922; P = .3738	R2 = .11542; P = .2800
		Maximum Negative	R2 = .60721; P = .1203	R2 = .104842; P = .3046
	Medial Plateau	Average Positive	R2 = .050921; P = .7151	R2 = .126807; P = .2559
		Average Negative	R2 = .129022; P = .5527	R2 = .02139; P = .6501
		Maximum Positive	R2 = .151705; P = .5169	R2 = .042714; P = .5193
		Maximum Negative	R2 = .281133; P = .3580	R2 = .007621; P = .7873

Table 1. Correlations between post-fracture bone surface deviations and Mankin score for arthritis at 8 weeks post-fracture. Bolded values are significant after Bonferroni correction with p<0.05/3.

Figure 1 - Registration of 3D Models. The medial plateau (red) of pre-fracture models (blue/purple) were selected for registration. An iterative closest point algorithm was used to register selected regions of pre-fracture models with the intact medial plateau of their corresponding post-fracture model (turqoise). After registration was complete the intact portions of both scans were well aligned and joint incongruities could be measured in the disrupted portion of the post-fracture joint surface.

Figure 2 – Quantifying Joint Incongruity with 3D Directional Deviation Analysis. Joint incongruity was quantified using 3D directional deviation analysis. Directional deviation was defined as the distance from a pre-fracture model surface to a post-fracture model surface along a single deviation axis, or unit vector. Positive deviations (left) represent outward projections of the post-fracture surface and negative deviations (right) represent inward projections. Bone surface deviations were measured along the axial, antero-posterior, and latero-medial anatomic axes.

Figure 3 – Normalizing Bone Surface Deviations for Mouse Size. To normalize for size differences between mice, deviations were reported as percentages of pre-fracture 3D model size as determined by anatomic landmarks. In this example, percent deviation = X/Y.

Figure 4 – Articular Fracture Creation. CT images of representative fractures in Black6 and MRL mice obtained immediately post-fracture and at 8 weeks post-fracture. In post-fracture scans, moderately severe articular fractures accompanied by multiple fracture fragments and displacement of fragments. In 8 week scans, white arrows point to regions of fracture healing.

Figure 5 – Markers of Bone Metabolism. Concentrations of PINP in the C57BL/6 mice were significantly lower than the MRL/MpJ mice post-fx (p=0.005), indicating a less robust acute bone anabolic response compared with the superhealer strain. Despite higher levels of CTXI in the C57BL/6 mice compared to the MRL/MpJ at pre-fracture (p=0.005), no differences were found in CTXI levels post-fracture between strains or at any time point.

Figure 6 – Progression of Post-Fracture Deviations. Progression of axial bone surface deviation in a single mouse from immediately post-fracture to 8 weeks. A color map (far right) highlights a spectrum of positive and negative deviations. Analyzing deviations at each time point provided a unique visual of the fracture healing process. In post-fracture and 1 week models, an increase in negative deviation of the lateral tibial plateau can be appreciated as a shift from light blue to dark blue coloration. This early change in deviation may suggest fracture fragment instability. The non-disturbed center region of all the models progressively increases in positive deviation from post-fracture to 8 weeks as demonstrated by a shift towards yellow/red coloration. In turn, these progressive changes may suggest remodeling.

Figure 7 – Progression of Average Axial Bone Surface Deviation. Average positive axial deviation plotted as a function of time. In the lateral plateau (left), Black6 mice exhibit deviations immediately post-fracture which continue to significantly increase at 4 and 8 weeks. In comparision, MRL mice also exhibit deviations immediately post-fracture but with no significant change overtime. By 8 weeks, deviation in MRL mice was significantly lower than in Black6 mice. In the medial plateau (right), deviation remained relatively constant for Black6 mice, but gradually increased in MRL mice which could be explained by bone remodeling. Error bars represent 95% confidence interval of mean. Repeated measures ANOVA with Tukey Post-hoc test. Letters represent levels of significance ($p < 0.05$). A significant effect of Strain*Time interaction term across time points was seen in both plots ($p < 0.05$). A deviation of 0% corresponds to perfect alignment of pre-fracture and post-fracture tibial plateaus.

Figure 8 – Post-Fracture Axial Deviation Correlates with Arthritis in C57BL/6 Mice. (A) Mankin score for arthritis vs. maximum positive axial deviation measured immediately post-fracture. For Black6 mice, a significant correlation is seen between deviation and the development of arthritis. There was no correlation between deviation and the development of arthritis in MRL mice. (B) Mankin score for arthritis vs. maximum negative axial deviation measured immediately post-fracture. Again, in Black6 mice, a strong correlation exists between deviation and the development of arthritis, with no significant correlation observed in the MRL mice.
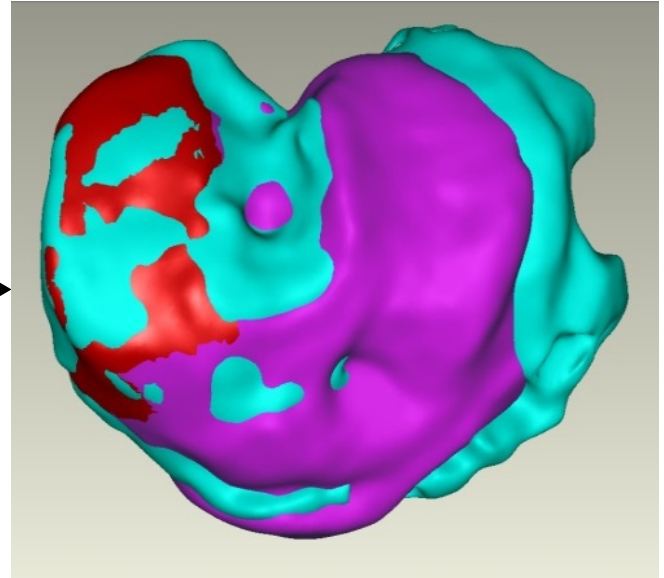
Pre-fracture 3D Model

Registered 3D Models
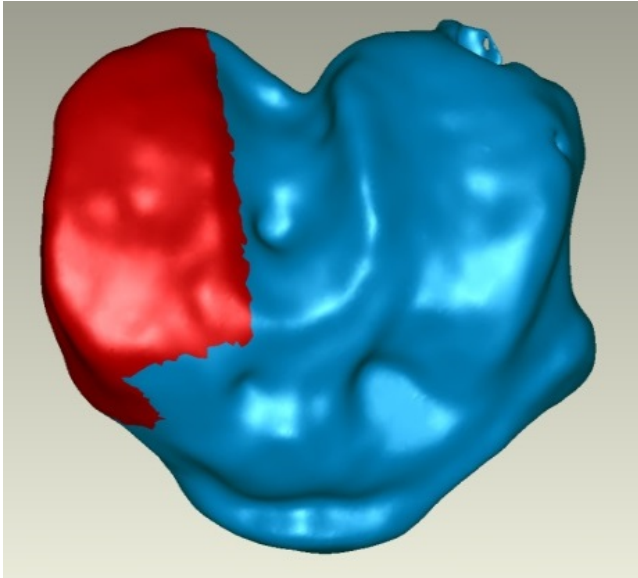
Registration

Iterative Closest Point Algorithm
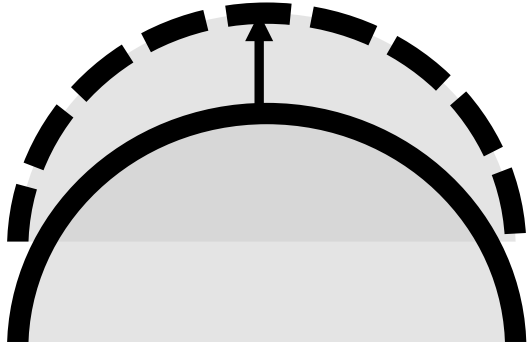
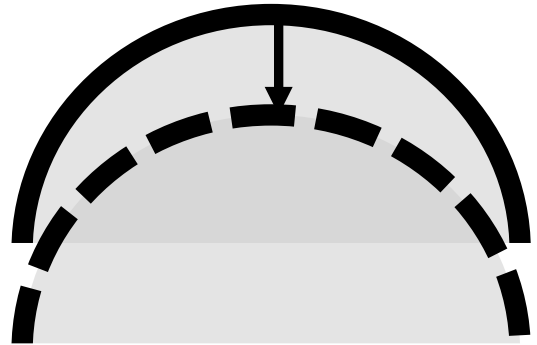■ = Region Selected for Registration

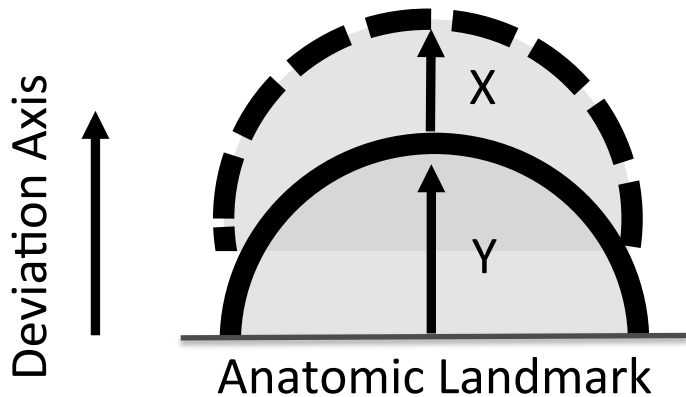■ = Pre-fracture Model

■ = Post-fracture Model

Positive Deviation   Negative Deviation

Deviation Axis

= Pre-fracture Model

= Post-fracture Model

Deviation Axis

Anatomic Landmark

X

Y

= Post-fracture Model

= Pre-fracture Model

	C57BL/6	MRL/MpJ
Post-Fracture		
8 Weeks		

Serum PINP

PINP (ng/ml) vs Pre, Post, 2wks, 4wks, 6wks

*

B6
MRL

Serum CTX-I

CTXI (ng/ml) vs Pre, Post, 2wks, 4wks, 6wks

*

B6
MRL
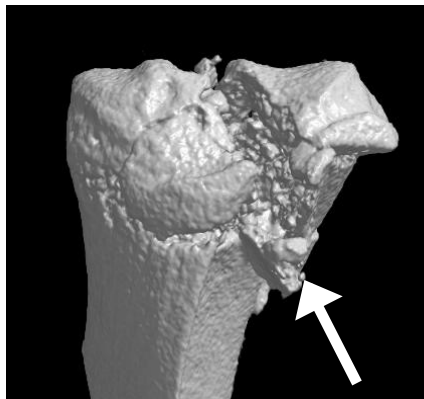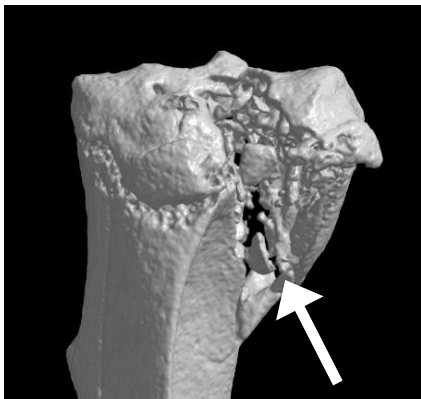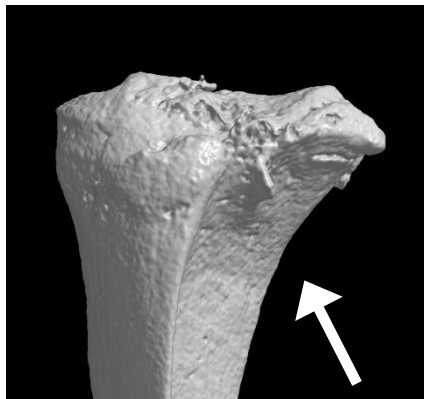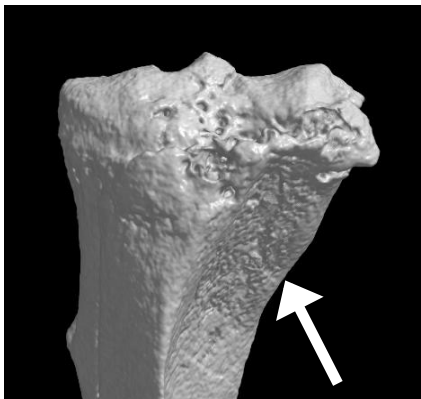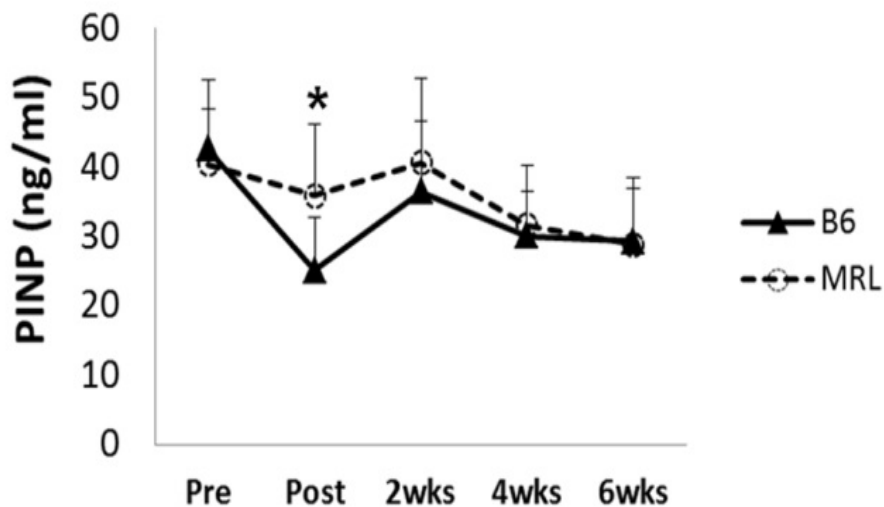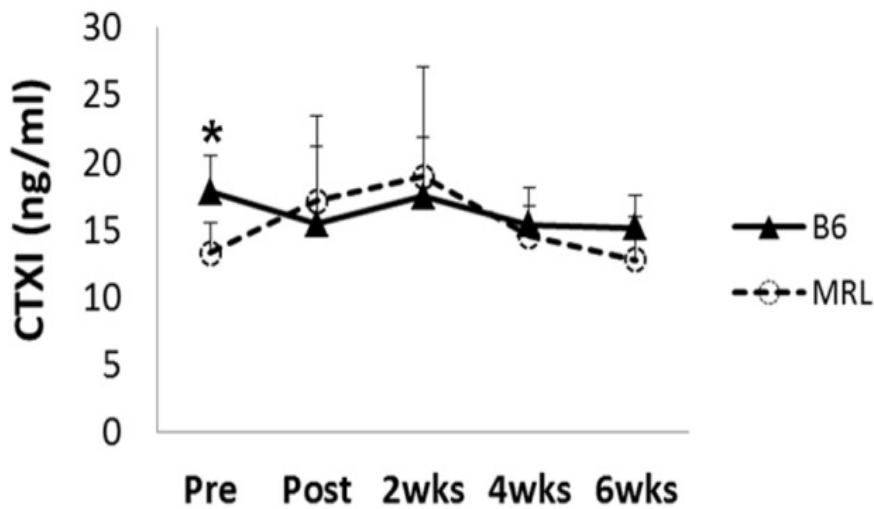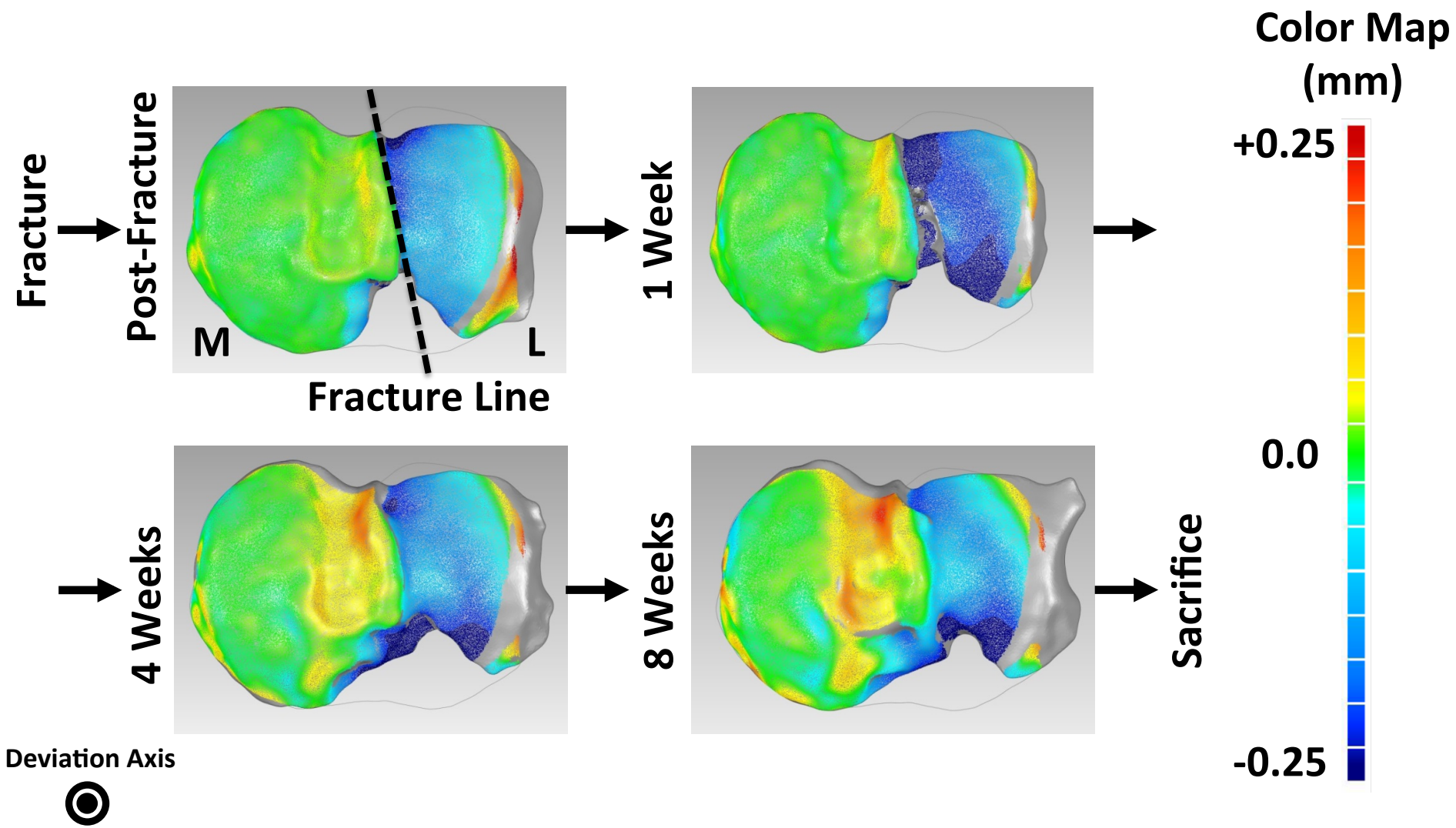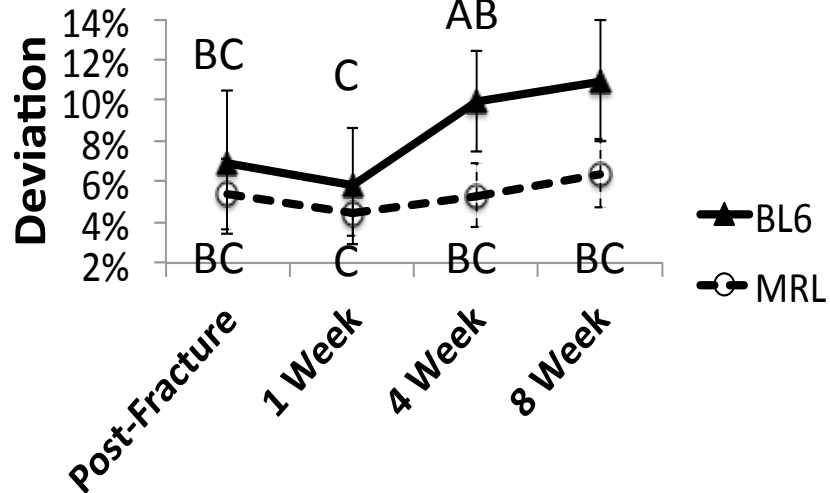
Average Positive Axial Deviation (Lateral) / Average Positive Axial Deviation (Medial)

$R^2 = 0.0207$
$P = 0.6554$

BL6

MRL

$R^2 = 0.9891$
$P = 0.0005$
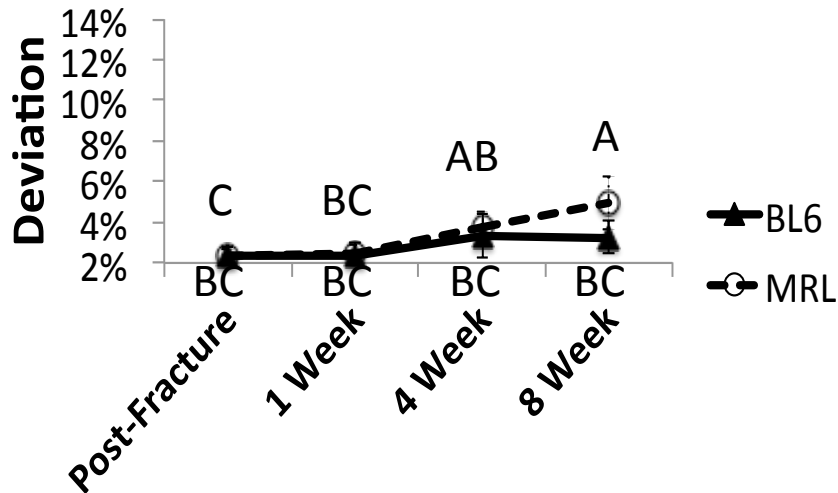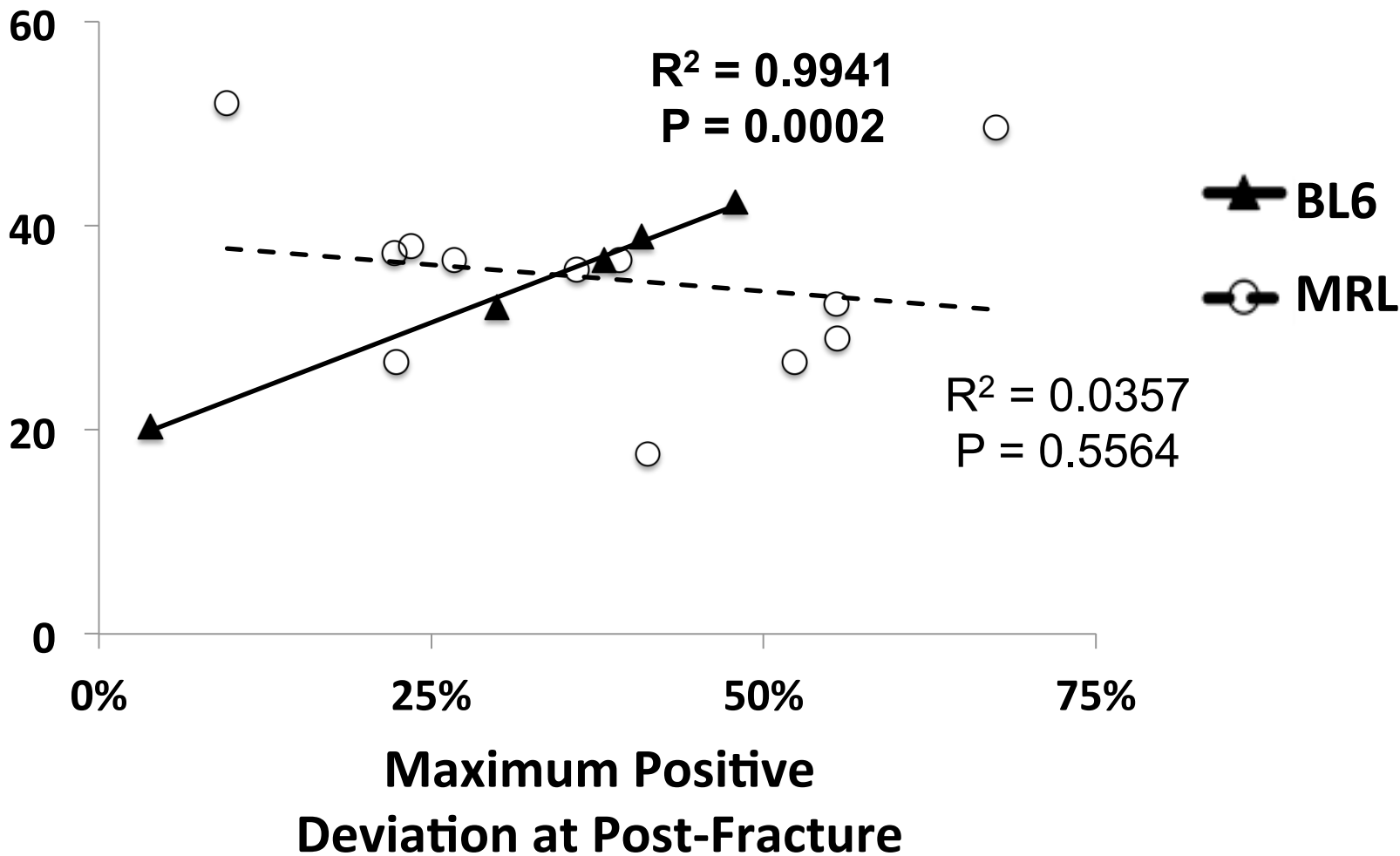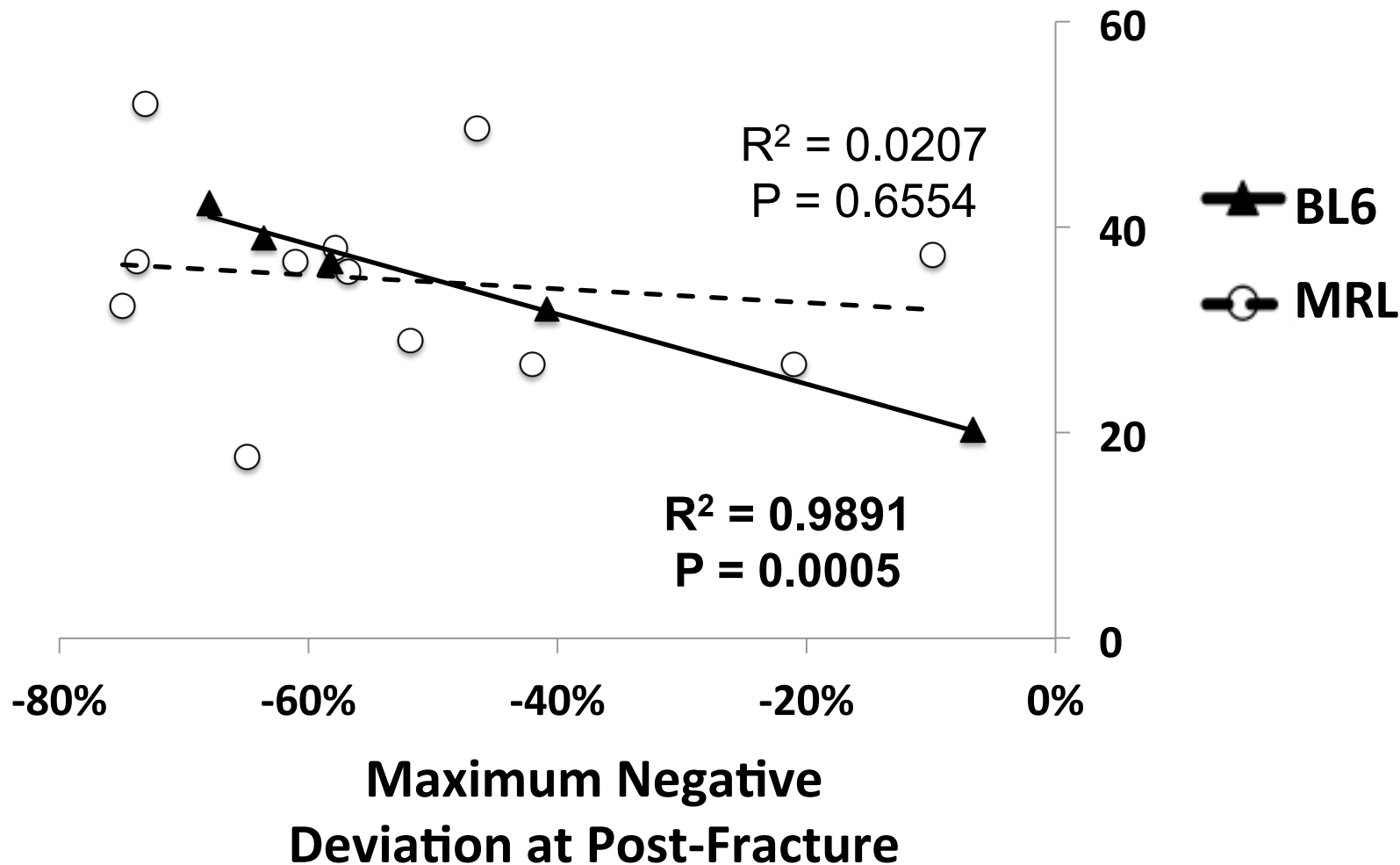
Appendix III. Personnel

DoD-TRP Award – Assessment of Biomarkers Associated with Joint Injury and Subsequent Posttraumatic Arthritis

Award Number: W81XWH-12-1-0621
PI: Steven A. Olson
Personnel: Steven Olson, Louis DeFrate, Bridgette Furman, Maria Manson, Gangadhar Utturkar

Award Number: W81XWH-12-1-0622
PI: Virginia B. Kraus
Personnel: Virginia Kraus, Janet Huebner

Award Number: W81XWH-12-1-0623
PI: Farshid Guilak
Personnel: Farshid Guilak, Bridgette Furman, Robert Nielsen, Kelly Kimmerling, Halei Benefield, Stephen Johnson, Dawn Chasse

Assessment of Biomarkers Associated with Joint Injury and Subsequent Post-Traumatic Arthritis

PRORP: Translational Research Partnership Award / OR110100P1
W81XWH-12-1-0622

PI: Virginia B. Kraus   **Org:** Duke University Medical Center   **Award Amount:** $750,000
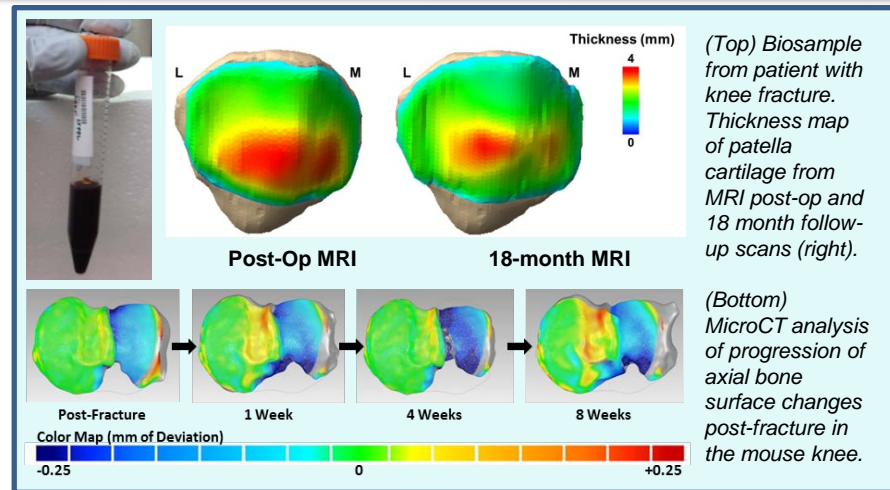
Study/Product Aim(s)

• The overall objective is to identify biomarkers following articular fracture that may be predictive of the development of post-traumatic arthritis (PTA).
• PTA is a severe burden in active duty and discharged soldiers. Compared to other forms of arthritis, PTA has a more rapid clinical onset. The goal of this work is to establish the basis for future use of biomarkers to predict the potential risk for developing PTA after acute joint injury.

Approach

• To accomplish this we will conduct a two part study:
• Biomarkers will be looked at in humans after knee joint fractures in biosamples (blood, synovial fluid, and urine) collected after injury. Special radiographic imaging will allow us to determine 18 months after injury which patients developed PTA from those who did not. We will then look for differences in biosamples between those with and without PTA.
• A companion series of animal experiments with two strains of mice will compare the human and mouse response following joint fracture. The low cost of mouse models lends itself to this type of work, and the results will provide a validated model for assessing future therapies to prevent PTA.

(Top) Biosample from patient with knee fracture. Thickness map of patella cartilage from MRI post-op and 18 month follow-up scans (right).

Post-Op MRI   18-month MRI

(Bottom) MicroCT analysis of progression of axial bone surface changes post-fracture in the mouse knee.

Post-Fracture   1 Week   4 Weeks   8 Weeks
Color Map (mm of Deviation)
-0.25   0   +0.25

Accomplishments: Enrollment has closed with 20 patients enrolled in the study. Biosamples have been collected from all subjects and are stored for analyses. MRI scans are being obtained and analyzed. Mice microCT analysis is near completion, and histology is underway.

Timeline and Cost

Activities CY	13	14	15	16*
Enroll knee fracture patients, collect biosamples, initial MRI	▨	▨		
Create articular fracture in knee of mice and harvest samples	▨	▨		
Analysis of mice samples, and obtain MRI at 18 months.		▨	▨	▮
Analyze biosamples and compare human data to mice			▨	▮
Estimated Budget ($K)	**$238**	**$233**	**$279**	**NCE***

*No Cost Extension (NCE)

Updated: 15 December 2016

Goals/Milestones

CY13 Goals – *Begin patient biosample collection, MRI scans, and animal studies*
☑ Obtained IRB approval of human use in study, enrolled 9 patients, processed and stored biosamples, and obtained initial MRI scans.
☑ Obtained IACUC approval for animal use in study, created fractures in mice, and harvested samples for early time points.

CY14 Goals – *Continue patient biosample collection, MRI scans, and animal studies*
☑ Enrolled 9 additional patients, collected biosamples, obtained initial MRI scans, and collected 18 month follow-up MRI scans from first two patients.
☑ Created fractures in mice, harvested samples, started microCT and histologic analysis.

CY15 Goal – *Biomarker analyses of human and mouse samples*
☑ Perform assays to measure biomarkers, metabolomics and proteomics analysis.
☑ Complete animal study histology, microCT analysis.

NCE CY16 Goal – *Complete all statistical analyses for human and mouse studies*
☑ Complete analyses of follow-up MRI scans.
☑ Complete animal and human biomarker assays and compare.

Budget Expenditure:
Projected-$750K Actual-$750K